The Second RPA and its connection to the nuclear multipole response

Danilo Gambacurta
gambacurta@lns.infn.it
INFN-LNS Catania

Nuclear excitations and resonances
18-22 November 2024, Saclay, France

Outline

- RPA and Second RPA (SRPA)
- First (1980s, 90s, 2000s) SRPA applications
  (small model spaces and "approximated")
- Large scale SRPA (2010s) calculations
- The SRPA within the EDF approach: $\mapsto$ the Subtracted SRPA (SSRPA)
- Applications of the SSRPA
- Conclusions and Outlook

The Random Phase Approximation (RPA)

- The RPA is a widely used tool for the description of collective excitations
- Very successful especially within the Energy Density Functional framework (interactions á la Skyrme or Gogny, covariant versions)
- It provides global properties: centroid energies and total strength

However, extensions of the RPA are required for:

- Strength Fragmentation
- Fine Structure
- Spreading Width
- Low Lying excitations in closed shell nuclei
- Double exctiations and Anharmonicities, ...

The Method of the Equations of Motion

Set of exact eigenstates of the Hamiltonian H

$$H|\nu\rangle = E_\nu \mid \nu\rangle$$

where $\mid 0\rangle$ is the ground state with energy E_0

Phonon operators

Let us introduce the operators $Q's$:

$$Q_\nu^\dagger \mid 0\rangle = \mid \nu\rangle$$

$$Q_\nu \mid 0\rangle = 0.$$

Equations of Motion:

$$\langle 0 \mid \left[\delta Q, [H, Q_\nu^\dagger]\right] \mid 0\rangle = \omega_\nu \langle 0 \mid [\delta Q, Q_\nu^\dagger] \mid 0\rangle$$

where

$$\omega_\nu = E_\nu - E_0.$$

Phonon Operators: RPA vs SRPA

Random Phase Approximation (RPA)

$$Q^{\dagger}_{\nu} = \underbrace{\sum_{ph} X^{(\nu)}_{ph} \underbrace{a^{\dagger}_{p} a_{h}}_{\text{1p-1h}} - \sum_{ph} Y^{(\nu)}_{ph} \underbrace{a^{\dagger}_{h} a_{p}}_{\text{1h-1p}}}_{\text{Only Landau Damping, Centroid Energy and Total Strength of GRs}}$$

Second Random Phase Approximation (SRPA)

$$Q^{\dagger}_{\nu} = \sum_{ph} (X^{(\nu)}_{ph} a^{\dagger}_{p} a_{h} - Y^{(\nu)}_{ph} a^{\dagger}_{h} a_{p})$$

$$+ \underbrace{\sum_{p_1<p_2, h_1<h_2} (X^{(\nu)}_{p_1 h_1 p_2 h_2} \underbrace{a^{\dagger}_{p_1} a_{h_1} a^{\dagger}_{p_2} a_{h_2}}_{\text{2p-2h}} - Y^{(\nu)}_{p_1 h_1 p_2 h_2} \underbrace{a^{\dagger}_{h_1} a_{p_1} a^{\dagger}_{h_2} a_{p_2}}_{\text{2h-2p}})}_{\textbf{Spreading Width, Fragmentation}, \text{ Double GRs and Anharmonicites, Low-Lying States}}$$

Phonon Operators: RPA vs SRPA

Random Phase Approximation (RPA)

$$Q^{\dagger}_{\nu} = \underbrace{\sum_{ph} X^{(\nu)}_{ph} \underbrace{a^{\dagger}_{p} a_{h}}_{\text{1p-1h}} - \sum_{ph} Y^{(\nu)}_{ph} \underbrace{a^{\dagger}_{h} a_{p}}_{\text{1h-1p}}}_{\text{Only Landau Damping, Centroid Energy and Total Strength of GRs}}$$

Second Random Phase Approximation (SRPA)

$$Q^{\dagger}_{\nu} = \sum_{ph} (X^{(\nu)}_{ph} a^{\dagger}_{p} a_{h} - Y^{(\nu)}_{ph} a^{\dagger}_{h} a_{p})$$

$$+ \underbrace{\sum_{p_1<p_2, h_1<h_2} (X^{(\nu)}_{p_1 h_1 p_2 h_2} \underbrace{a^{\dagger}_{p_1} a_{h_1} a^{\dagger}_{p_2} a_{h_2}}_{\text{2p-2h}} - Y^{(\nu)}_{p_1 h_1 p_2 h_2} \underbrace{a^{\dagger}_{h_1} a_{p_1} a^{\dagger}_{h_2} a_{p_2}}_{\text{2h-2p}})}_{\textbf{Spreading Width, Fragmentation}, \text{ Double GRs and Anharmonicites, Low-Lying States}}$$

Quasi Boson Approximation (QBA)

The phonon vacumm $|\,0\rangle$ is not known: it is replaced by the HF one

$$|\,0\rangle \mapsto |\,HF\rangle$$

RPA Equations of Motion (1$\mapsto$ 1p-1h)

$$\begin{pmatrix} \mathcal{A}_{11} & \mathcal{B}_{11} \\ -\mathcal{B}^*_{11} & -\mathcal{A}^*_{11} \end{pmatrix} \begin{pmatrix} \mathcal{X}^\nu_1 \\ \mathcal{Y}^\nu_1 \end{pmatrix} = \omega_\nu \begin{pmatrix} \mathcal{X}^\nu_1 \\ \mathcal{Y}^\nu_1 \end{pmatrix}$$

RPA Equations of Motion (1$\mapsto$ 1p-1h)

$$\begin{pmatrix} \mathcal{A}_{11} & \mathcal{B}_{11} \\ -\mathcal{B}^*_{11} & -\mathcal{A}^*_{11} \end{pmatrix} \begin{pmatrix} \mathcal{X}^\nu_1 \\ \mathcal{Y}^\nu_1 \end{pmatrix} = \omega_\nu \begin{pmatrix} \mathcal{X}^\nu_1 \\ \mathcal{Y}^\nu_1 \end{pmatrix}$$

SRPA Equations of Motion (1$\mapsto$ 1p-1h, 2$\mapsto$ 2p-2h)

$$\begin{pmatrix} \mathcal{A}_{11} & \mathcal{A}_{12} & \mathcal{B}_{11} & \mathcal{B}_{12} \\ \mathcal{A}_{21} & \mathcal{A}_{22} & \mathcal{B}_{21} & \mathcal{B}_{22} \\ -\mathcal{B}^*_{11} & -\mathcal{B}^*_{12} & -\mathcal{A}^*_{11} & -\mathcal{A}^*_{12} \\ -\mathcal{B}^*_{21} & -\mathcal{B}^*_{22} & -\mathcal{A}^*_{21} & -\mathcal{A}^*_{22} \end{pmatrix} \begin{pmatrix} \mathcal{X}^\nu_1 \\ \mathcal{X}^\nu_2 \\ \mathcal{Y}^\nu_1 \\ \mathcal{Y}^\nu_2 \end{pmatrix} = \omega_\nu \begin{pmatrix} \mathcal{X}^\nu_1 \\ \mathcal{X}^\nu_2 \\ \mathcal{Y}^\nu_1 \\ \mathcal{Y}^\nu_2 \end{pmatrix}$$

Transition Probabilities in RPA and SRPA

- Let us consider a one-body operator $F = \sum_{\alpha,\beta} F_{\alpha\beta} a^\dagger_\alpha a_\beta$
- The RPA and SRPA transition amplitudes are

$$\langle \nu | F | 0 \rangle = \langle 0 | [Q_\nu, F] | 0 \rangle \approx \langle HF | [Q_\nu, F] | HF \rangle = \sum_{ph} \{ X^{\nu *}_{ph} F_{ph} + Y^{\nu *}_{ph} F_{hp} \}$$

Thouless Theorem

The first moment

$$m_1 = \sum_\nu \omega_\nu |\langle \nu \mid F \mid 0 \rangle|^2$$

is the same in RPA and SRPA[a] and Thouless theorem holds [b]

$$\sum_\nu \omega_\nu |\langle \nu \mid F \mid 0 \rangle|^2 = \frac{1}{2} \langle HF \mid [F, [H, F]] \mid HF \rangle,$$

Energy Weighted Sum Rules are preserved.

---

[a] C. Yannouleas, Phys. Rev. C35, 1159 (1987)

[b] For self-consistent calculations

Computationally very demanding

- Number of 2ph ($\sim 10^{6,7}$ for a medium-mass nucleus) is considerable higher than 1ph ($\sim$ a few hundreds) in J-coupled scheme
- Old applications used strong approximations
  - Restricted 2ph spaces
  - Unperturbed 2ph configurations, e.g. no residual interaction, diagonal approximation (see later)
  - Real part of the self-energy neglected

Some references

- B. Schwesinger and J. Wambach, Nuclear Physics A426 (1984) 253-275
- S.Drozdz, S. Nishizaki, J. Speth and J. Wambach, Physics Reports 197,1 (1990) and references therein
- S. Ait-Tahar and D.M. Brink, Nuclear Physics A560 (1993) 765-796
- S. Nishizaki, J. Wambach, Physics Letters B 349 (1995) 7-10
- S. Ayik, D. Lacroix and P. Chomaz, PRC, 61, 014608 (1999)
- D. Lacroix *et al.*, Physics Letters B 479 (2000) 15

From SRPA to an Energy dependent RPA-like problem

- The SRPA problem can be reduced to an RPA eigenvalue problem but with $\mathcal{A}_{1,1}$ **depending on the Energy** ω

$$A_{1,1'} \mapsto \tilde{A}_{1,1'}(\omega) = A_{1,1'} + \sum_{2,2'} A_{1,2}(\omega + i\eta - A_{2,2'})^{-1} A_{2',1'}$$

- Exact projection onto the 1ph space
- The matrix inversion is very **cumbersome**
- If we neglect the **residual interaction** among the $2p-2h$ states

$$A_{2,2} \simeq \delta_{h_1 h_1'} \delta_{p_1 p_1'} \delta_{h_2 h_2'} \delta_{p_2 p_2'} (\epsilon_{p_1} + \epsilon_{p_2} - \epsilon_{h_1} - \epsilon_{h_2})$$

the inversion is algebraic, (**diagonal approximation**)

SRPA as an energy-dependent RPA problem

$$\begin{pmatrix} \mathcal{A}_{11}(\omega) & \mathcal{B}_{11} \\ -\mathcal{B}_{11}^{*} & -\mathcal{A}_{11}^{*}(-\omega) \end{pmatrix} \begin{pmatrix} \mathcal{X}_1^{\nu}(\omega) \\ \mathcal{Y}_1^{\nu}(\omega) \end{pmatrix} = \omega_{\nu} \begin{pmatrix} \mathcal{X}_1^{\nu}(\omega) \\ \mathcal{Y}_1^{\nu}(\omega) \end{pmatrix}$$

Second RPA calculations of the charge-exchange quadrupole response functions in closed-shell nuclei

Nuclear Physics A560 (1993) 765–796
North-Holland

S. Ait-Tahar [a,b] and D.M. Brink [a]

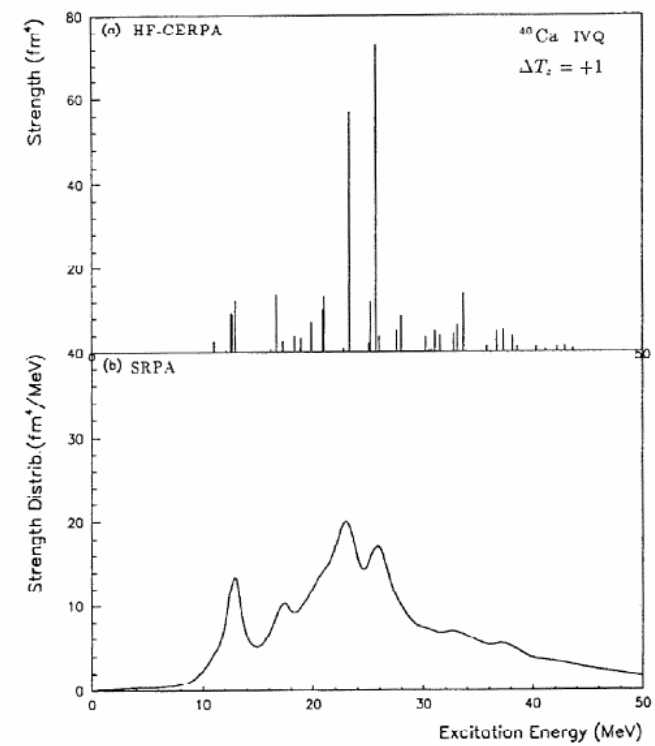

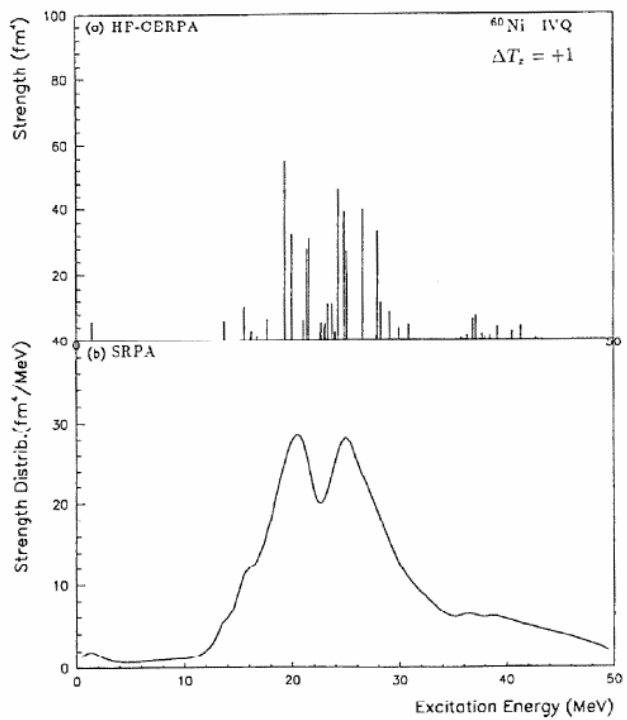

Fig. 3. The same as fig. 1 for ^{60}Ni.

PHYSICAL REVIEW C, VOLUME 61, 014608

Fragmentation and damping of the collective response in extended random-phase approximati

Sakir Ayik,[1] Denis Lacroix,[2] and Philippe Chomaz[2]

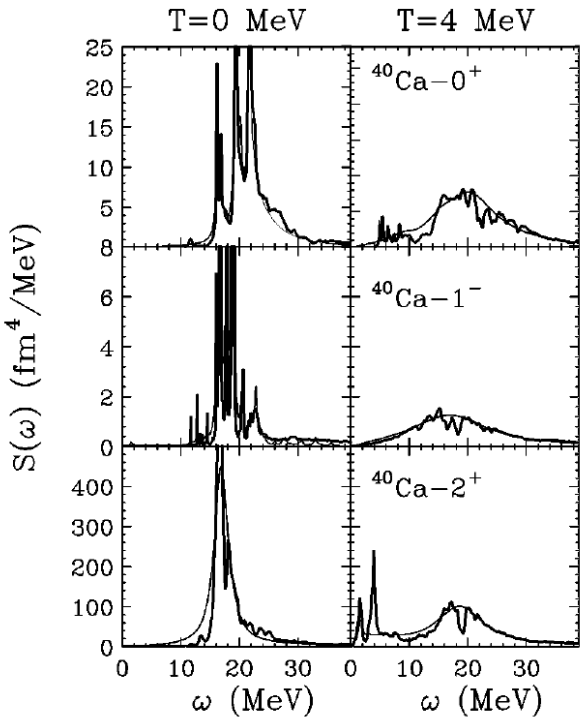

FIG. 2. The extended RPA strength distributions of the monopole, dipole, and quadrupole excitations at $T=0$ MeV (left) and $T=4$ MeV (right). Thin lines represent the strength obtained in the pole approximation whereas thick lines are obtained by including the frequency dependence of the imaginary part of the self-energy. In both cases, the real part of the self-energy is neglected.

B. Energy shift with zero-range effective forces

A zero range Skyrme-type force provides a good description for the mean-field properties, but it is not very suitable for calculation of $2p$-$2h$ self-energies of the collective modes. Matrix elements of a zero range force with a quadratic momentum dependence does not involve a natural cutoff for large values of the momentum transfer. This behavior is not a serious problem for the damping width since the high frequency matrix elements are naturally cut off due to the Lorentzian factor in $\Gamma_\lambda(\omega)$ [Eq. (14)]. However, the situation is different for the energy shift. The frequency dependent factor in the expression of $\Delta_\lambda(\omega)$ does not provide such a cutoff. As a result, the shift of the collective frequency $\Delta_\lambda(\omega)$ is strongly affected by the unrealistic large matrix elements for high momentum transfers. As an example, Fig. 3 shows the strength distribution for quadrupole excitations at temperature $T=4$ MeV. Thin lines are obtained in the pole approximation and neglecting the shift of the resonance due to the real part of the self-energy, whereas, thick line is the result of full calculations including the real and imaginary parts of the self-energy. The strength is shifted down by an unreasonable amount of about 10 MeV from the RPA value. A similar result was reported in [23]. Moreover, the magnitude of the energy shift depends on the size of the $2p$-$2h$ space, which clearly indicates a serious weakness of the zero range forces in the calculation of $2p$-$2h$ self-energies.

PHYSICAL REVIEW C, VOLUME 61, 014608

Fragmentation and damping of the collective response in extended random-phase approximati

Sakir Ayik,[1] Denis Lacroix,[2] and Philippe Chomaz[2]

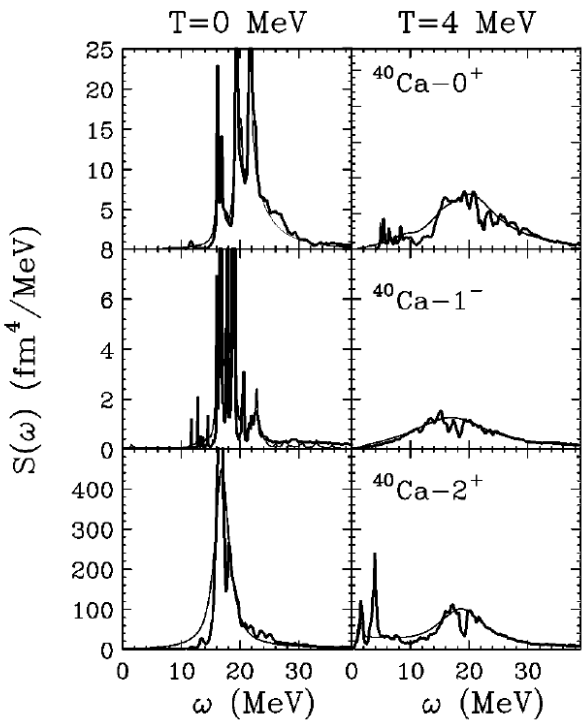

FIG. 2. The extended RPA strength distributions of the monopole, dipole, and quadrupole excitations at $T=0$ MeV (left) and $T=4$ MeV (right). Thin lines represent the strength obtained in the pole approximation whereas thick lines are obtained by including the frequency dependence of the imaginary part of the self-energy. In both cases, the real part of the self-energy is neglected.

B. Energy shift with zero-range effective forces

A zero range Skyrme-type force provides a good description for the mean-field properties, but it is not very suitable for calculation of $2p$-$2h$ self-energies of the collective modes. Matrix elements of a zero range force with a quadratic momentum dependence does not involve a natural cutoff for large values of the momentum transfer. This behavior is not a serious problem for the damping width since the high frequency matrix elements are naturally cut off due to the Lorentzian factor in $\Gamma_\lambda(\omega)$ [Eq. (14)]. However, the situation is different for the energy shift. The frequency dependent factor in the expression of $\Delta_\lambda(\omega)$ does not provide such a cutoff. As a result, the shift of the collective frequency $\Delta_\lambda(\omega)$ is strongly affected by the unrealistic large matrix elements for high momentum transfers. As an example, Fig. 3 shows the strength distribution for quadrupole excitations at temperature $T=4$ MeV. Thin lines are obtained in the pole approximation and neglecting the shift of the resonance due to the real part of the self-energy, whereas, thick line is the result of full calculations including the real and imaginary parts of the self-energy. The strength is shifted down by an unreasonable amount of about 10 MeV from the RPA value. A similar result was reported in [23]. Moreover, the magnitude of the energy shift depends on the size of the $2p$-$2h$ space, which clearly indicates a serious weakness of the zero range forces in the calculation of $2p$-$2h$ self-energies.

Physics Letters B 349 (1995) 7–10

Double-dipole excitations in ^{40}Ca

S. Nishizaki [1], J. Wambach [2]

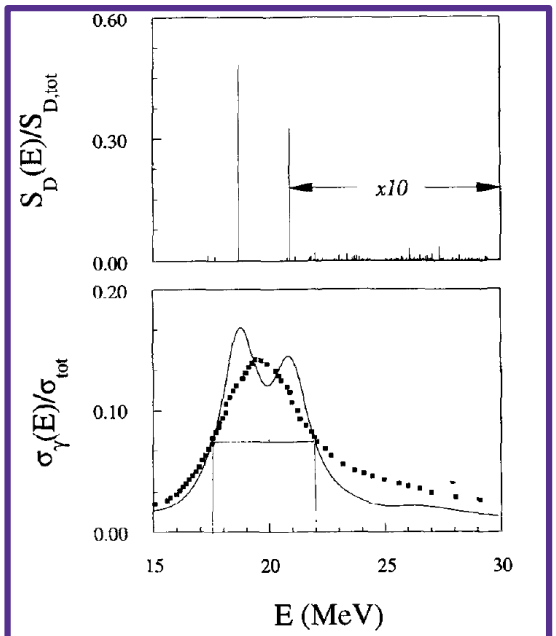

ig. 1. Upper part: the calculated dipole transition strength distri-ution in ^{40}Ca (Eq. (8)). The high-energy tail has been multi-ied by a factor of 10; lower part: the photoabsorption cross sec-on, normalized to the TRK sum rule. The data, indicated by the lled squares, are inferred from the Compton-scattering analysis f [11].

On the other hand, the single-dipole state

$$|D\rangle \equiv \sum_{i=1}^{Z} r_i \tau_i^z |0\rangle,$$

as well as the double-dipole state

$$|DD\rangle \equiv (\sum_{i=1}^{Z} r_i \tau_i^z)(\sum_{j=1}^{Z} r_j \tau_j^z)|0\rangle,$$

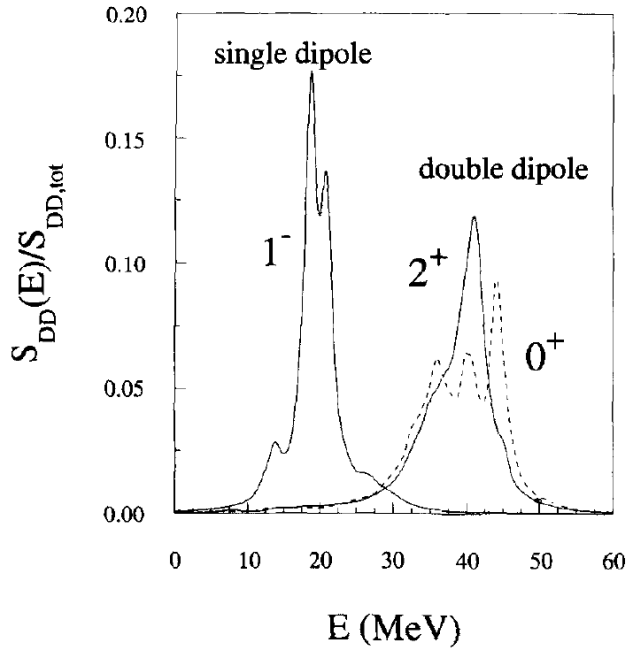

Fig. 2. The transition-strength distribution for the 0^+-component (dashed line) and 2^+-component (full line) the DGDR in ^{40}Ca. For comparison the single-dipole strength function is also given

Large scale SRPA calculations

- Only recently full large scale SRPA calculations have been performed [a]
- Model spaces large enough to preserve EWSRs
- No approximation in the evaluation of the matrix elements
- Self-consistency (same interaction in mean-field and in linear response)

[a] P. Papakonstantinou and R. Roth, PLB 671, 356 (2009); D.G et al. PRC 81, 054312 (2010)

.

Some references

- P. Papakonstantinou and R. Roth, Physics Letters B 671, 356 (2009), Phys. Rev. C.81, 024317 (2010)
- P. Papakonstantinou, Phys. Rev. C 90, 024305 (2014)
- DG, M. Grasso and F. Catara, PRC 81, 054312 (2010), PRC 84, 034301 (2011)
- D. G., M. Grasso and F. Catara, Journal of Physics G 38 035103 (2011)
- D. G. *et al.*, Phys. Rev. C 86 021304 (2012)

P. Papakonstantinou and R. Roth, Phys. Lett. B 671 (2009), 356

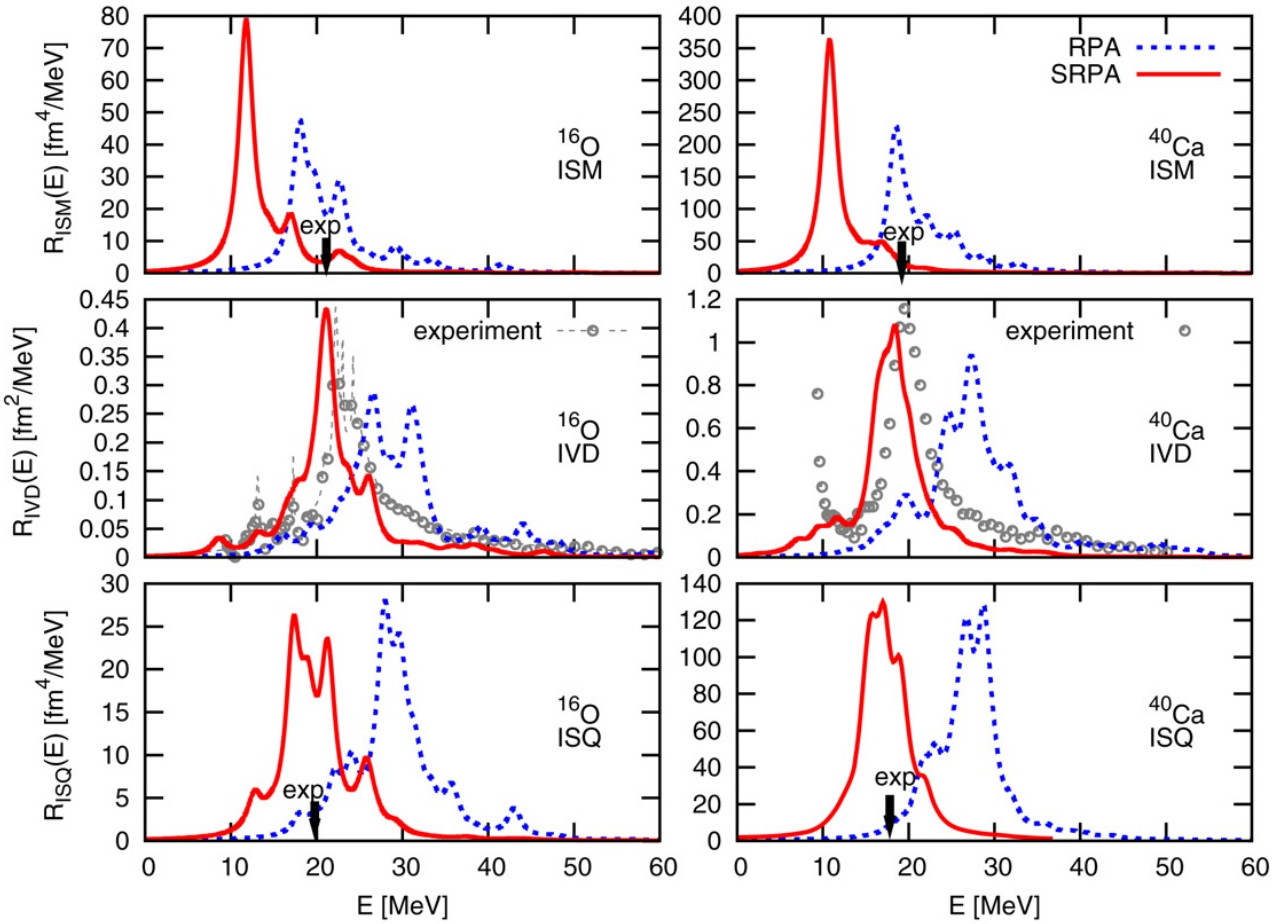

SRPA with UCOM method

SRPA for closed-shell nuclei using an interaction derived from the Argonne V18 potential with the Unitary Correlation Operator Method

PHYSICAL REVIEW C **81**, 054312 (2010)

Collective nuclear excitations with Skyrme-second random-phase approximation

D. Gambacurta,[1,2,*] M. Grasso,[3] and F. Catara[1,2]
[1]*Dipartimento di Fisica e Astronomia dell'Universitá di Catania, Via S. Sofia 64, I-95123 Catania, Italy*
[2]*Istituto Nazionale di Fisica Nucleare, Sezione di Catania, Via S. Sofia 64, I-95123 Catania, Italy*
[3]*Institut de Physique Nucléaire, Université Paris-Sud, IN2P3-CNRS, F-91406 Orsay Cedex, France*
(Received 22 February 2010; published 20 May 2010)

PHYSICAL REVIEW C **86**, 021304(R) (2012)

Second random-phase approximation with the Gogny force: First applications

D. Gambacurta,[1] M. Grasso,[2] V. De Donno,[3] G. Co',[3] and F. Catara[4]
[1]*Grand Accélérateur National d'Ions Lourds (GANIL), CEA/DSM-CNRS/IN2P3, Boulevard Henri Becquerel, F-14076 Caen, France*
[2]*Institut de Physique Nucléaire, Université Paris-Sud, IN2P3-CNRS, F-91406 Orsay Cedex, France*
[3]*Dipartimento di Matematica e Fisica "E. De Giorgi," Università del Salento and INFN, Sezione di Lecce, I-73100 Lecce, Italy*
[4]*Dipartimento di Fisica e Astronomia and INFN, Via Santa Sofia 64, I-95123 Catania, Italy*
(Received 7 May 2012; published 30 August 2012)

Numerical details

- Skyrme-HF equations are solved in the coordinate space
- 1ph and 2ph configurations with a given J^{π} are build (J-coupling)
- In SRPA calculations **all kinds of couplings** among all 1p-1h and 2p-2h configurations are taken into account
- Comparison with the diagonal approximation

EWSR Monopole Case in ^{16}O

First moment

$$m_1 = \sum_{\nu}^{\omega_{max}} \omega_\nu |\langle \nu \mid F \mid 0 \rangle|^2; \qquad m_1^{RPA} = m_1^{SRPA}?$$

Isoscalar and Isovector EWSR

EWSR		
	$m_1(T=0)$	$m_1(T=1)$
RPA	671.6516	201.2494
ω_{max}	SRPA	SRPA
40	626.4381	115.4153
50	648.9699	147.8026
60	661.0194	182.7364
70	664.3803	193.7896
80	669.7185	197.6874
90	671.4575	200.6472
100	671.6515	201.2473
110	671.6515	201.2473

Monopole Strength Distribution in ^{16}O

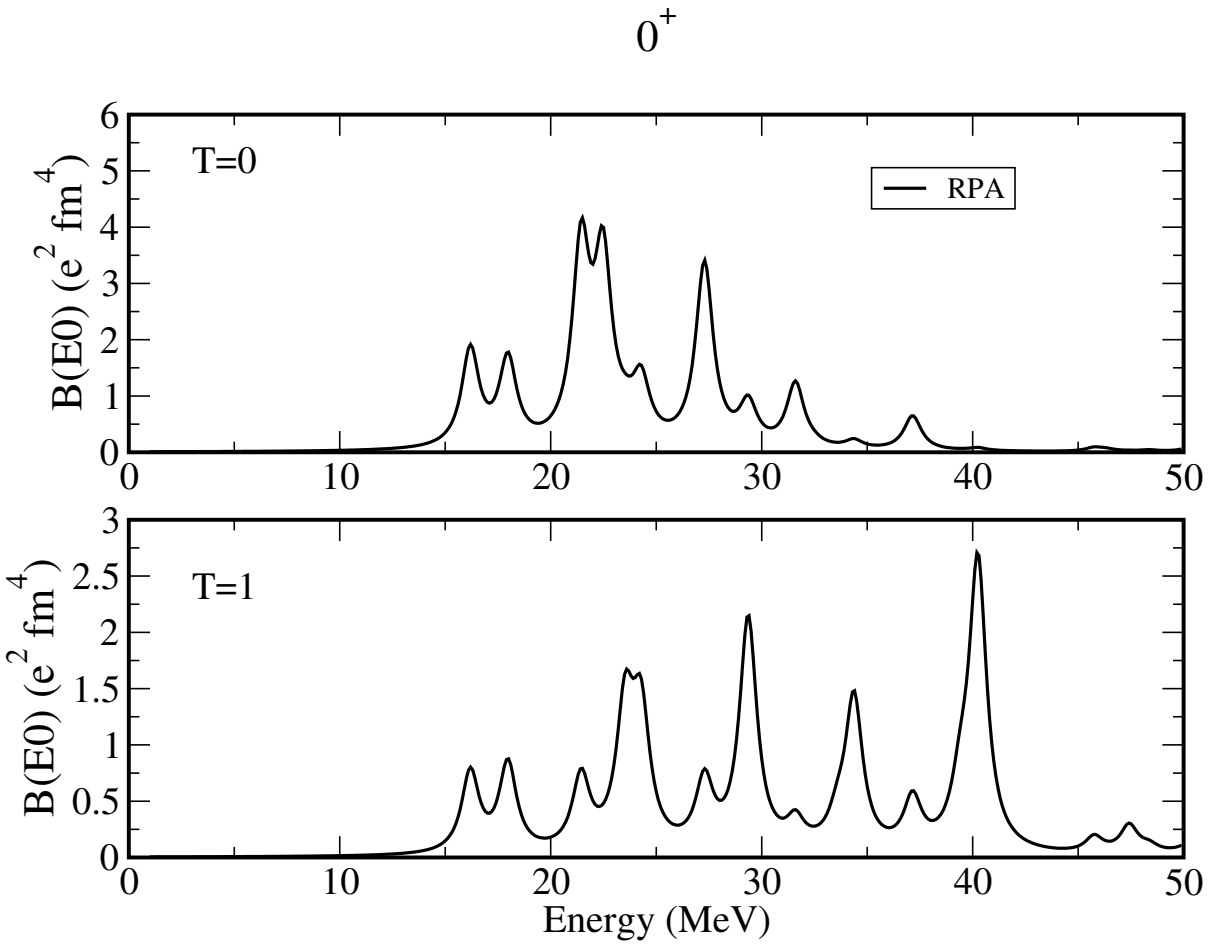

Monopole Strength Distribution in ^{16}O

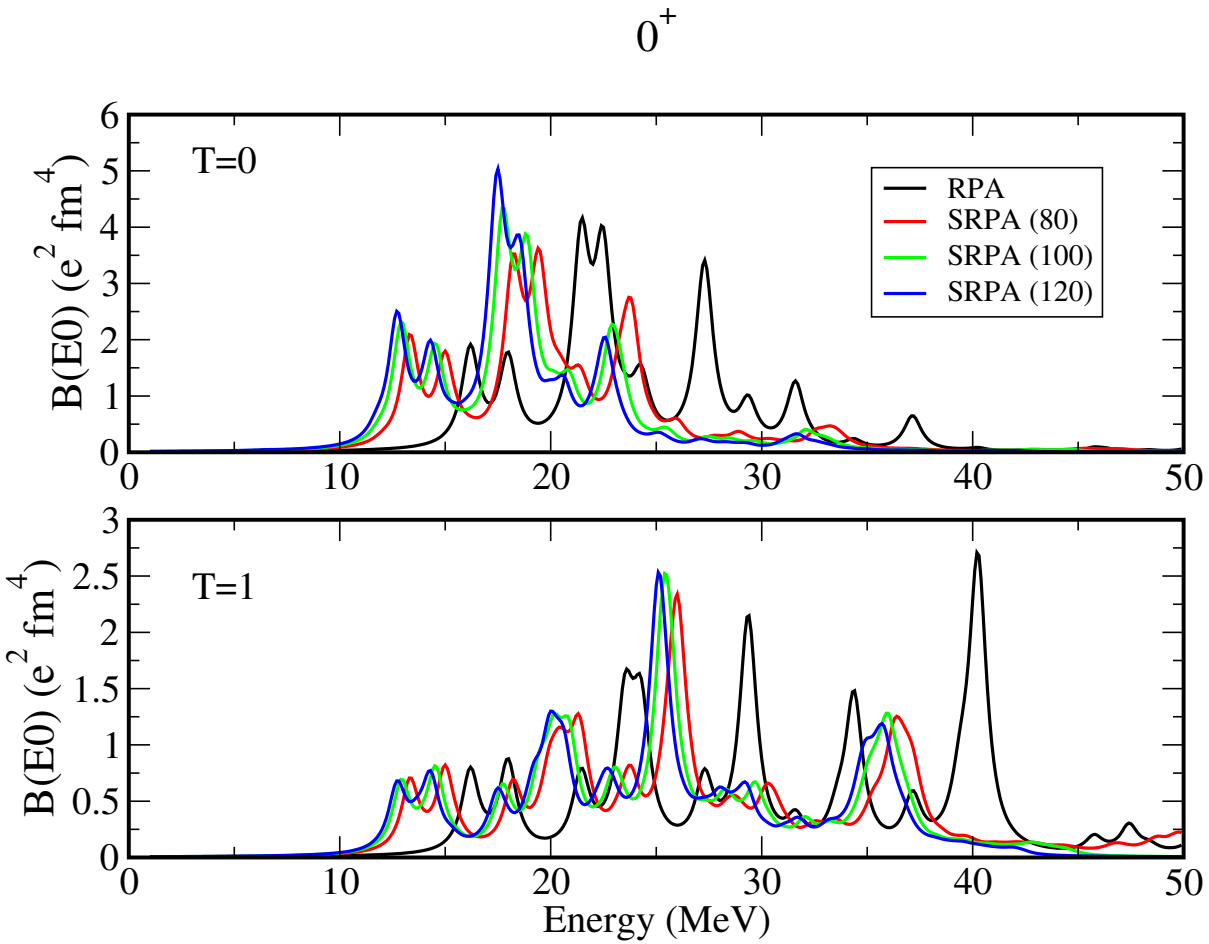

Monopole Strength Distribution in ^{16}O

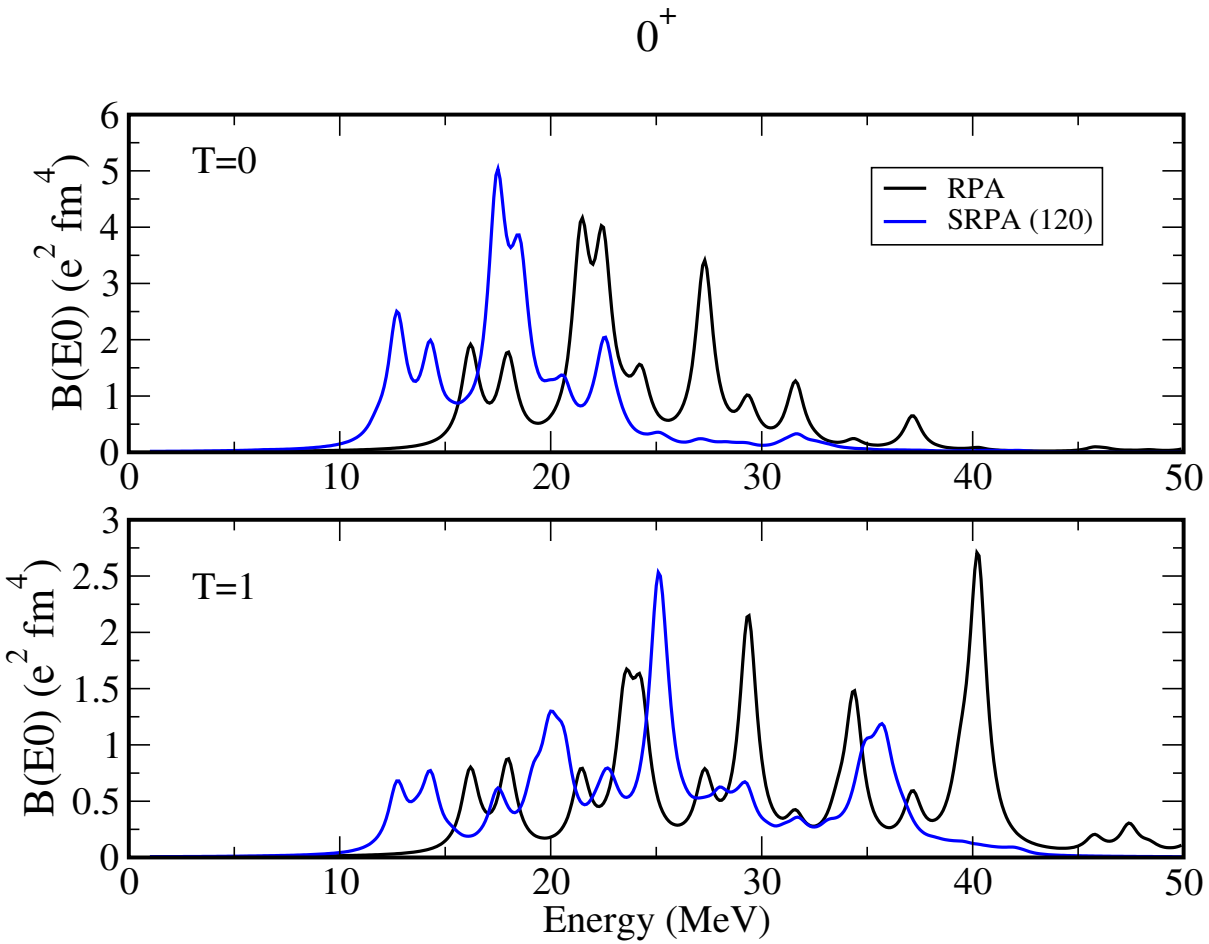

Monopole Strength Distribution in ^{16}O

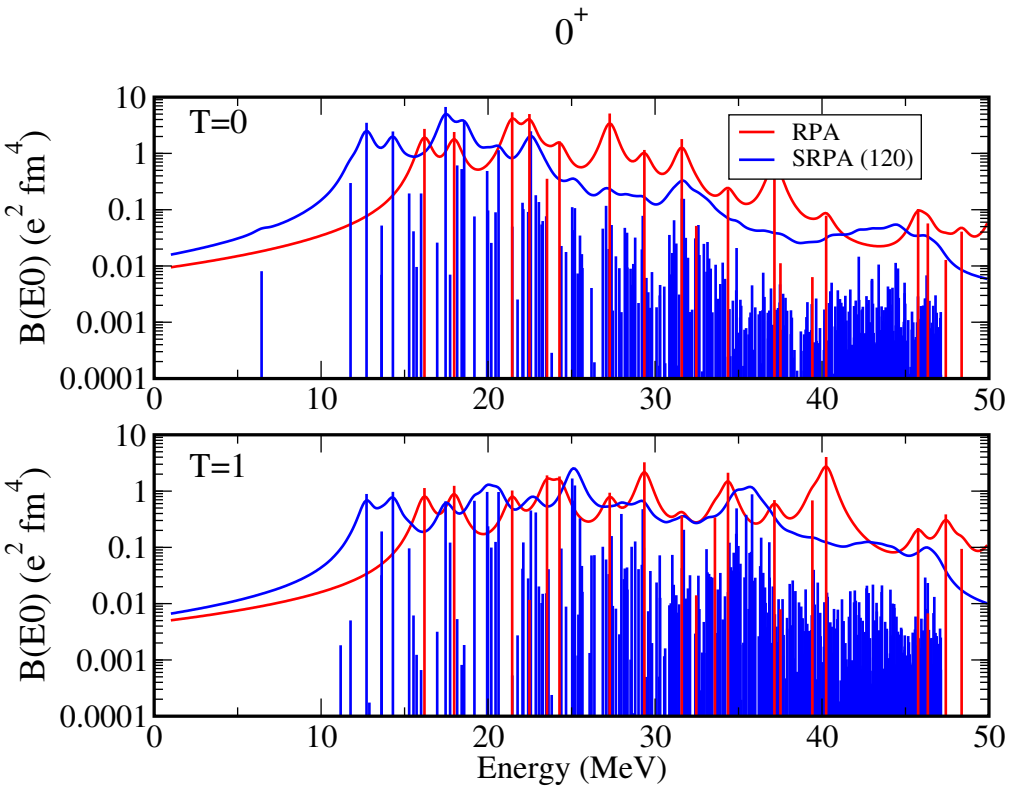

Monopole Strength in ^{16}O, Full Vs Diagonal

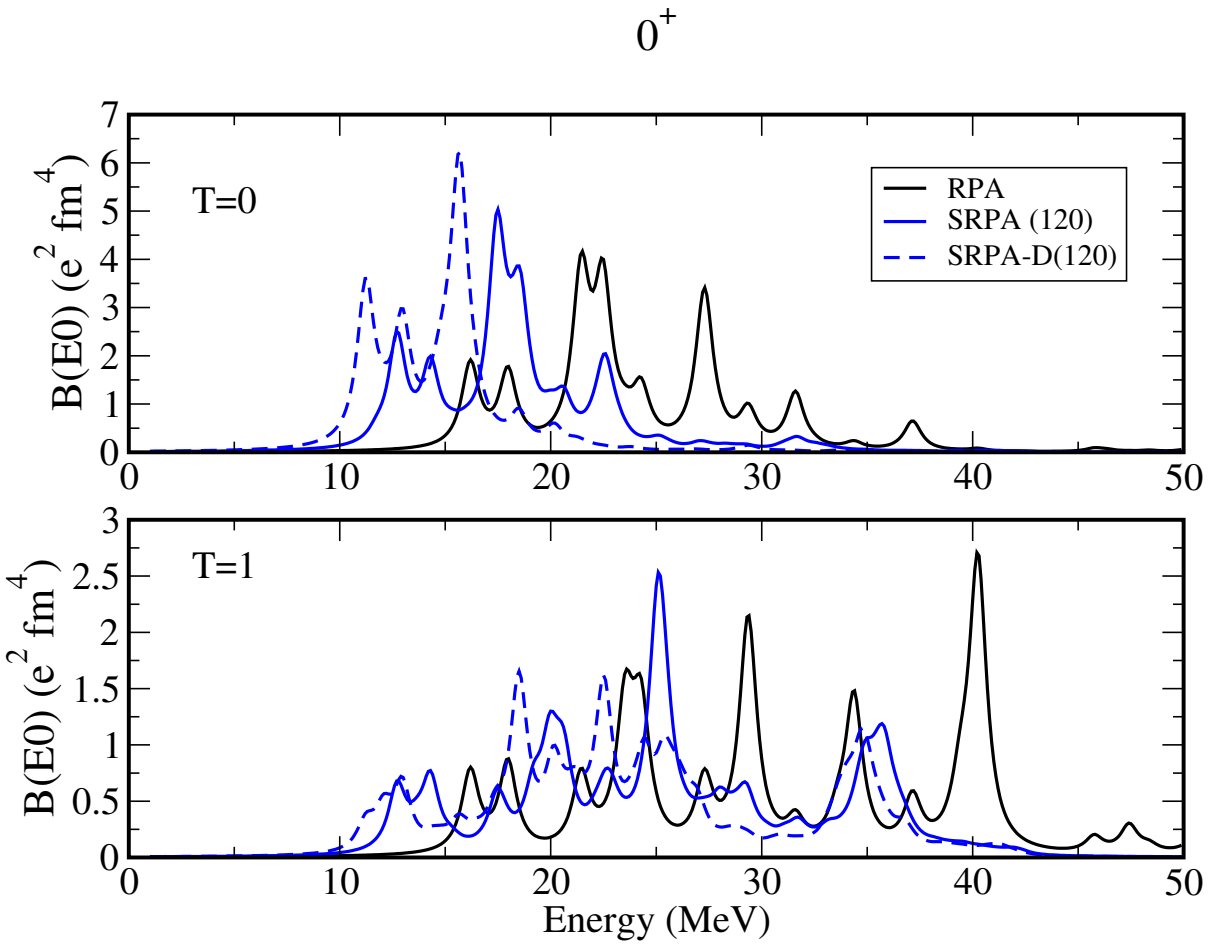

Monopole Case in ^{16}O

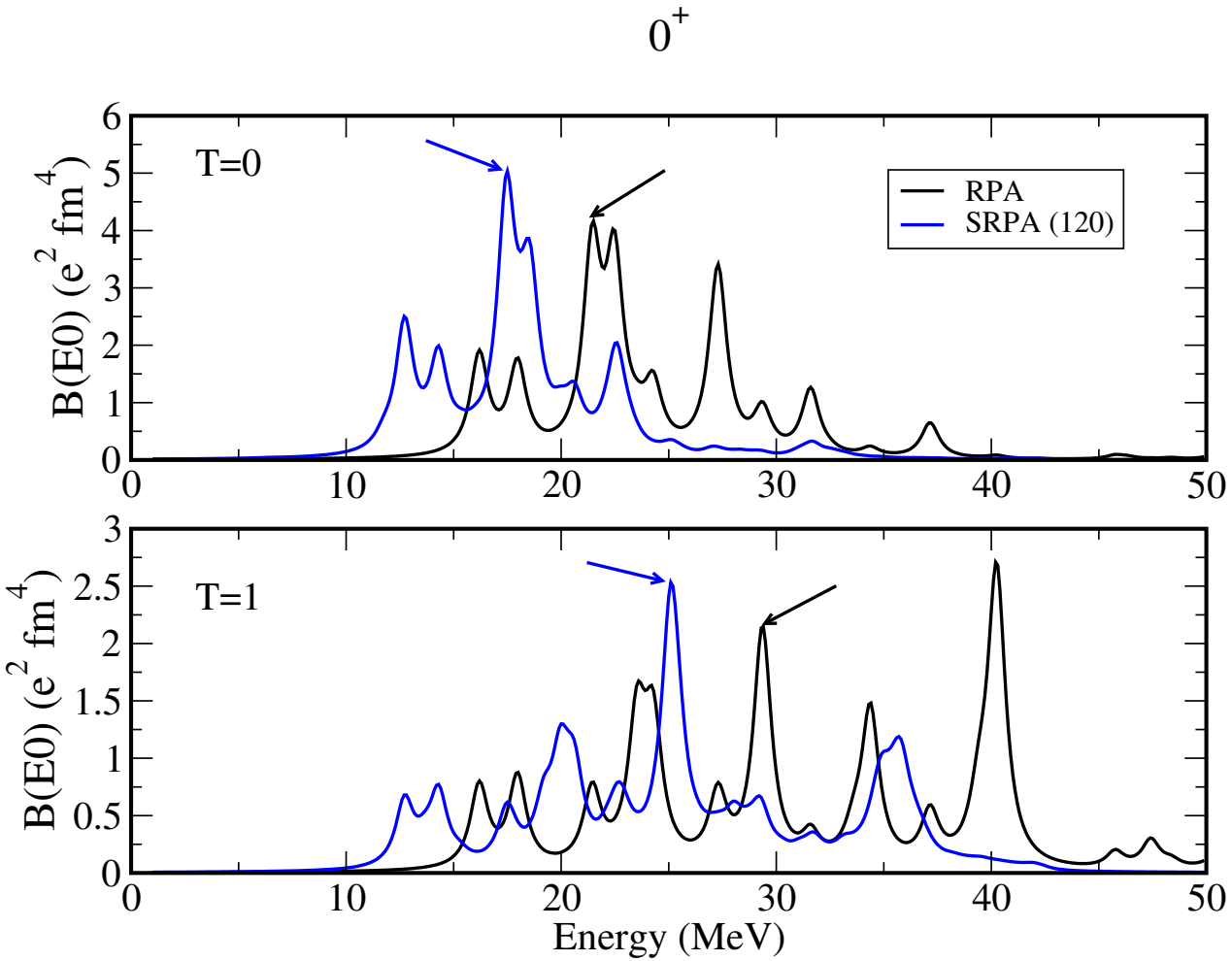

Monopole Transition Densities in ^{16}O

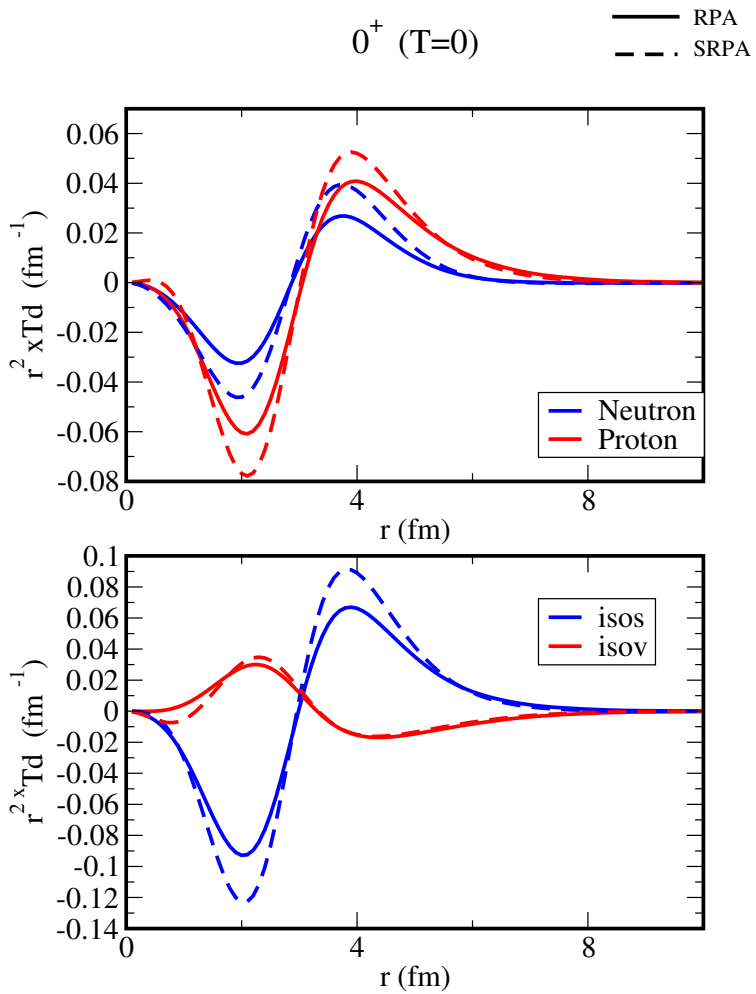

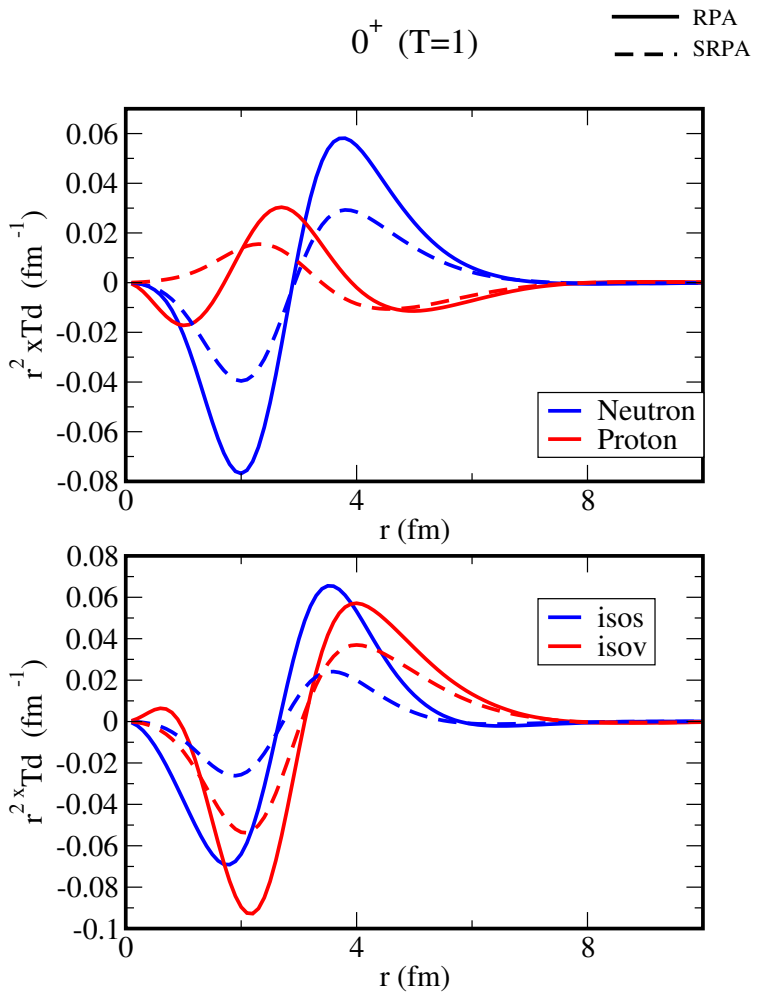

Low Lying States in ^{16}O

Monopole State

Low Lying 0^+ state (MEV)			
Exp*	RPA	SRPA	SRPA-D
$\sim$6	16.19	6.43	11.23

Quadrupole State

Low Lying 2^+ state (MEV)			
Exp	RPA	SRPA	SRPA-D
$\sim$7	16.03	7.16	12.44

Transition Probabilities

However the $B(E0)$ and $B(E2)$ data values are underestimated (factor 5)

*Nucl. Phys. A375, 1 (1982);Progress in Part. and Nucl. Phys. 61 (2008)

The Subtraction procedure

Large scale SRPA calculations have shown that:

- The SRPA strength distribution is sistematically shifted towards lower energies compared to the RPA one
- This shift is very strong ($\simeq$ 5-7 MeV), RPA description often spoiled

Origins and Causes:

1. Quasi Boson Approximation more severe in SRPA [a]
2. Use of effective interactions in beyond-mean field methods

[a] K. Takayanagi *et al.*, Nucl. Phys. A477 (1988); A. Mariano et al. PRC 49, 2824 (1994).

The Subtraction procedure (I. Tselyaev Phys. Rev. C 75, 024306 (2007))

- Designed for beyond RPA approaches
- Static ($\omega = 0$) limit of the SRPA imposed to be equal to the RPA one

PHYSICAL REVIEW C **92**, 034303 (2015)

Subtraction method in the second random-phase approximation: First applications with a Skyrme energy functional

D. Gambacurta,[1] M. Grasso,[2] and J. Engel[3]
[1]*Dipartimento di Fisica e Astronomia and INFN, Via Santa Sofia 64, I-95123 Catania, Italy*
[2]*Institut de Physique Nucléaire, IN2P3-CNRS, Université Paris-Sud, F-91406 Orsay Cedex, France*
[3]*Department of Physics and Astronomy, University of North Carolina, Chapel Hill, North Carolina 27516-3255*

PHYSICAL REVIEW LETTERS **125,** 212501 (2020)

Gamow-Teller Strength in ^{48}Ca and ^{78}Ni with the Charge-Exchange Subtracted Second Random-Phase Approximation

D. Gambacurta,[1] M. Grasso,[2] and J. Engel[3]
[1]*INFN-LNS, Laboratori Nazionali del Sud, 95123 Catania, Italy*
[2]*Université Paris-Saclay, CNRS/IN2P3, IJCLab, 91405 Orsay, France*
[3]*Department of Physics and Astronomy, CB 3255, University of North Carolina, Chapel Hill, North Carolina 27599-3255*

From SRPA to an Energy dependent RPA-like problem

- The SRPA problem as an energy-dependent RPA problem

$$A_{1,1'} \mapsto \tilde{A}_{1,1'}(\omega) = A^{RPA}_{1,1'} + \sum_{2,2'} A_{1,2}(\omega + i\eta - A_{2,2'})^{-1} A_{2',1'} = A^{RPA}_{1,1'} + A^{Cor}_{1,1'}(\omega)$$

From SRPA to an Energy dependent RPA-like problem

- The SRPA problem as an energy-dependent RPA problem

$$A_{1,1'} \mapsto \tilde{A}_{1,1'}(\omega) = A^{RPA}_{1,1'} + \sum_{2,2'} A_{1,2}(\omega + i\eta - A_{2,2'})^{-1} A_{2',1'} = A^{RPA}_{1,1'} + A^{Cor}_{1,1'}(\omega)$$

The Subtraction procedure is SRPA (SSRPA)

- Subtraction of the zero–frequency limit of the SRPA correction

$$A^{Cor}_{1,1'} \mapsto \tilde{A}^{Cor}_{1,1'}(\omega) = A_{1,1'}(\omega) - A_{1,1'}(\omega = 0) \Rightarrow$$

$$\tilde{A}_{1,1'}(\omega = 0) = A^{RPA}_{1,1'}$$

$$\Rightarrow \Pi^{SSRPA}(\omega = 0) = \Pi^{RPA}$$

From SRPA to an Energy dependent RPA-like problem

- The SRPA problem as an energy-dependent RPA problem

$$A_{1,1'} \mapsto \tilde{A}_{1,1'}(\omega) = A^{RPA}_{1,1'} + \sum_{2,2'} A_{1,2}(\omega + i\eta - A_{2,2'})^{-1} A_{2',1'} = A^{RPA}_{1,1'} + A^{Cor}_{1,1'}(\omega)$$

The Subtraction procedure is SRPA (SSRPA)

- Subtraction of the zero–frequency limit of the SRPA correction

$$A^{Cor}_{1,1'} \mapsto \tilde{A}^{Cor}_{1,1'}(\omega) = A_{1,1'}(\omega) - A_{1,1'}(\omega = 0) \Rightarrow$$

$$\tilde{A}_{1,1'}(\omega = 0) = A^{RPA}_{1,1'}$$

$$\Rightarrow \Pi^{SSRPA}(\omega = 0) = \Pi^{RPA}$$

$$\Pi^{RPA} \propto m_{-1}$$

The Subtraction procedure

First applications (Skyrme interaction):

- 0^+ and 2^+ response in ^{16}O
- $2p2h$ energy cutoff < 70 (50) MeV for 0^+ (2^+)
- In this way full inversion is possible $\Rightarrow$SSRPA$_F$
- We can thus check the inversion in the diagonal approximation $\Rightarrow$ SSRPA$_D$
- D. Gambacurta, M. Grasso and J. Engel Phys. Rev. C 92, 034303 (2015)

Quadrupole Strength Distribution in ^{16}O: RPA, SRPA and SSRPA

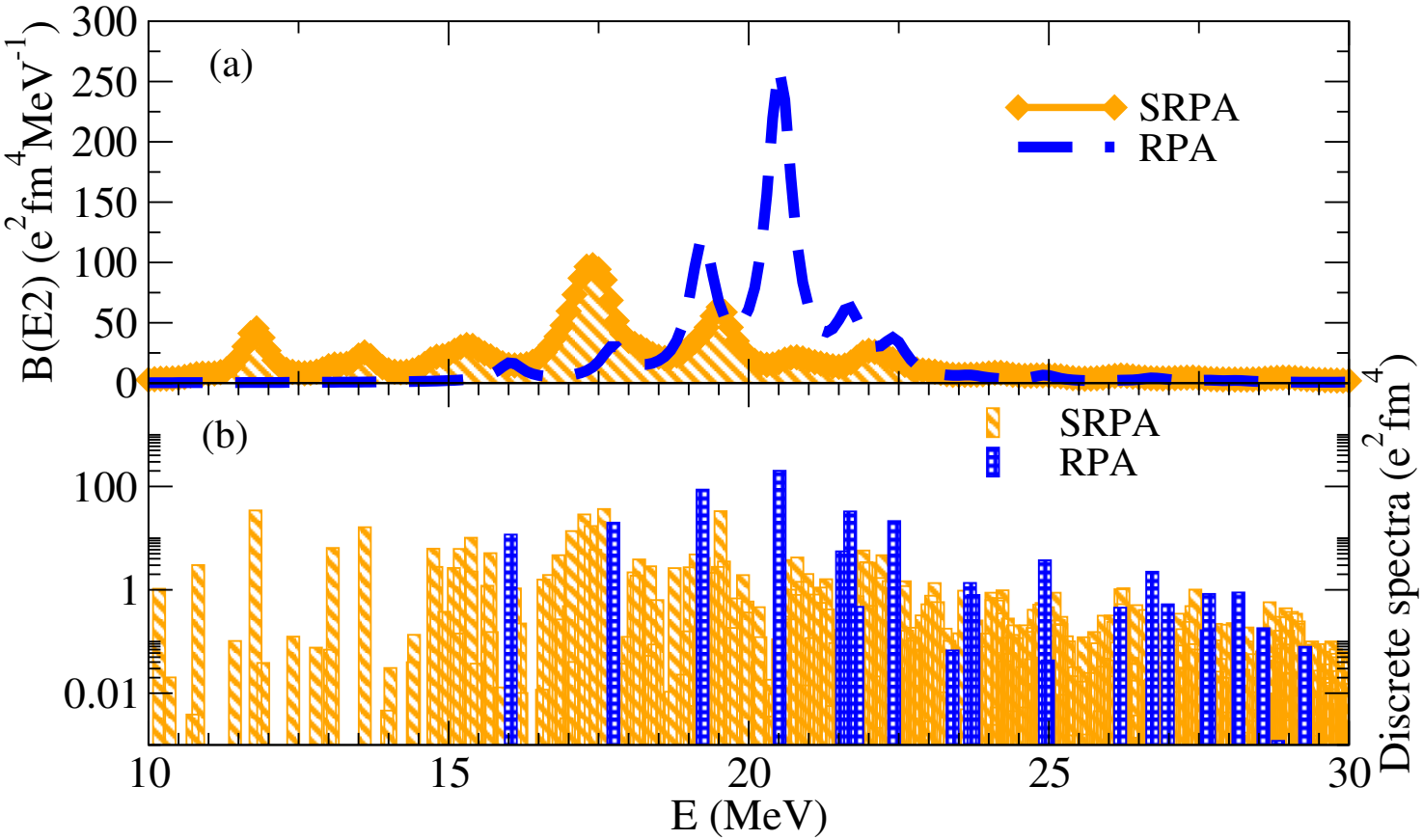

D. G., M. Grasso and J.Engel, Phys. Rev. C 92 , 034303 (2015)

Quadrupole Strength Distribution in ^{16}O: RPA, SRPA and SSRPA

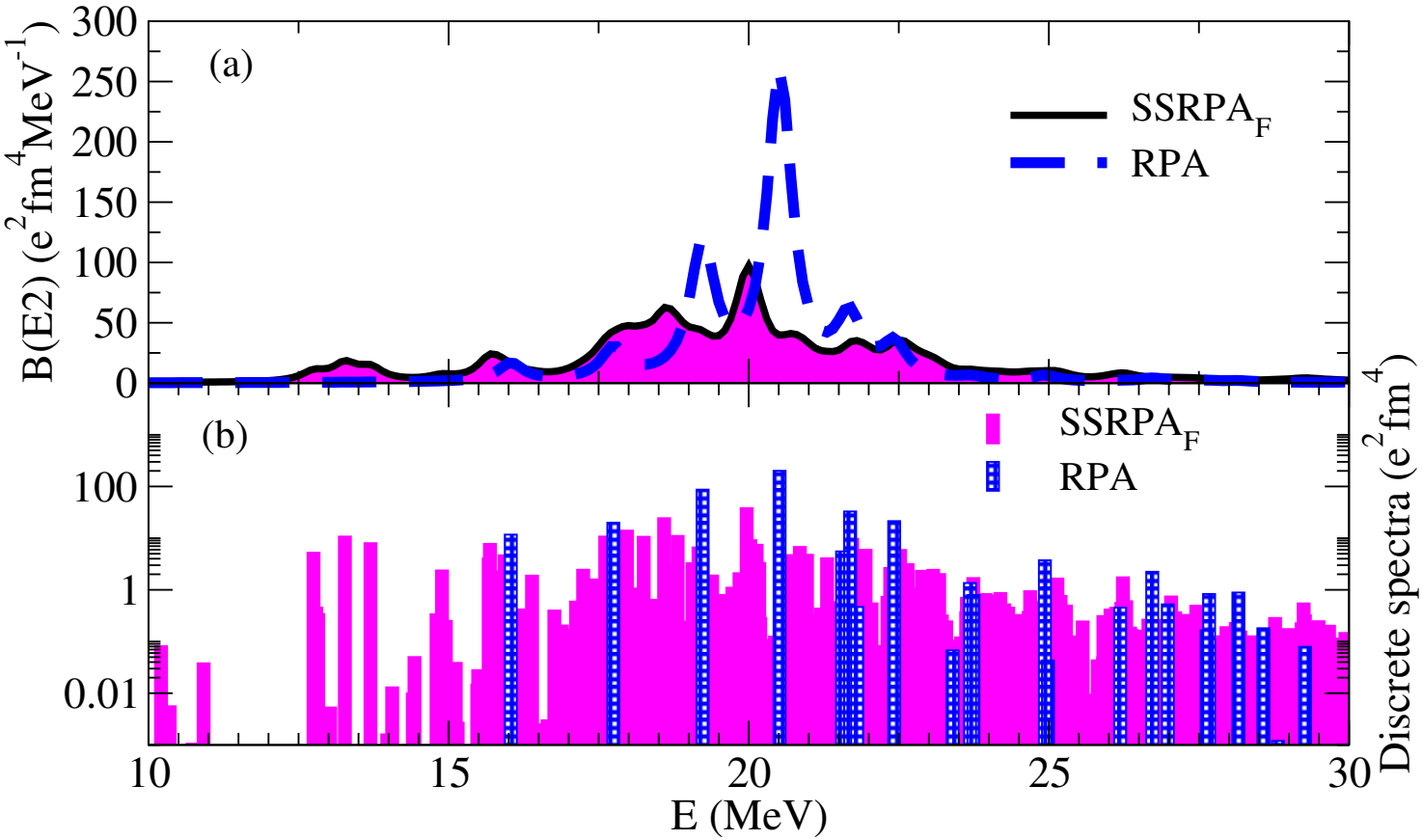

D. G., M. Grasso and J.Engel, Phys. Rev. C 92 , 034303 (2015)

Quadrupole Strength Distribution: $SSRPA_F$ vs $SSRPA_D$

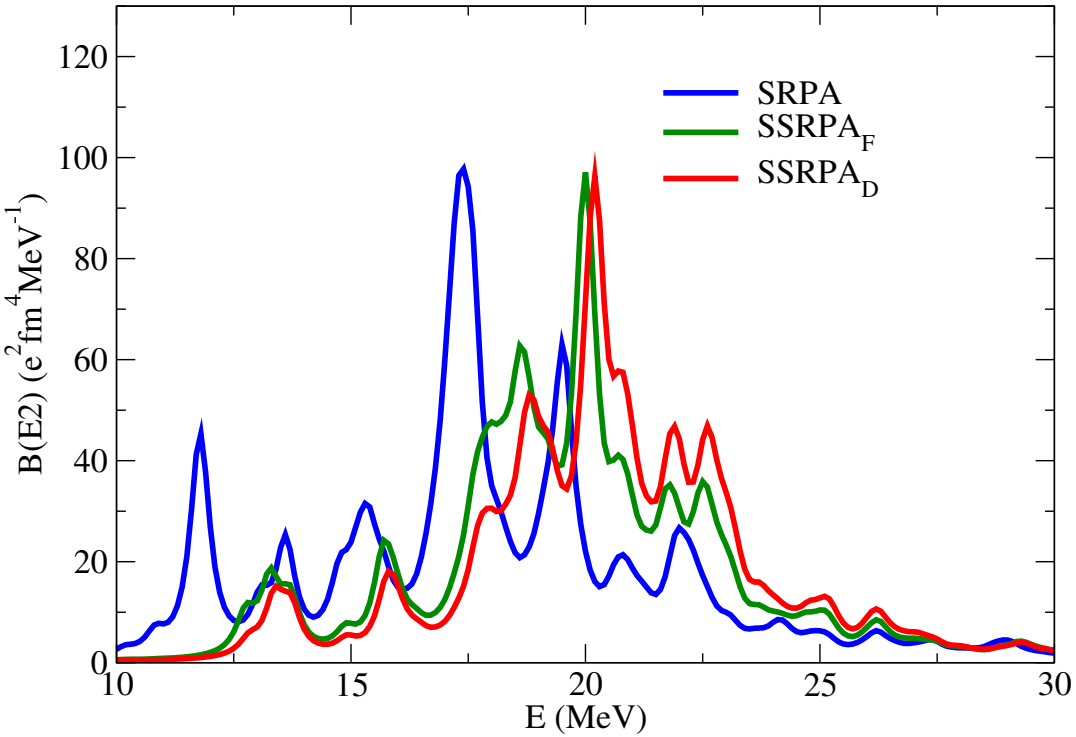

Monopole Strength Distribution: cutoff dependence

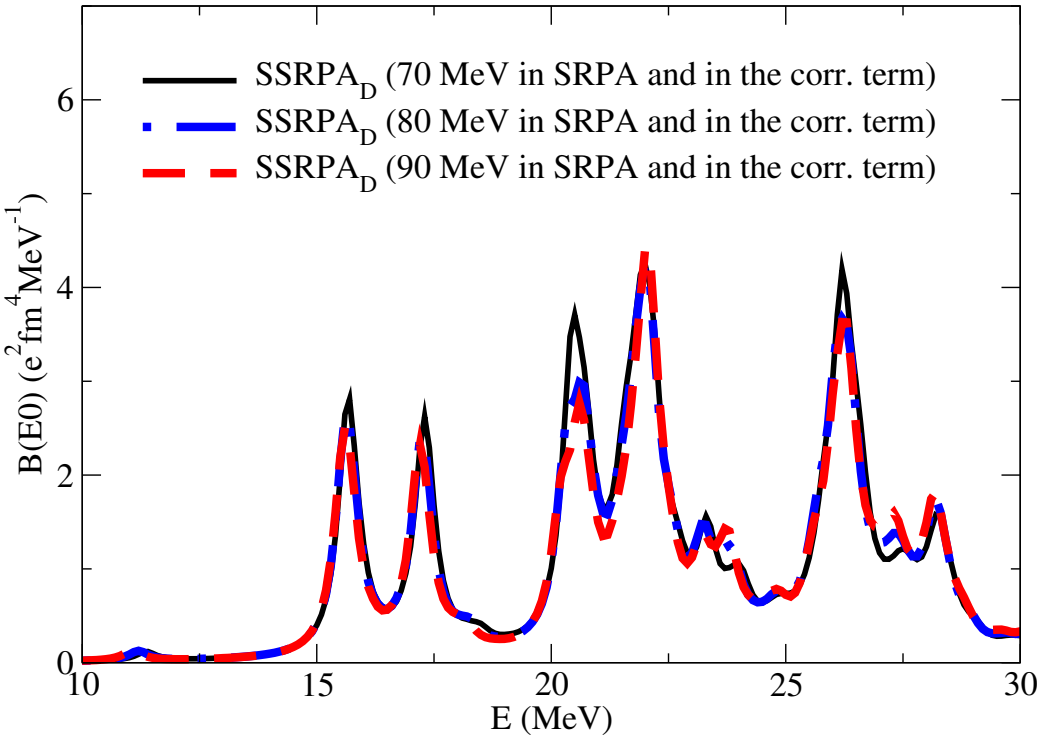

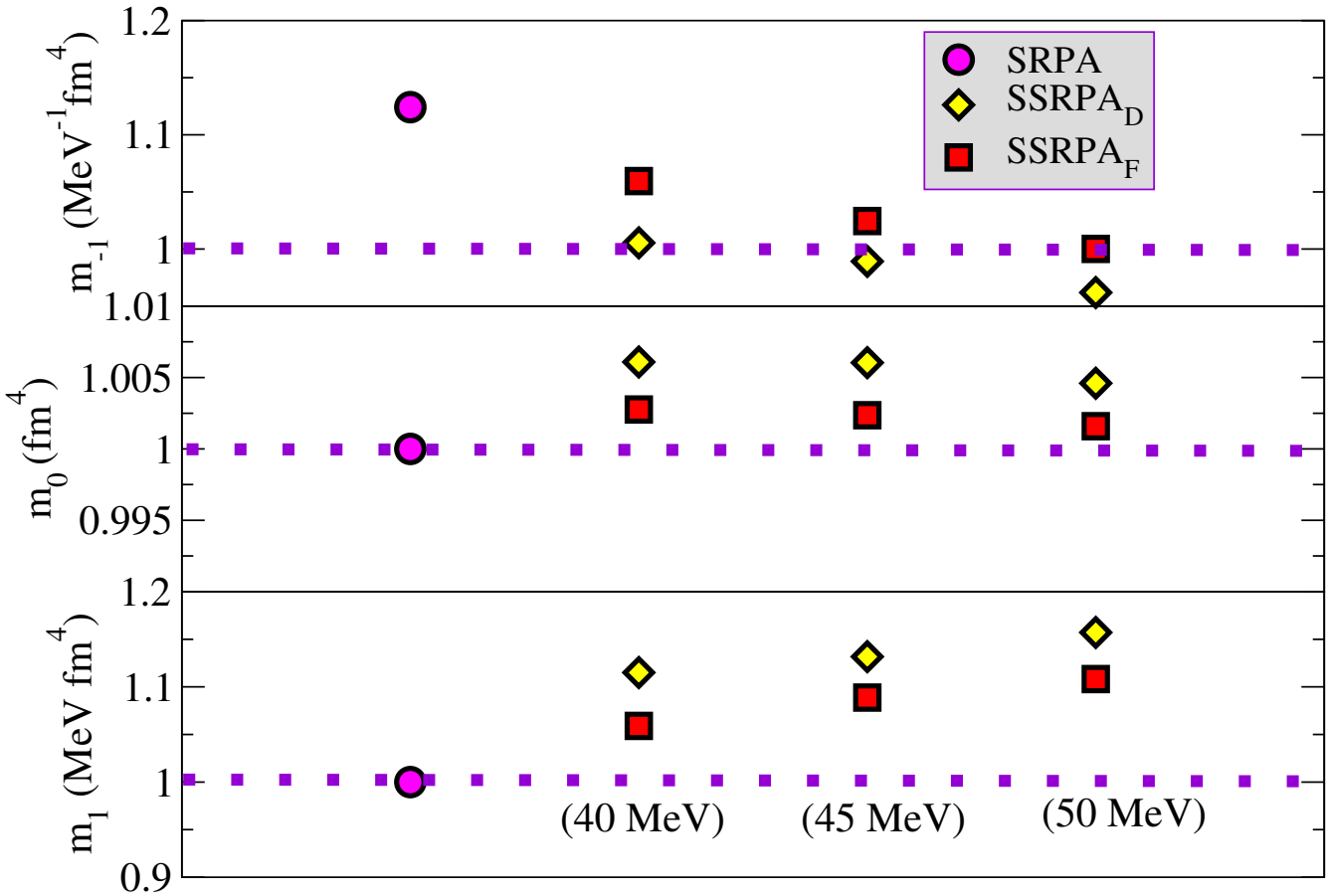

Ratios of the moments m_{-1}, m_0, and m_1 of the quadrupole strength distribution in the SRPA (purple circles), the SSRPA$_F$ (red squares), and the SSRPA$_D$ (yellow diamonds) to those in the RPA for increasingly high cutoffs in the correction terms, at 40, 45, and 50 MeV.

Some SSRPA applications

- Dipole response in ^{48}Ca
- Soft monopole modes in neutron-rich nuclei
- Isoscalar quadrupole giant resonance
- Gamow-Teller excitations and beta-decay

Low-lying dipole response in ^{48}Ca: Motivation

- Experimental low-lying dipole (from 5 to 10 MeV) response in ^{48}Ca stronger than in ^{40}Ca
- Pygmy Dipole Resonance (PDR) type?
- Not described in relativistic and non-relativistic RPA models
- What happens in SRPA [a] ?
- and in the SSRPA [b] ?

[a] D. G. , M. Grasso, and F. Catara, Phys. Rev. C 84, 034301 (2011)
[b] D. G., M. Grasso and O. Vasseur, Physics Letters B 777 (2018) 163–168

Experimental low-lying dipole strength in ^{40},^{48}Ca. (Photon Scattering)

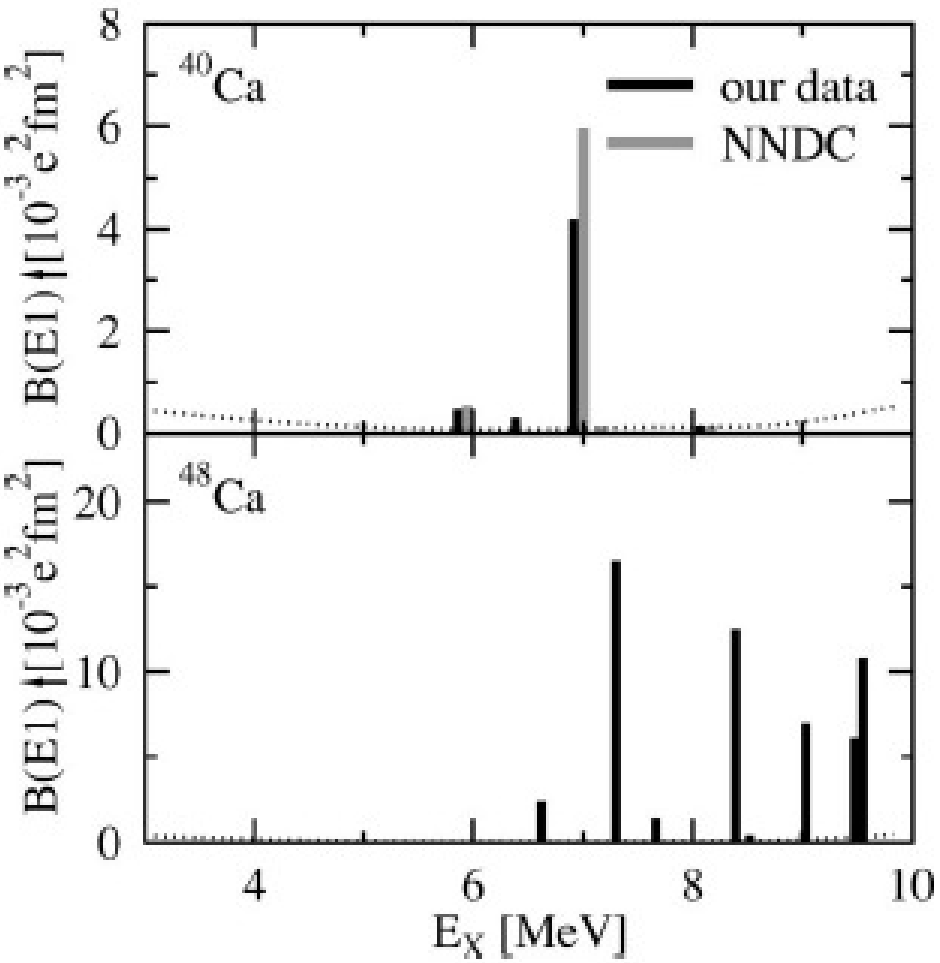

From T. Hartmann *et al.*, PRC 65, 034301, (2002)

$\sum$ B(E1)=5.1 $\pm$ 0.8 ($10^{-3}e^2fm^2$),

$\sum$ B(E1)=68.7 $\pm$ 7.5 ($10^{-3}e^2fm^2$),

Relativistic RPA results

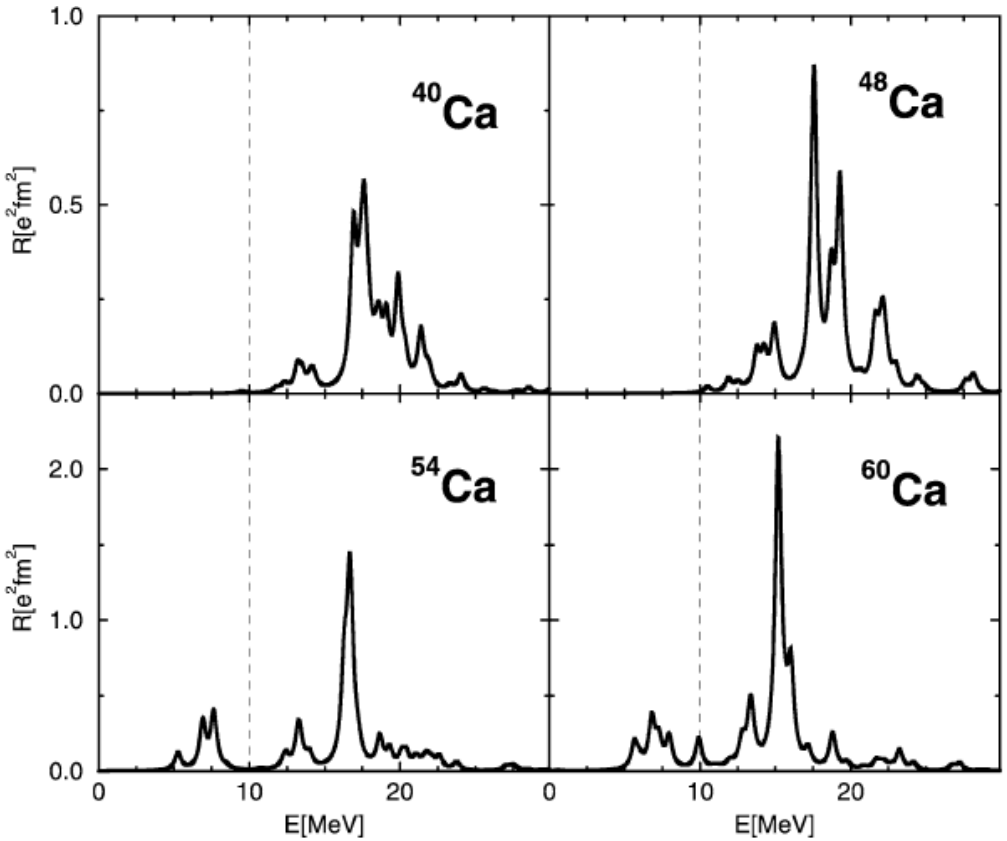

Fig. 5. RRPA isovector dipole strength distributions in Ca isotopes. The thin dashed line tentatively separates the region of giant resonances from the low-energy region below 10 MeV.

From D. Vretenar *et al.*, Nucl. Phys. A 692, 496 (2001)

RPA and SRPA Dipole Strength

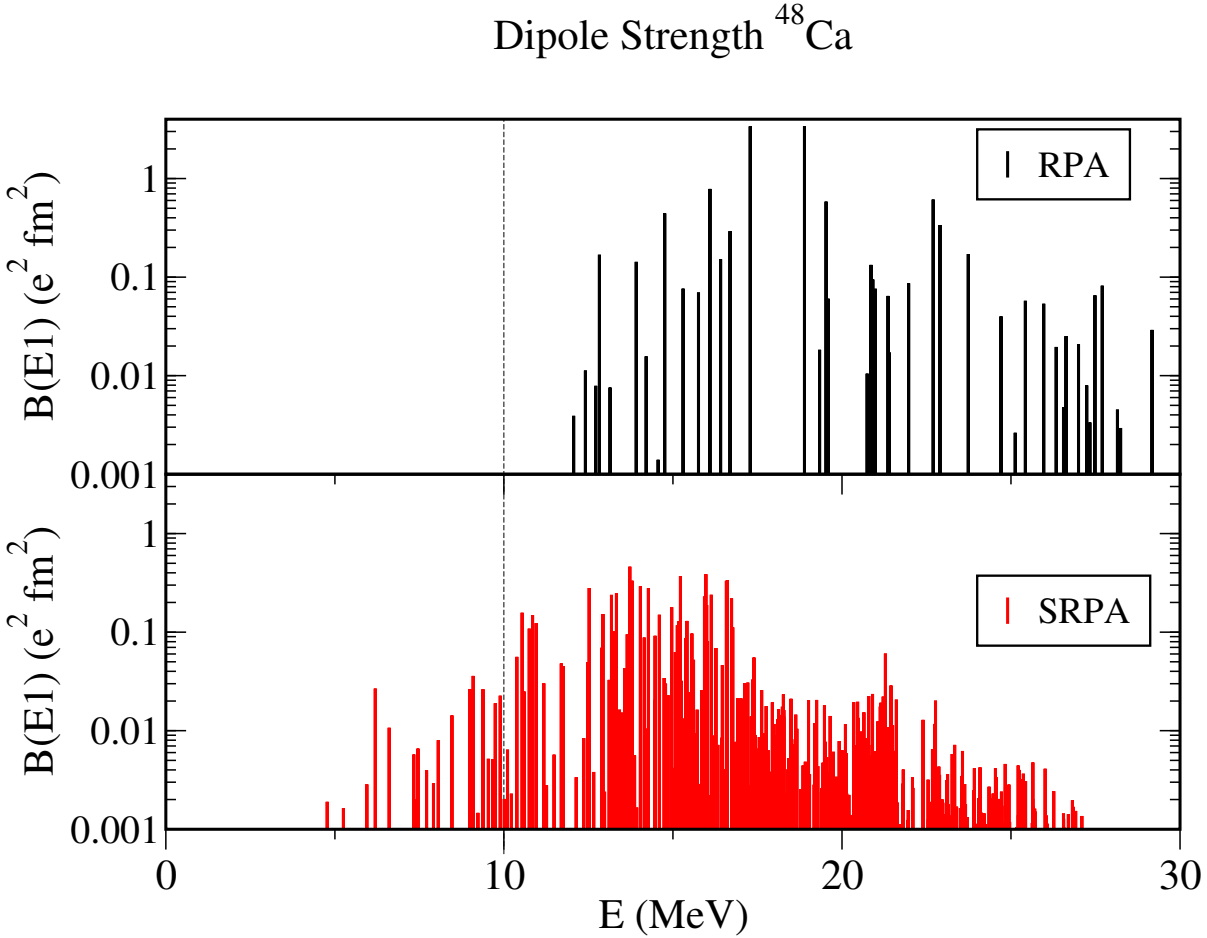

RPA and SRPA Dipole Strength

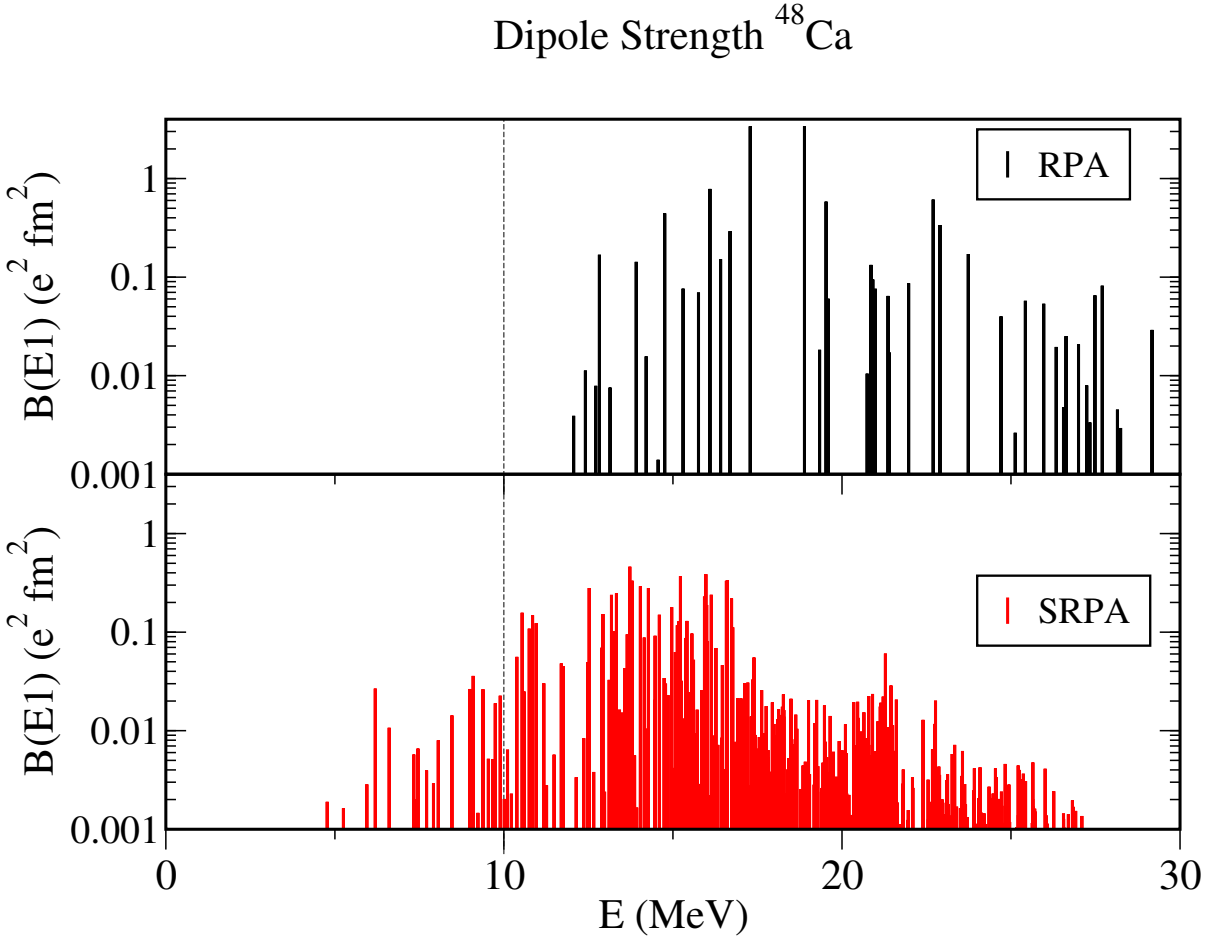

SRPA provides the strength below 10 MeV, but total strength is overestimated.

1p1h and 2p2h contents

$$\langle \nu|\nu\rangle = \sum_{ph}(\mid X^{\nu}_{ph} \mid^2 - \mid Y^{\nu}_{ph} \mid^2) + \sum_{p_1<p_2,h_1<h_2} (\mid X^{\nu}_{p_1h_1p_2h_2} \mid^2 - \mid Y^{\nu}_{p_1h_1p_2h_2} \mid^2)$$

$$= \quad N_1 \quad + \quad N_2 \quad = 1$$

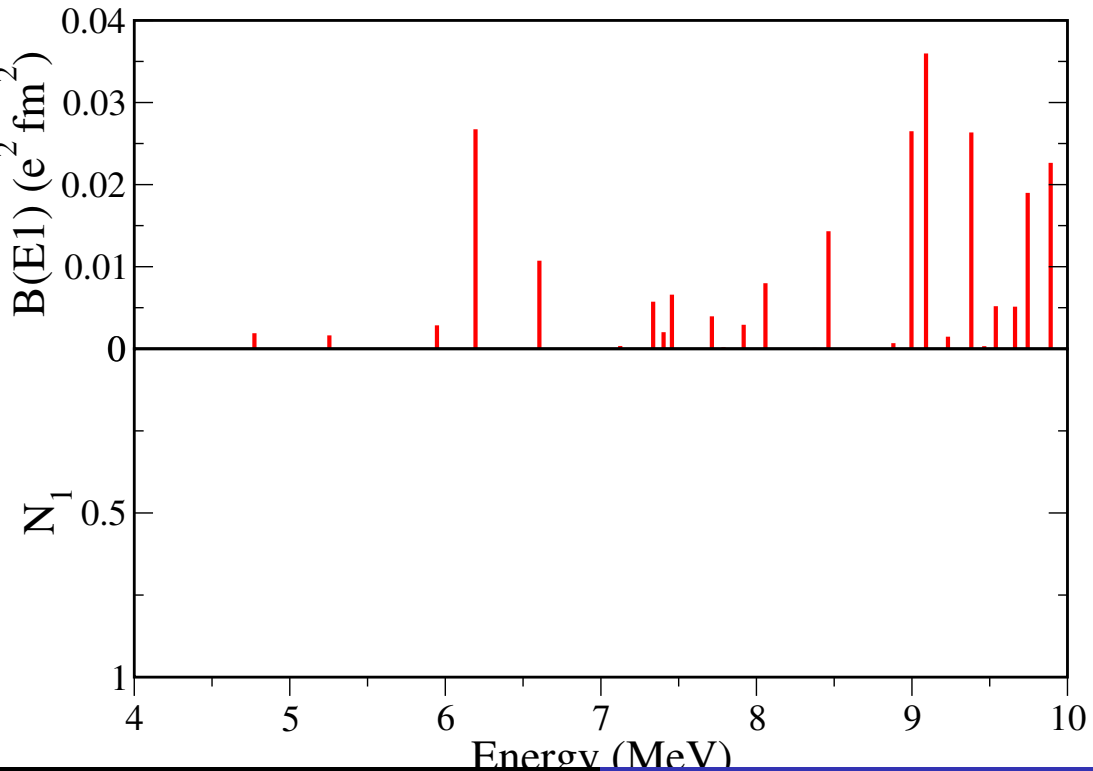

1p1h and 2p2h contents

$$\langle \nu|\nu\rangle = \sum_{ph}(\mid X^{\nu}_{ph} \mid^2 - \mid Y^{\nu}_{ph} \mid^2) + \sum_{p_1<p_2,h_1<h_2} (\mid X^{\nu}_{p_1h_1p_2h_2} \mid^2 - \mid Y^{\nu}_{p_1h_1p_2h_2} \mid^2)$$

$$= \quad N_1 \quad + \quad N_2 \quad = 1$$

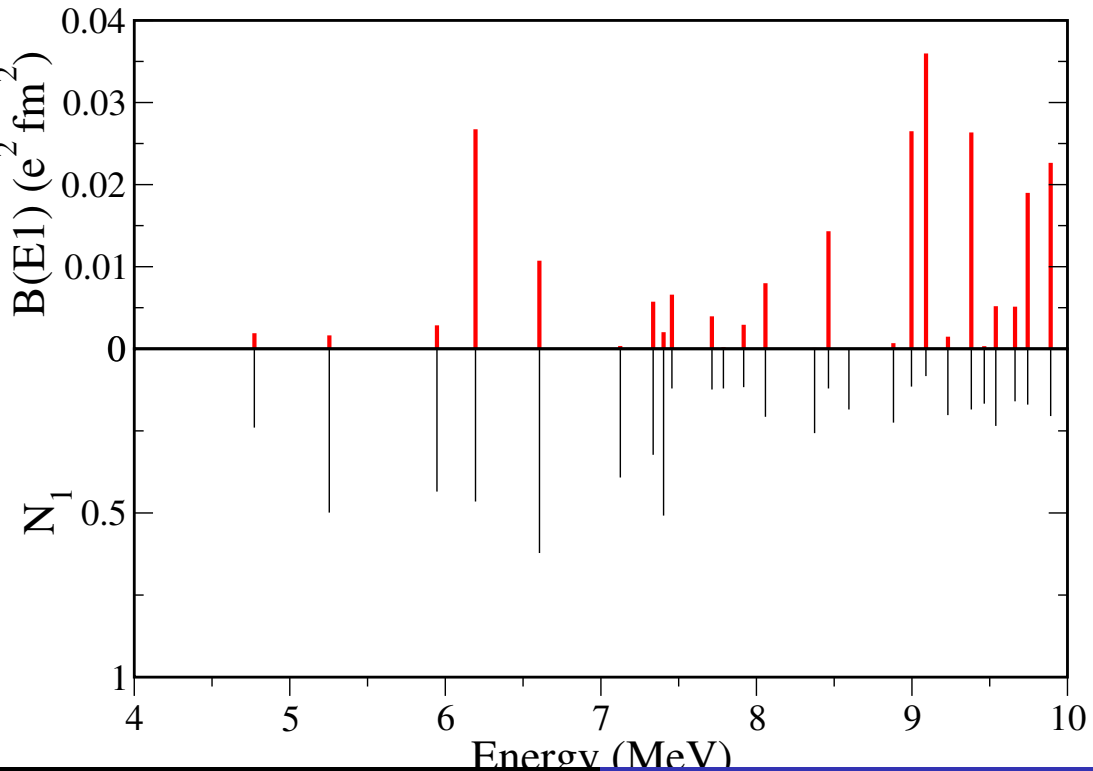

Coherence of the elementary $1p1h$ configurations in building the B(E1)

$$B^{\nu}(E\lambda) = |\sum_{ph}(X^{\nu}_{ph} - Y^{\nu}_{ph})F^{\lambda}_{ph}|^2 = |\sum_{ph} b^{\nu}_{ph}(E\lambda)|^2$$

where F^{λ}_{ph} are the dipole transition amplitudes of the operator

$$F = e\frac{N}{A}\sum_{i=1}^{Z} r_i Y_{10}(\Omega_i) - e\frac{Z}{A}\sum_{i=1}^{N} r_i Y_{10}(\Omega_i)$$

The IVGDR case

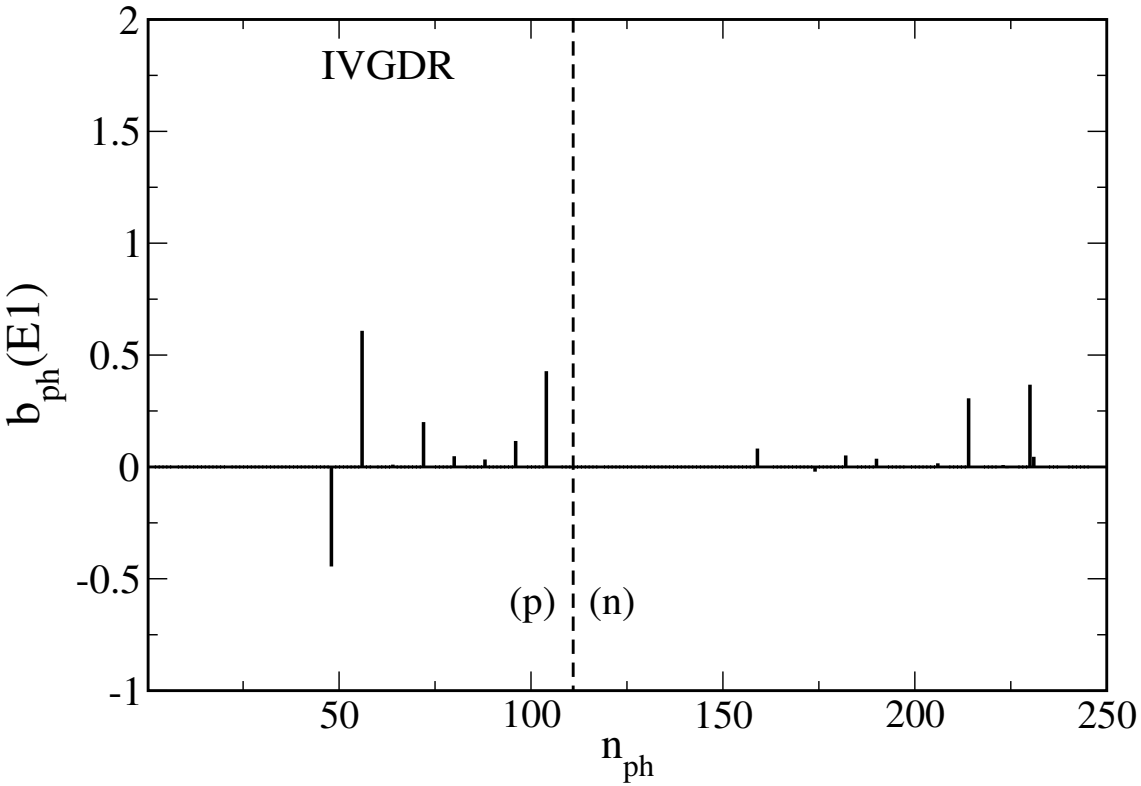

Bars are the single b_{ph}, the continuous line is the cumulative sum of the b_{ph}

The IVGDR case

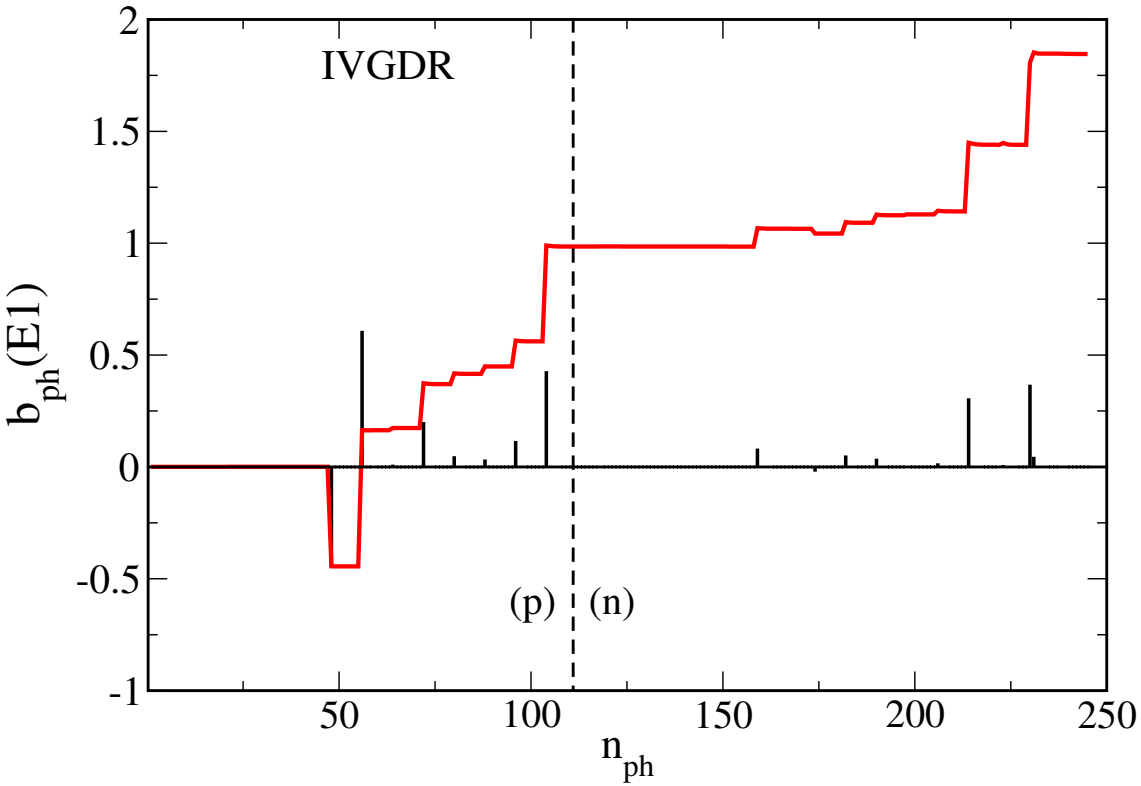

Bars are the single b_{ph}, the continuous line is the cumulative sum of the b_{ph}

Collectivity: coherence of the elementary contributions

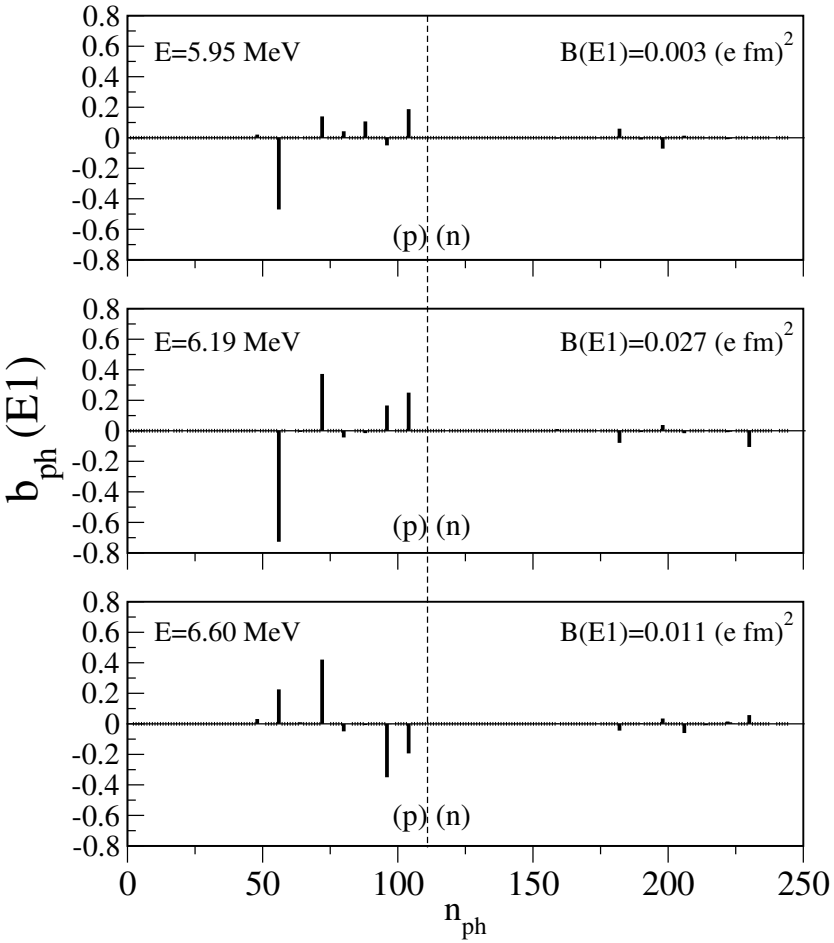

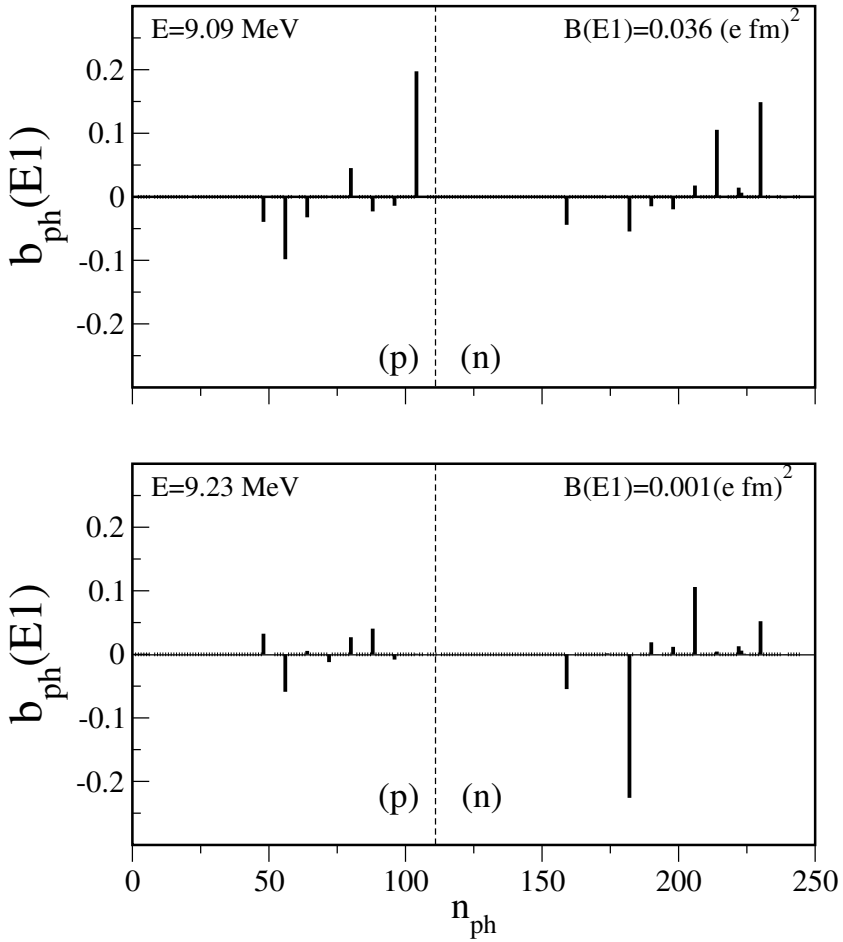

Collectivity: coherence of the elementary contributions

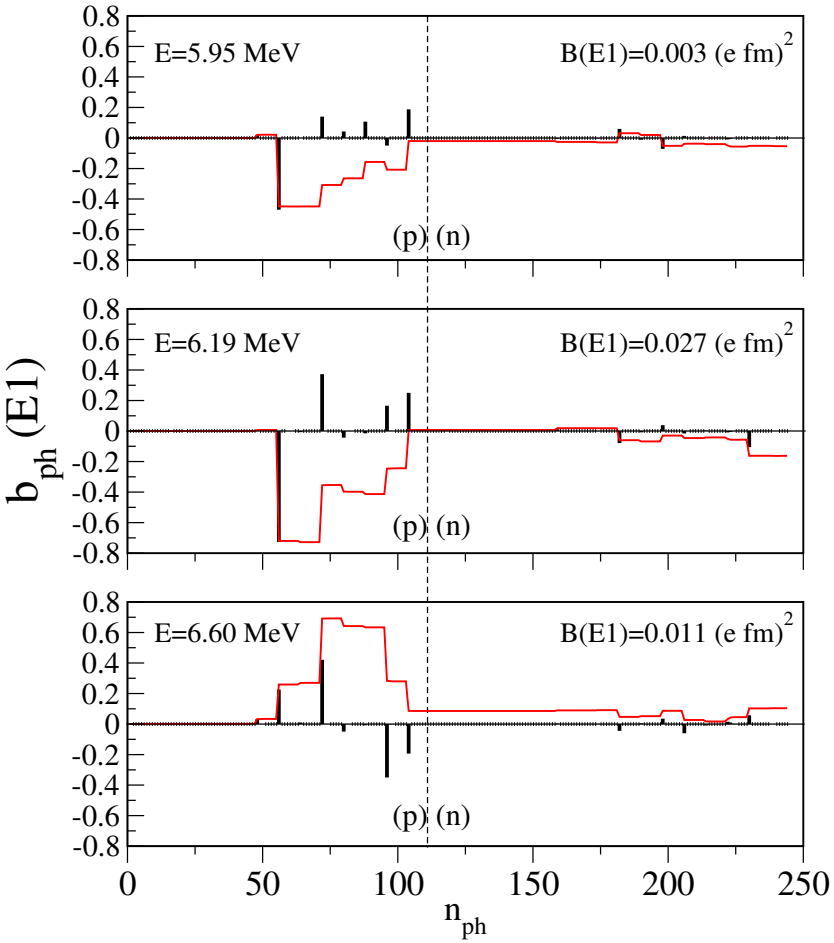

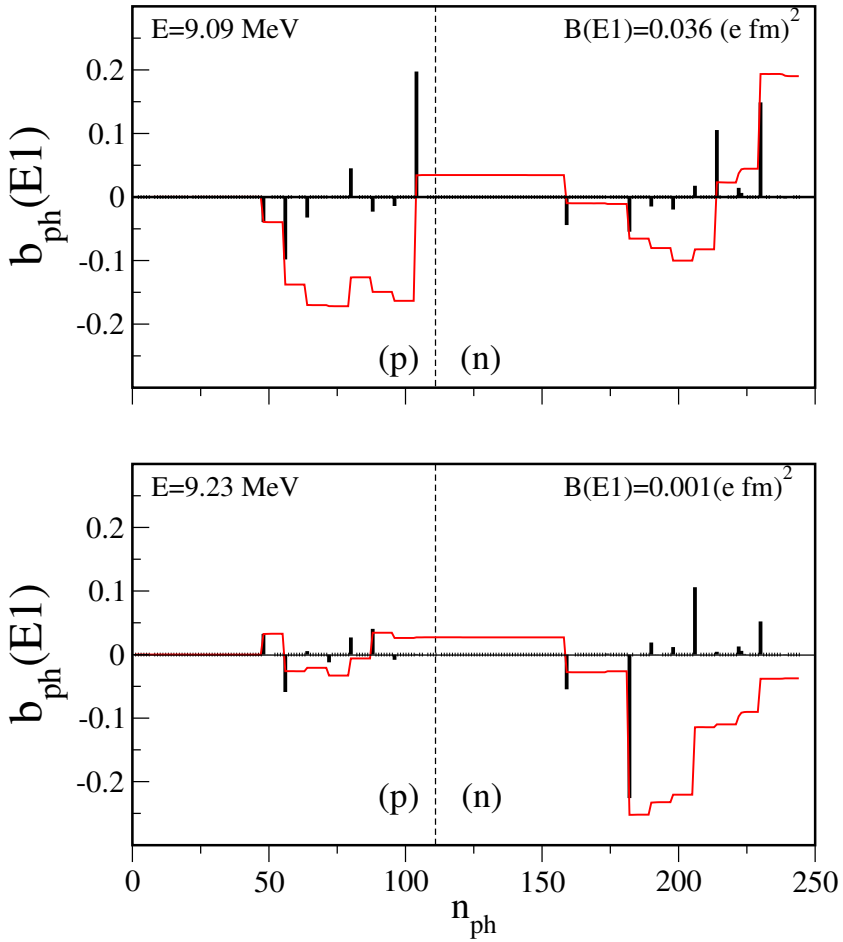

Collectivity: coherence of the elementary contributions

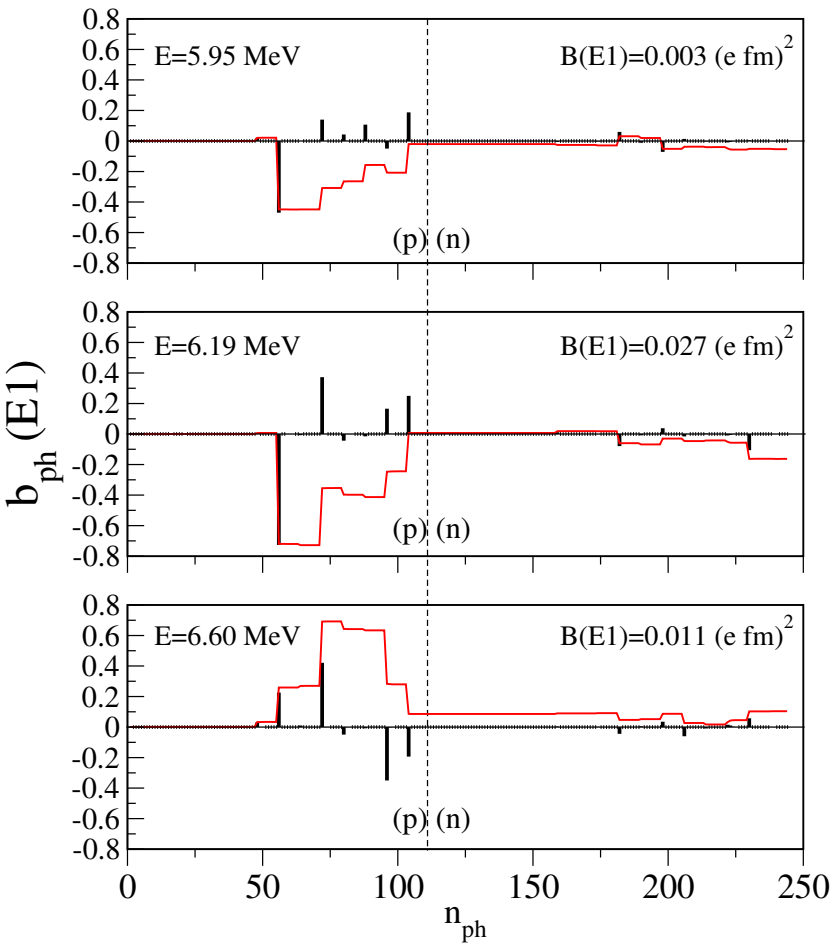

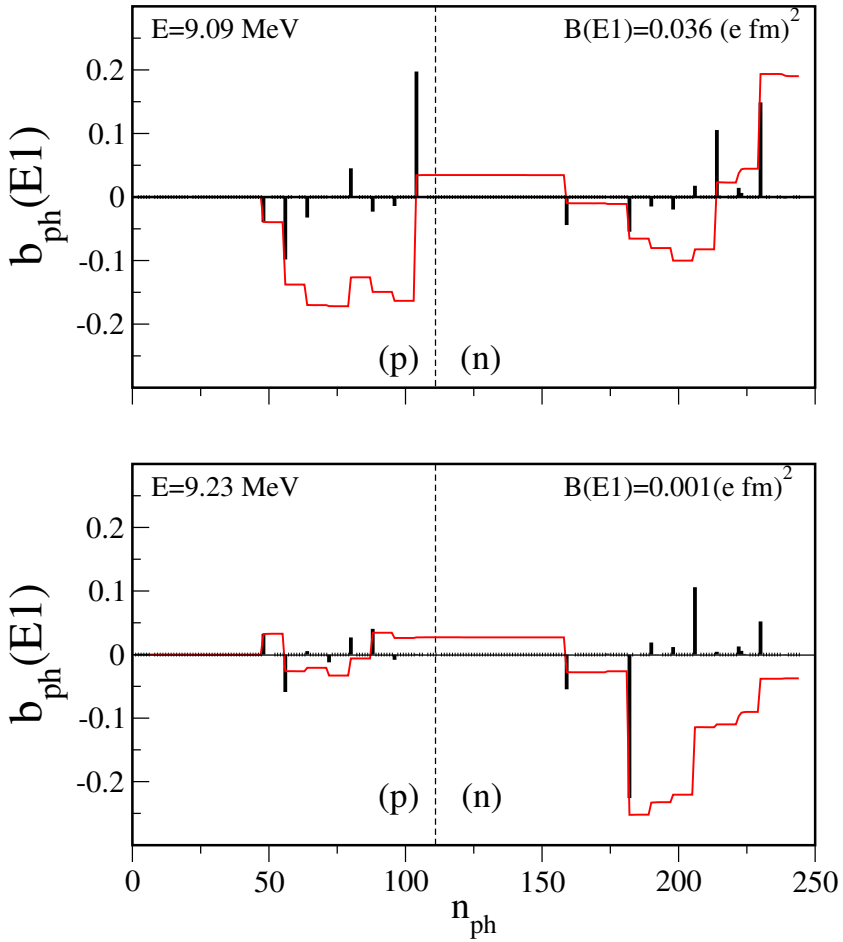

Several 1p-1h configurations participate but not coherently

SRPA, SSRPA vs Data

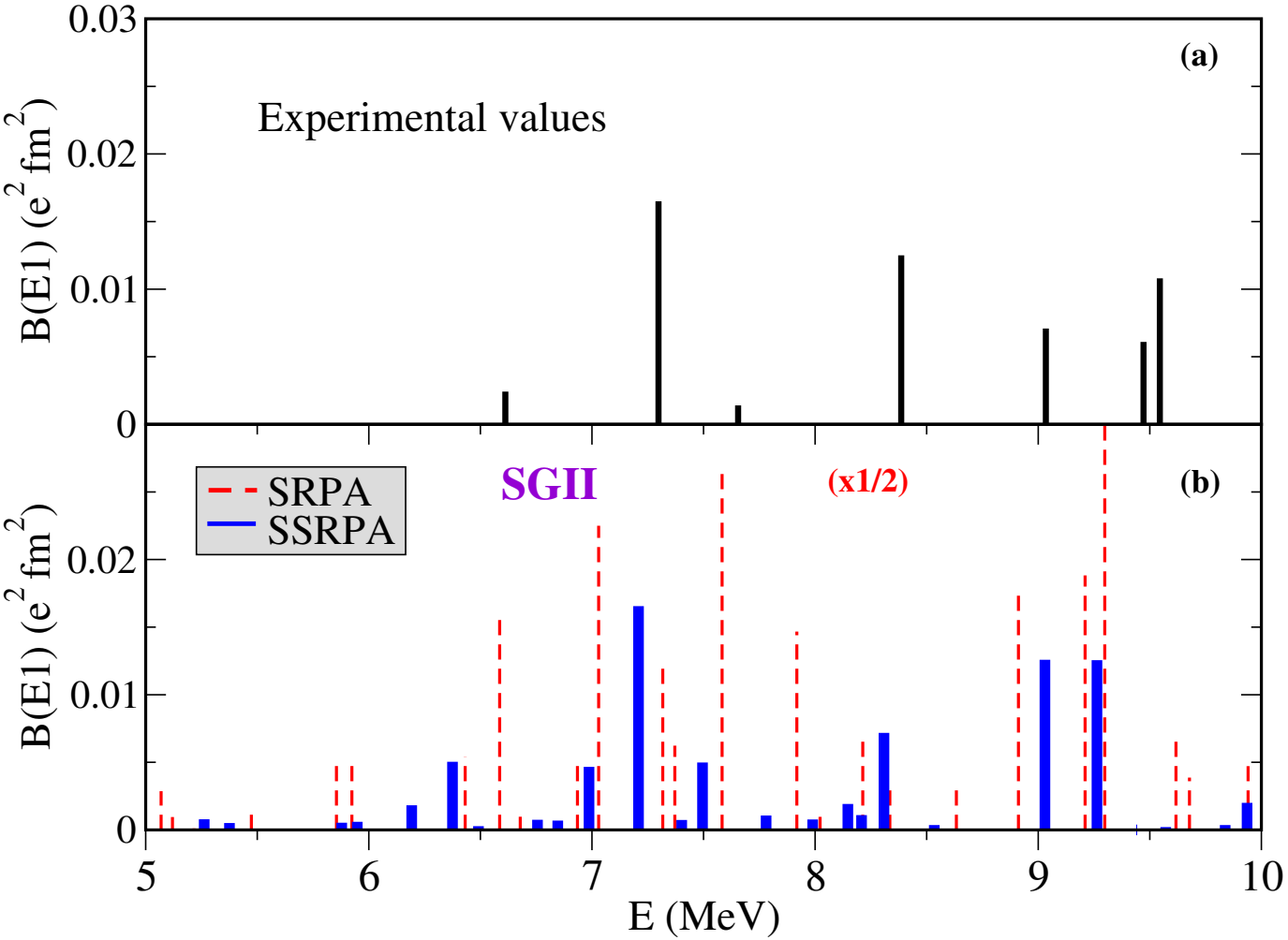

D. Gambacurta , M. Grasso , O. Vasseur, Physics Letters B 777 (2018) 163–168

Total $B(E1)$ and EWSRs (From 5 to 10 MeV)

	Exp	SRPA SGII	SSRPA SGII	SRPA SLy4	SSRPA SLy4
$\sum B(E1)$	0.068 $\pm$ 0.008	0.563	0.078	1.012	0.126
$\sum_i E_i B_i(E1)$	0.570 $\pm$ 0.062	4.618	0.621	8.795	1.062

Experimental and theoretical $\sum B(E1)$ in (e^2 fm^2) and $\sum_i E_i B_i(E1)$ in (MeV e^2 fm^2) summed between 5 and 10 MeV.
From D. G., M. Grasso , O. Vasseur, Physics Letters B 777 (2018) 163–168

Total $B(E1)$ and EWSRs (From 5 to 10 MeV)

	Exp	SRPA SGII	SSRPA SGII	SRPA SLy4	SSRPA SLy4
$\sum B(E1)$	0.068 $\pm$ 0.008	0.563	**0.078**	1.012	**0.126**
$\sum_i E_i B_i(E1)$	0.570 $\pm$ 0.062	4.618	**0.621**	8.795	**1.062**

Experimental and theoretical $\sum B(E1)$ in (e^2 fm^2) and $\sum_i E_i B_i(E1)$ in (MeV e^2 fm^2) summed between 5 and 10 MeV.
From D. G., M. Grasso , O. Vasseur, Physics Letters B 777 (2018) 163–168

SSRPA vs Data, GDR case

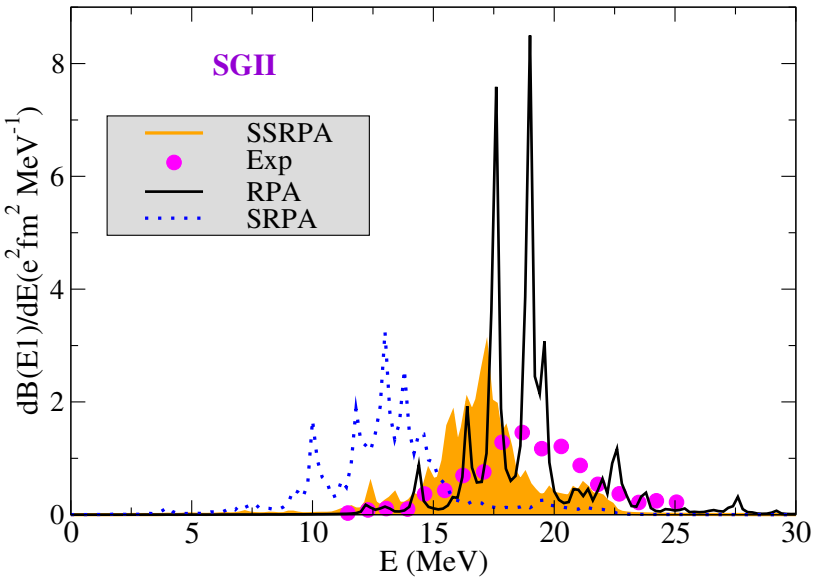

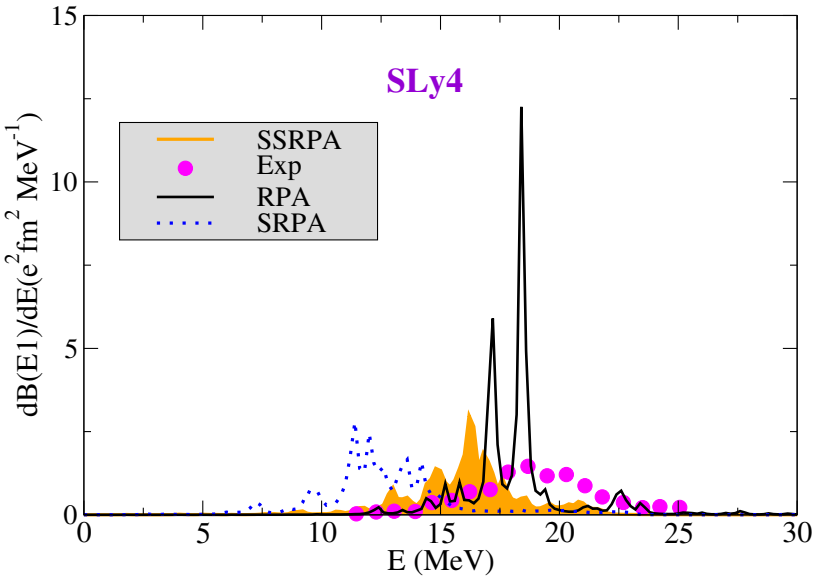

Data From J. Birkhan *et al.*, Phys. Rev. Lett. 118, 252501 (2017);
Theoretical results folded with a Lorentzian having a width of 0.25 MeV
D. G., M. Grasso , O. Vasseur, Physics Letters B 777 (2018) 163–168

SSRPA vs Data, GDR case

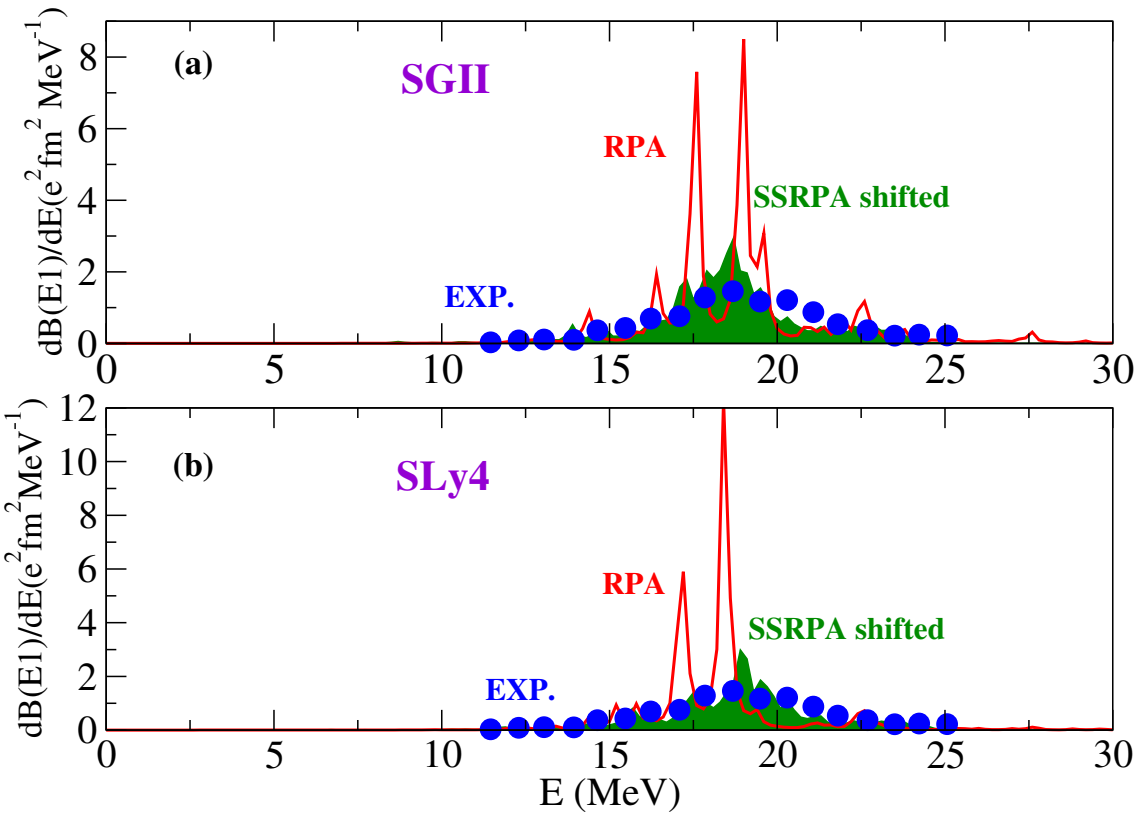

Shift $\sim$ 1 MeV (SGII), $\sim$ 1.5 MeV (SLy4);

SSRPA vs Data, GDR case

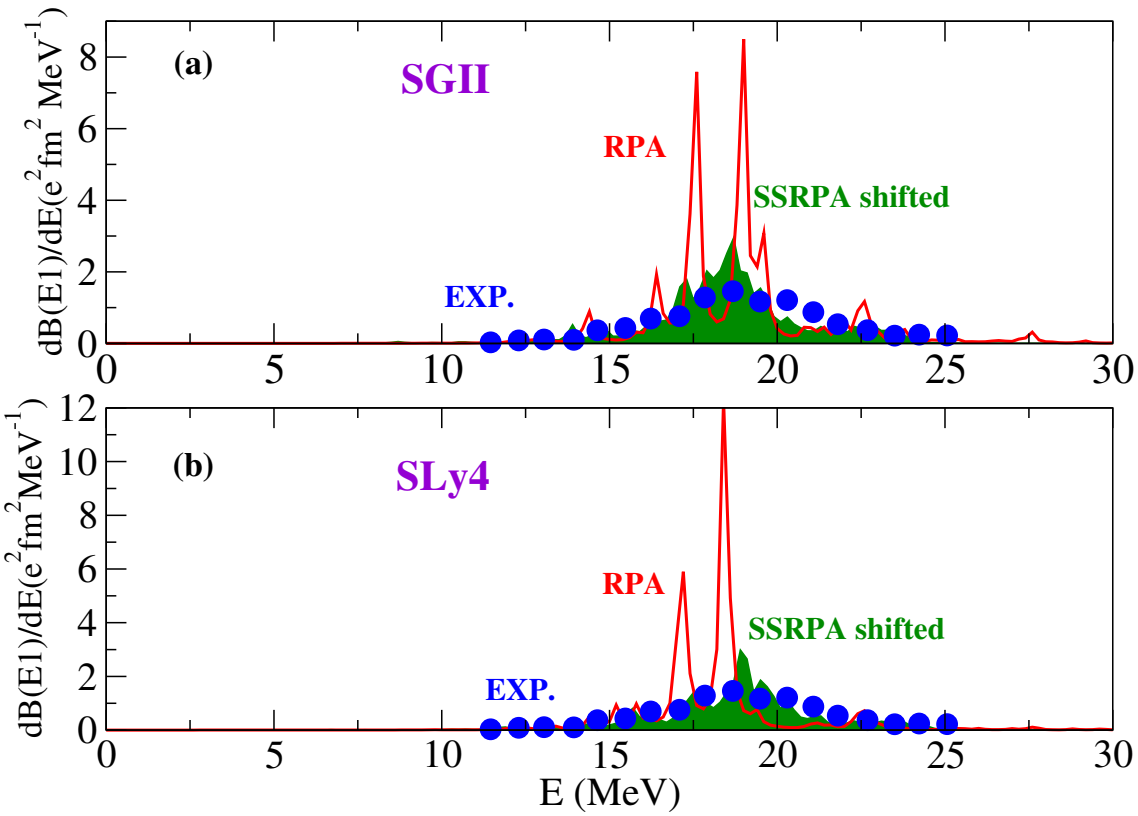

Shift $\sim$ 1 MeV (SGII), $\sim$ 1.5 MeV (SLy4);
Room to improve on that (overcoming the diagonal approximation in subtraction)

Monopole response in RPA and SSRPA

- Evolution of the response in Ca isotopes from ^{40}Ca to ^{60}Ca [a]
- $N = 20$ isotones : ^{40}Ca, ^{36}S and ^{34}Si
- The case of ^{68}Ni

[a] Phys. Rev. Lett. 121, (2018) @ RIKEN

The key-points of our study

- Similarities and differences with respect PDR
- Microscopic properties
- Properties as a function of the isospin asymmetry
- More details: DG, M. Grasso and O. Sorlin, PRC 100, 014317 (2019)

Monopole strength distribution in Ca isotopes

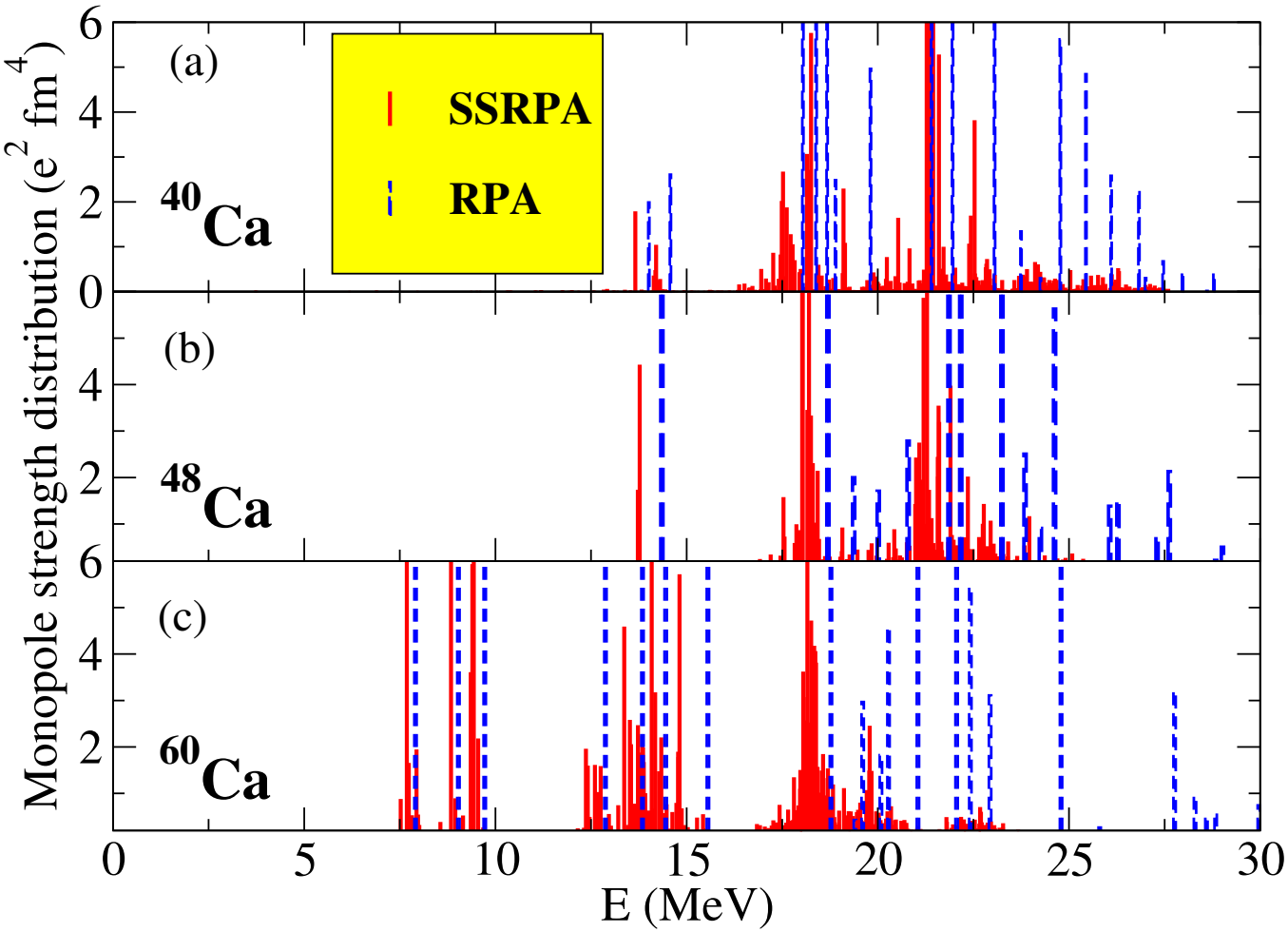

(a) Monopole strength distribution computed with RPA (dashed blue bars) and SSRPA (full red bars) for ^{40}Ca; (b) Same as in (a) but for ^{48}Ca; (c) Same as in (a) but for ^{60}Ca.

Comparison with data from Y.-W. Lui, et al., PRC 83, 044327 (2011)

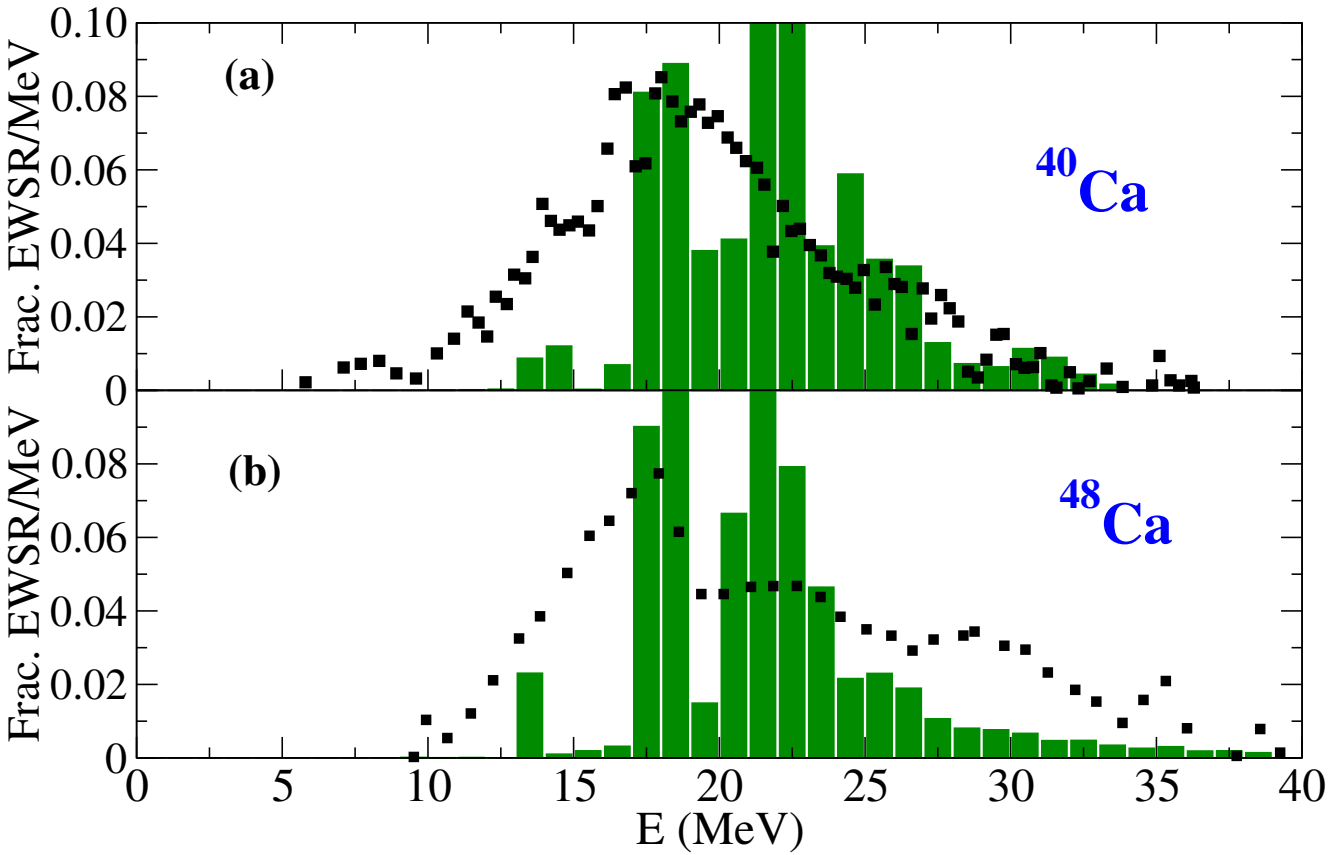

(a) Black squares: experimental results ; green bars: SSRPA predictions for ^{40}Ca; (b) Same as in (a) but for ^{48}Ca.

Comparison with data from Y.-W. Lui, et al., PRC 83, 044327 (2011)

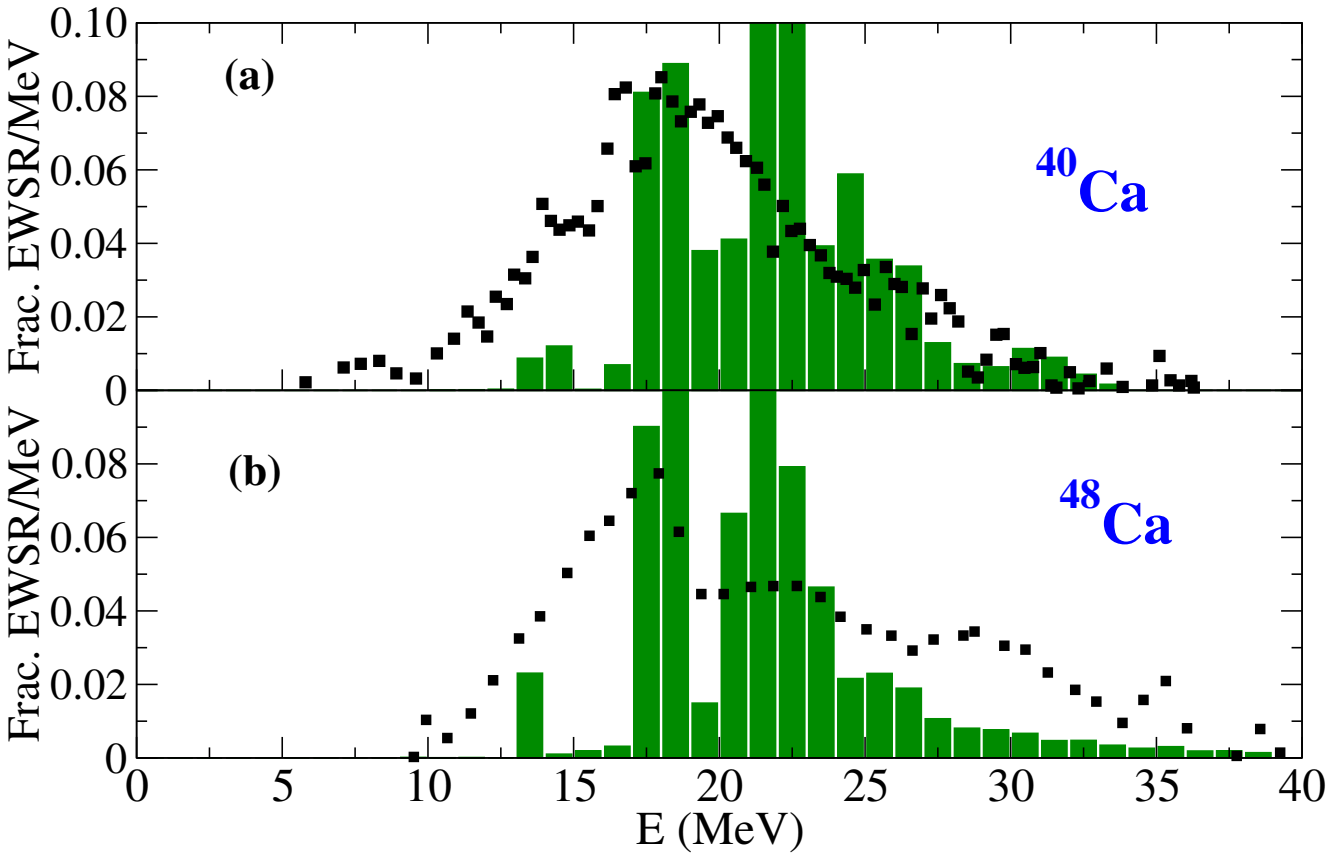

(a) Black squares: experimental results ; green bars: SSRPA predictions for ^{40}Ca; (b) Same as in (a) but for ^{48}Ca.

Centroids (MeV)

^{40}Ca: 21.3 (RPA), 20.7 (SSRPA), 18.3 (Exp)

^{48}Ca: 20.7 (RPA), 20.4 (SSRPA), 19.0 (Exp)

Transition densities in ^{40}Ca

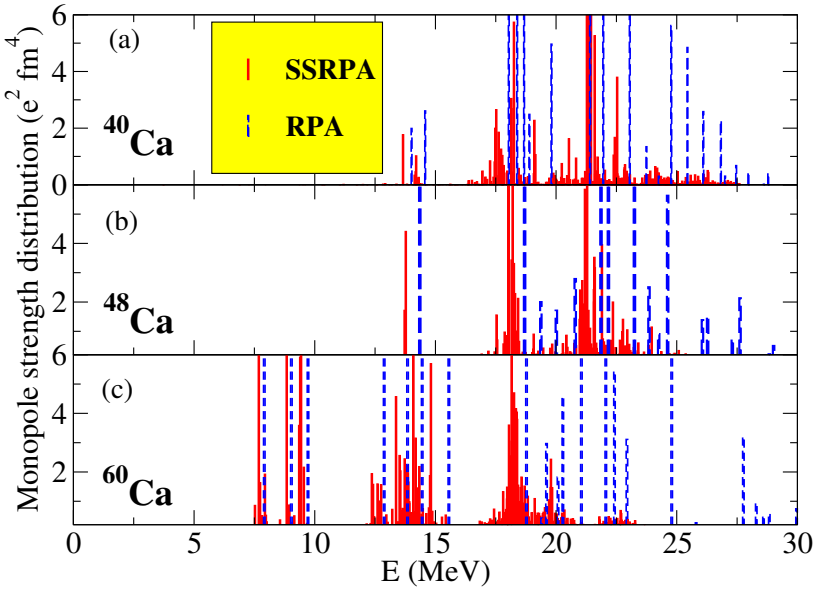

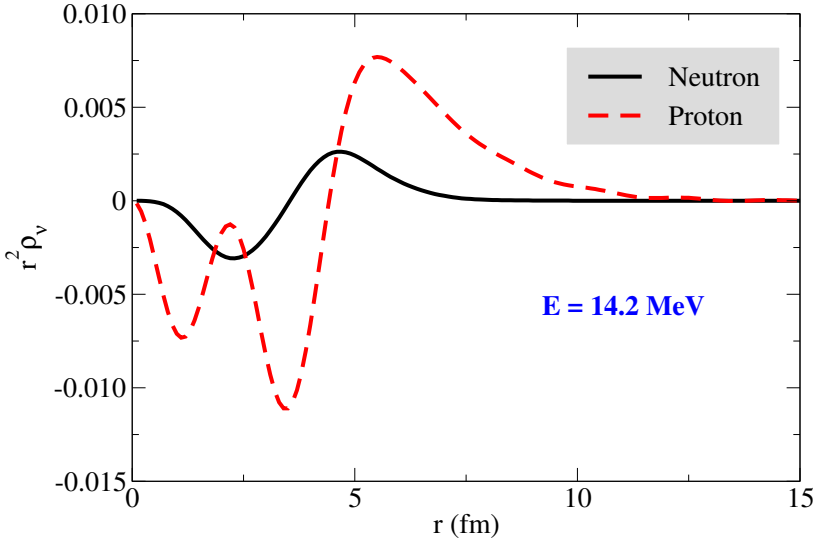

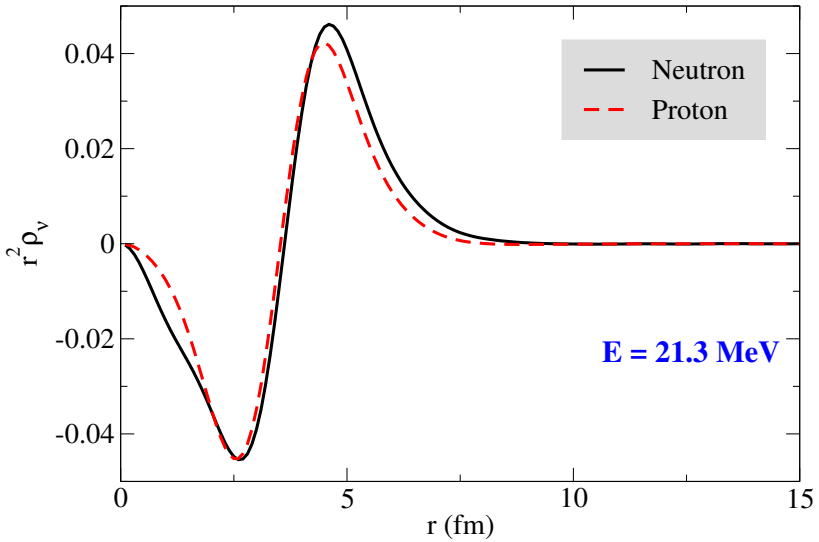

Transition densities in ^{48}Ca

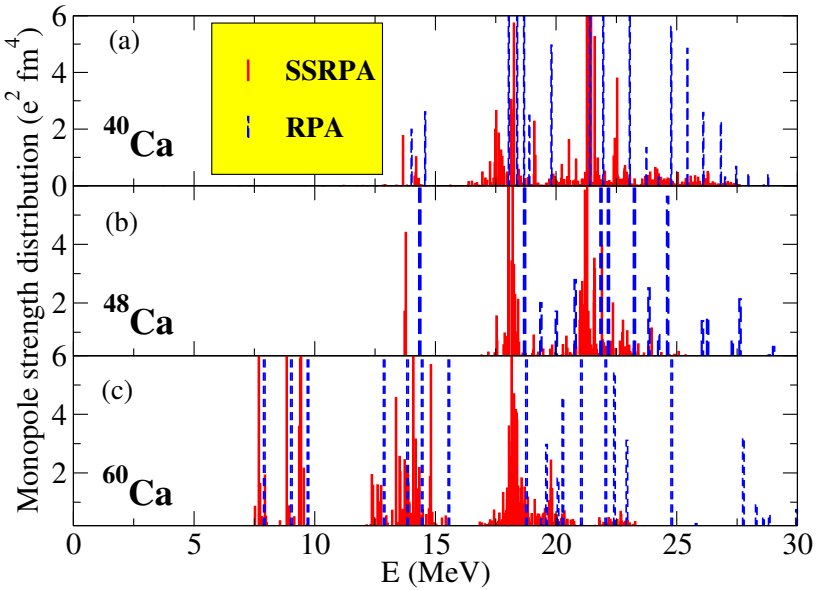

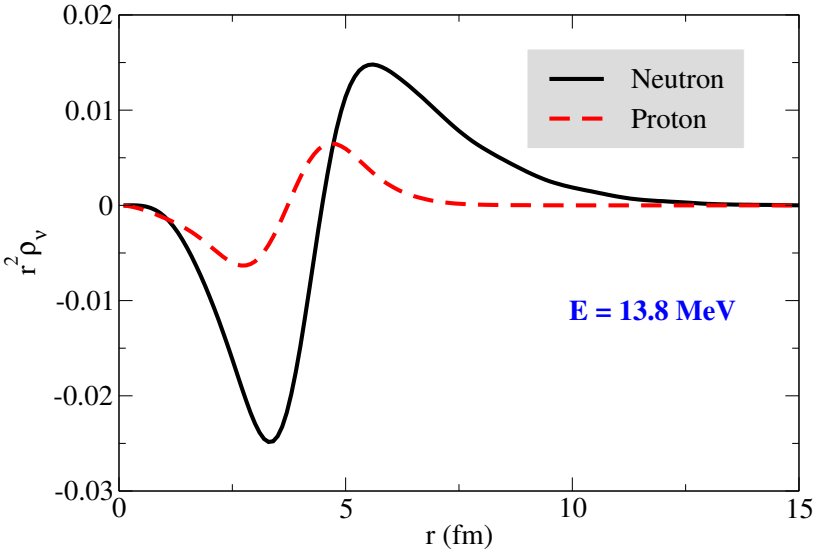

Transition densities in ^{60}Ca

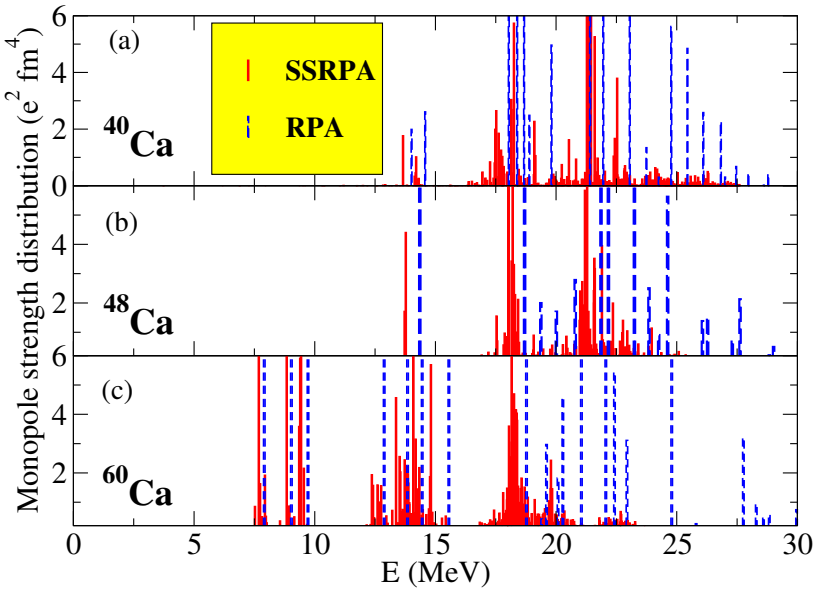

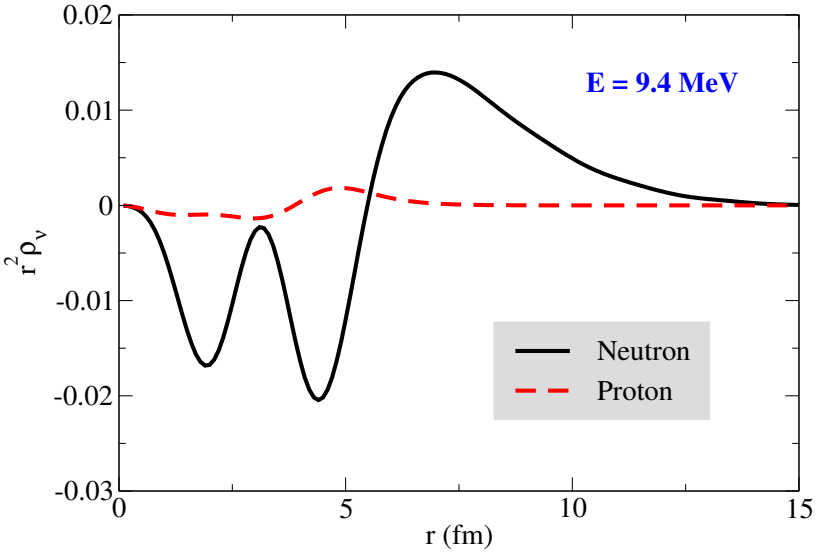

Transition densities in ^{60}Ca

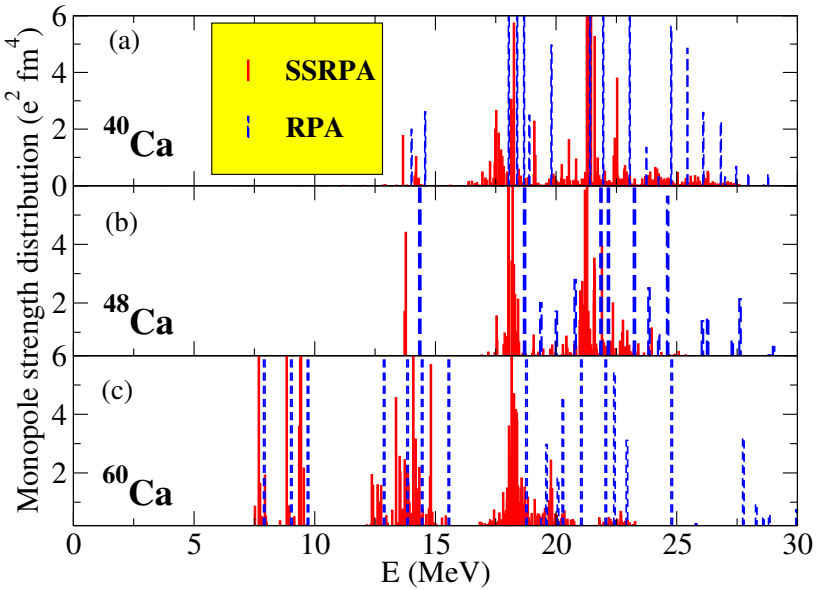

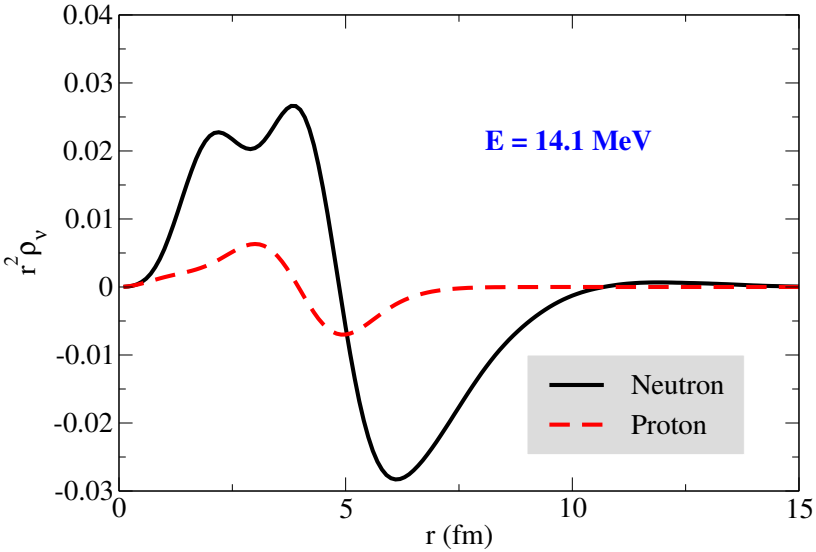

Monopole strength distributions and transition densities in ^{34}Si and ^{36}S

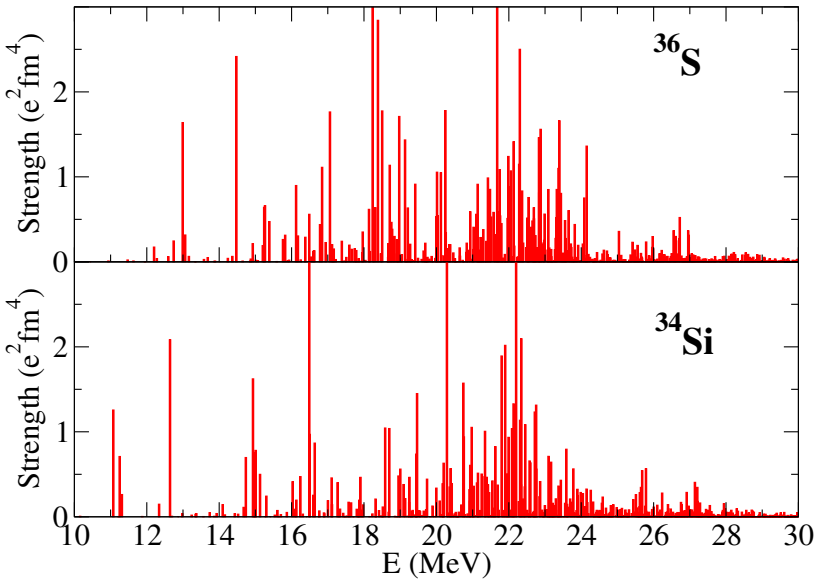

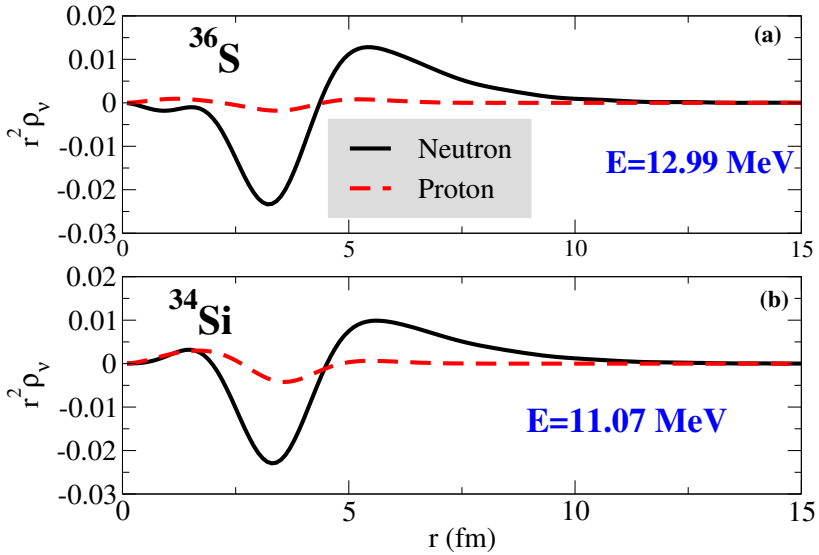

Composition of the peak located at 11.07 (12.99) MeV for ^{34}Si (^{36}S).

^{34}Si	1p1h 54 %	2p2h 46 %
	$[\nu 2d_{3/2}, \nu 1d_{3/2}]^{J=0}$	$[[\pi 3p_{1/2}, \nu 3f_{7/2}]^{J_p=3}[\pi 1d_{5/2}, \nu 2s_{1/2}]^{J_h=3}]^{J=0}$ $[[\pi 4p_{1/2}, \nu 1f_{5/2}]^{J_p=2}[\pi 1d_{5/2}, \nu 2s_{1/2}]^{J_h=2}]^{J=0}$ $[[\pi 4p_{1/2}, \nu 1f_{5/2}]^{J_p=3}[\pi 1d_{5/2}, \nu 2s_{1/2}]^{J_h=3}]^{J=0}$ $[[\pi 6s_{1/2}, \nu 2d_{3/2}]^{J_p=2}[\pi 1d_{5/2}, \nu 1d_{3/2}]^{J_h=2}]^{J=0}$ $[[\pi 6s_{1/2}, \nu 2d_{5/2}]^{J_p=2}[\pi 1d_{5/2}, \nu 1d_{3/2}]^{J_h=2}]^{J=0}$ $[[\pi 3d_{3/2}, \nu 3s_{1/2}]^{J_p=2}[\pi 1d_{5/2}, \nu 1d_{3/2}]^{J_h=2}]^{J=0}$ $[[\pi 3d_{3/2}, \nu 2d_{5/2}]^{J_p=1}[\pi 1d_{5/2}, \nu 1d_{3/2}]^{J_h=1}]^{J=0}$ $[[\pi 3d_{3/2}, \nu 2d_{5/2}]^{J_p=2}[\pi 1d_{5/2}, \nu 1d_{3/2}]^{J_h=2}]^{J=0}$
^{36}S	1p1h 52 %	2p2h 48 %
	$[\nu 2d_{3/2}, \nu 1d_{3/2}]^{J=0}$	$[[\pi 3d_{3/2}, \nu 4d_{3/2}]^{J_p=2}[\pi 1d_{5/2}, \nu 1d_{3/2}]^{J_h=2}]^{J=0}$ $[[\pi 4d_{3/2}, \nu 4s_{1/2}]^{J_p=2}[\pi 2s_{1/2}, \nu 1d_{3/2}]^{J_h=2}]^{J=0}$ $[[\pi 4d_{3/2}, \nu 5s_{1/2}]^{J_p=1}[\pi 2s_{1/2}, \nu 1d_{3/2}]^{J_h=1}]^{J=0}$ $[[\pi 4d_{3/2}, \nu 4d_{3/2}]^{J_p=2}[\pi 2s_{1/2}, \nu 1d_{3/2}]^{J_h=2}]^{J=0}$ $[[\pi 4d_{3/2}, \nu 2d_{5/2}]^{J_p=1}[\pi 2s_{1/2}, \nu 1d_{3/2}]^{J_h=1}]^{J=0}$

Transition densities in ^{68}Ni

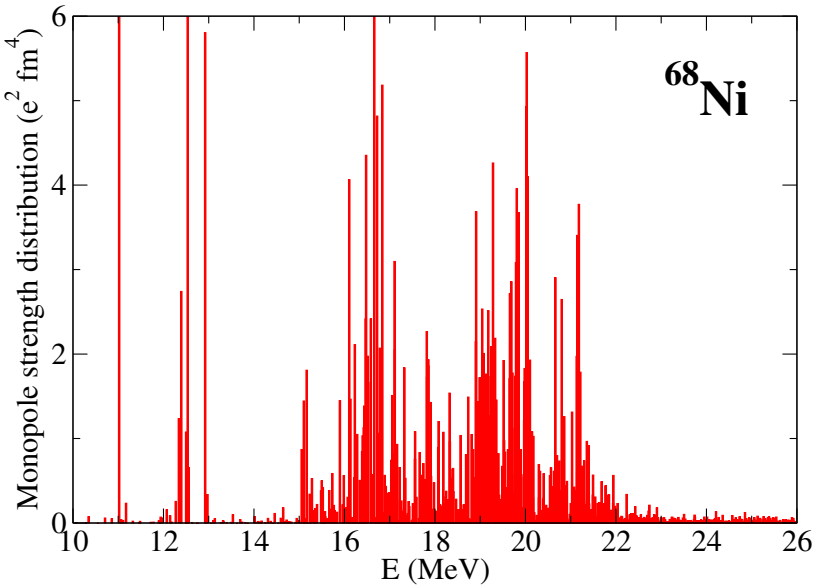

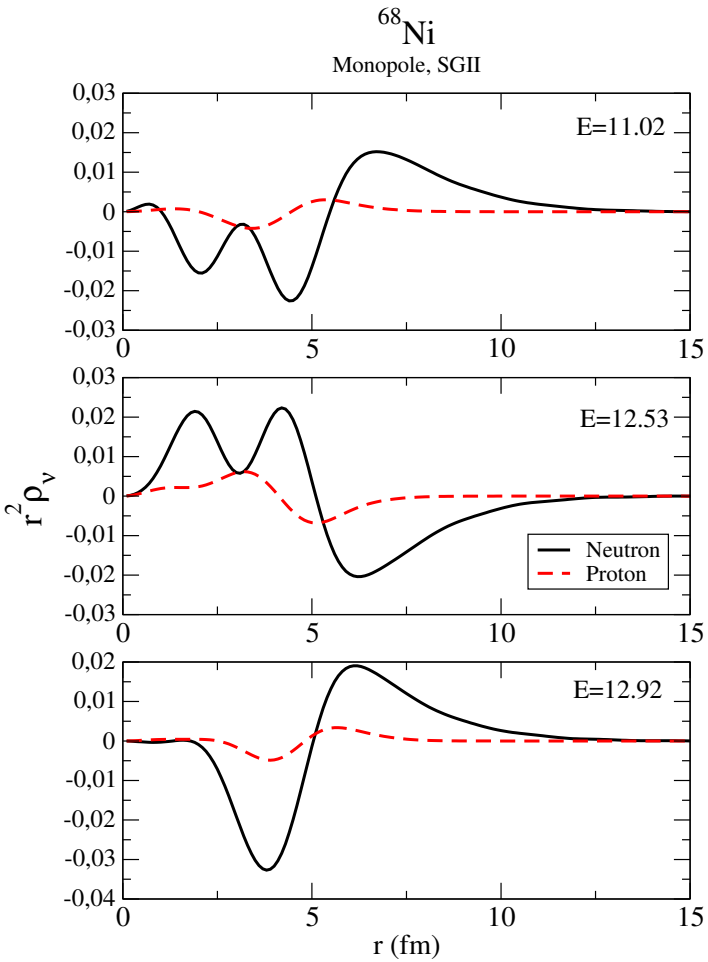

Transition densities in ^{68}Ni

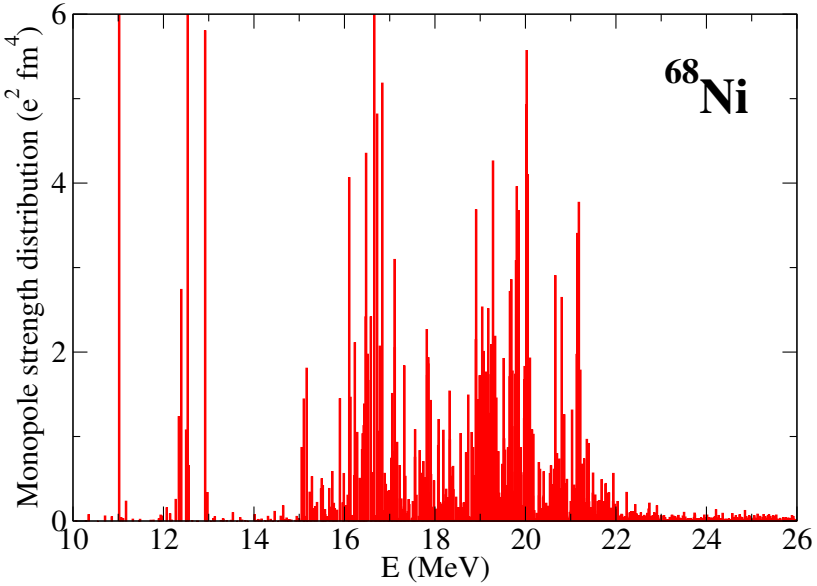

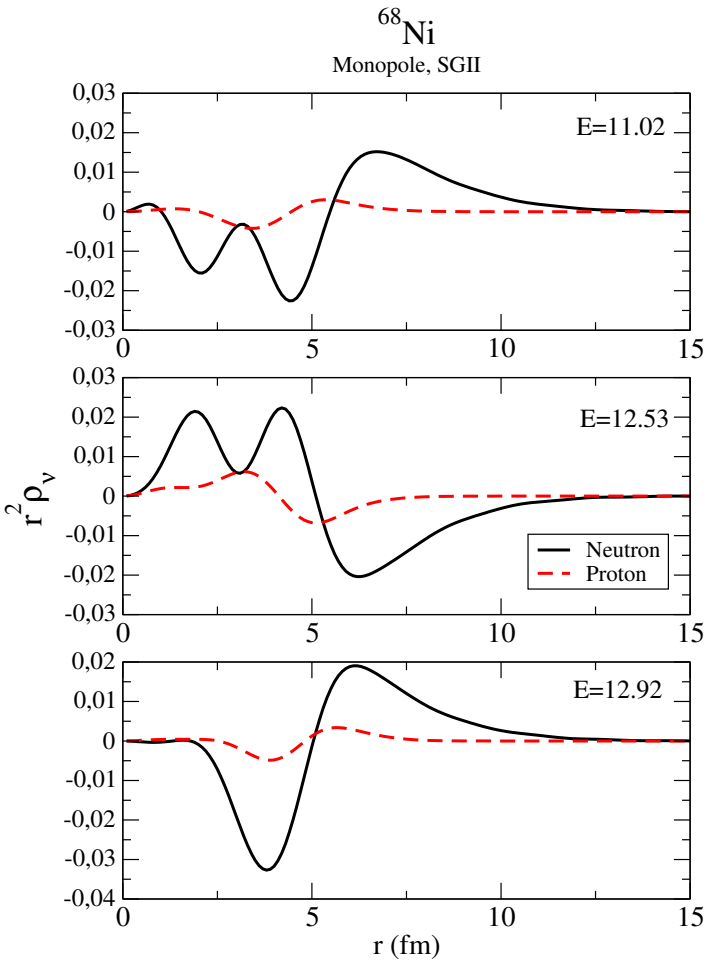

M. Vandebrouck et al. PRL 113, 032504 (2014)

E^{exp}_{ISGMR}=21.1±1.9 $E^{SSRPA}_{ISGMR} \sim 19.8$

$E^{exp}_{SOFT} = 12.9 \pm 1.0$ $E^{SSRPA}_{SOFT} \sim 12.92$ $70\%[\nu 2f_{5/2}, \nu 1f_{5/2}]^{J=0}$

Main results

- Low-lying states appear also in the monopole channel
- Strength increases with neutron excess
- Soft monopole modes driven by neutron excitations
- Not only at the surface of the nucleus but over its entire volume
- However, they have mostly single 1ph nature
- More details: DG, M. Grasso and O. Sorlin, PRC 100, 014317 (2019)

PHYSICAL REVIEW C **98**, 044313 (2018)

Systematic study of giant quadrupole resonances with the subtracted second random-phase approximation: Beyond-mean-field centroids and fragmentation

O. Vasseur,[1] D. Gambacurta,[2] and M. Grasso[1]

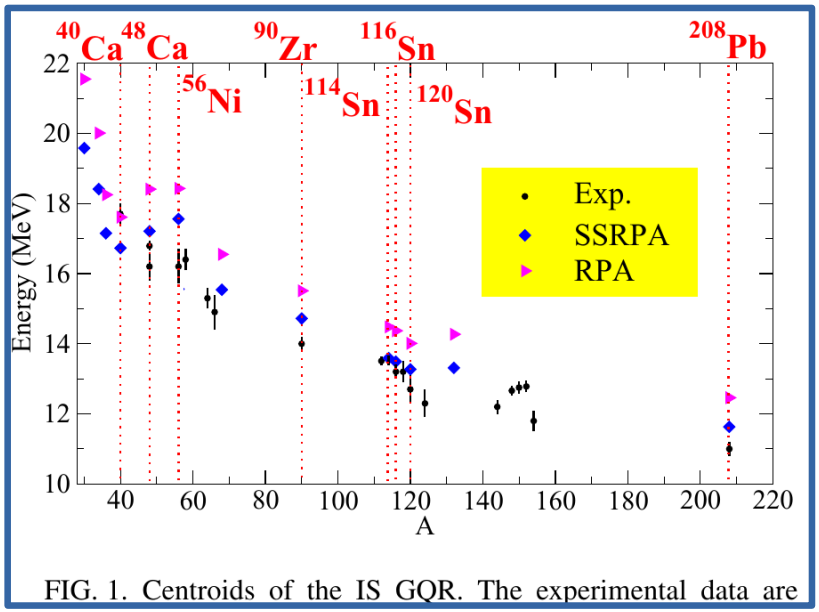

FIG. 1. Centroids of the IS GQR. The experimental data are

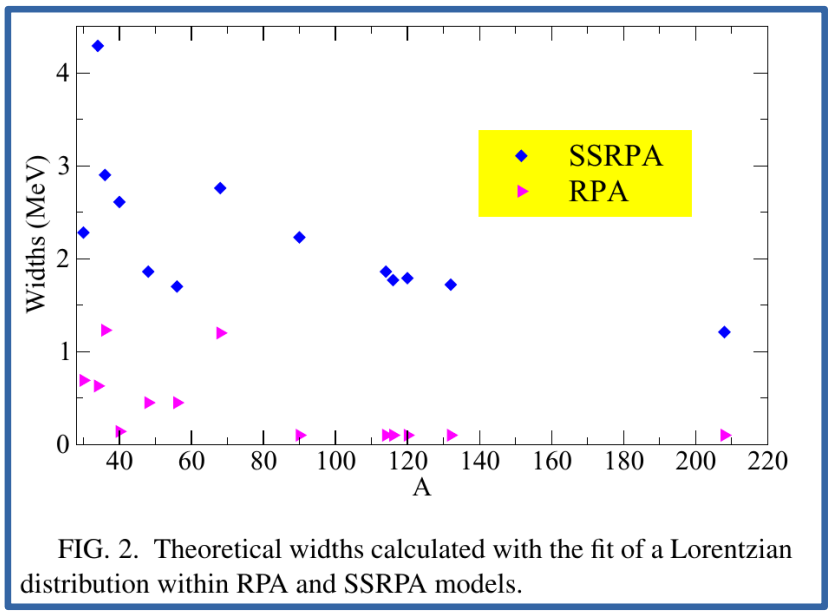

FIG. 2. Theoretical widths calculated with the fit of a Lorentzian distribution within RPA and SSRPA models.

Recent extension to the charge exchange (CE) case

Second RPA for CE excitations

- Extension of the SSRPA for the description of **CE excitations**
- First applications to ^{48}Ca (lightest double-β emitter) and ^{78}Ni in Ref [1]
- More applications (^{14}C, ^{22}O, ^{90}Zr and ^{132}Sn) in Ref [2,3]

More details in:

[1] D.Gambacurta, M. Grasso, J. Engel, Phys. Rev. Lett. 125, 212501 (2020)
[2] D.Gambacurta and M. Grasso, Phys. Rev. C 105, 014321, (2022)
[3] D.Gambacurta and M. Grasso, *in preparation*

The quenching problem

- Computed GT matrix elements **are larger** than the experimental ones.
- The problem is "cured" by **quenching** the strength by $q \sim 0.7$ or using effective axial constant g_A (~ 1) instead of the "bare" value ~ 1.27.

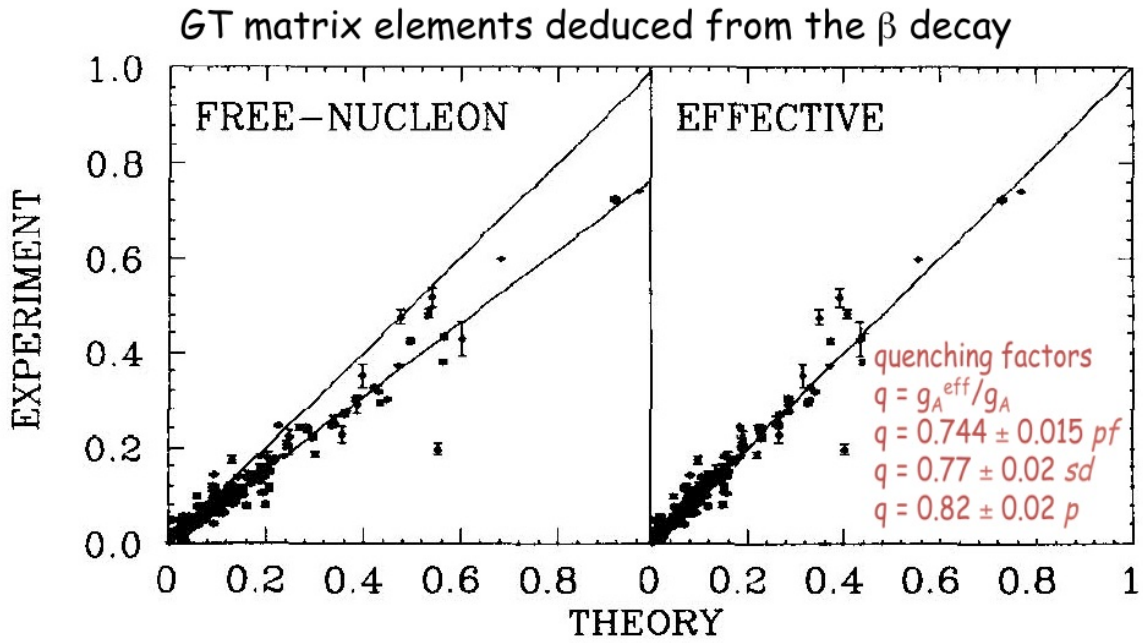

Shell Model calculations

The quenching problem

- Computed GT matrix elements **are larger** than the experimental ones.
- The problem is "cured" by **quenching** the strength by $q \sim 0.7$ or using effective axial constant g_A (~ 1) instead of the "bare" value ~ 1.27.

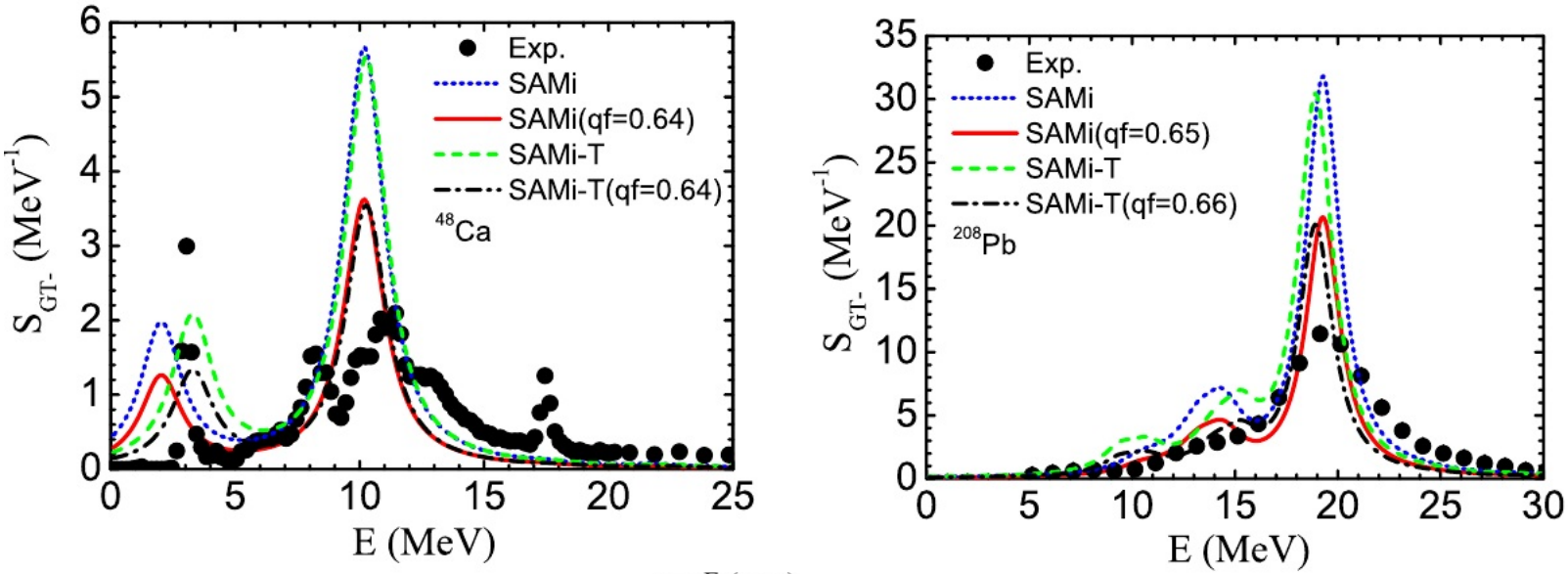

$$qf = \frac{\sum_{E_x=0}^{E_x(\max)} B(GT : E_x)_{\text{expt}}}{\sum_{E_x=0}^{E_x(\max)} B(GT)_{\text{calc}}}$$

Li-Gang Cao , Shi-Sheng Zhang, and H. Sagawa, PHYSICAL REVIEW C 100, 054324 (2019)

Skyrme-RPA calculations

Theory vs Experiment: the quenching problem

The quenching problem

- Computed GT matrix elements **are larger** than the experimental ones.
- The problem is "cured" by **quenching** the strength by $q \sim 0.7$ or using effective axial constant g_A (~ 1) instead of the "bare" value ~ 1.27.

Possible causes fall in two main classes:

- **Nuclear many-body correlations not included in the calculations**: (truncation of the model space, short-range correlations, multi-phonon states, multi particle-hole excitations, ...)
- **Non-nucleonic degrees of freedom**: (Many-nucleon weak currents, Δ-isobar excitations, in-medium modification of pion physics, ...)

GT^- Strength Distribution ^{48}Ca, SGII interaction

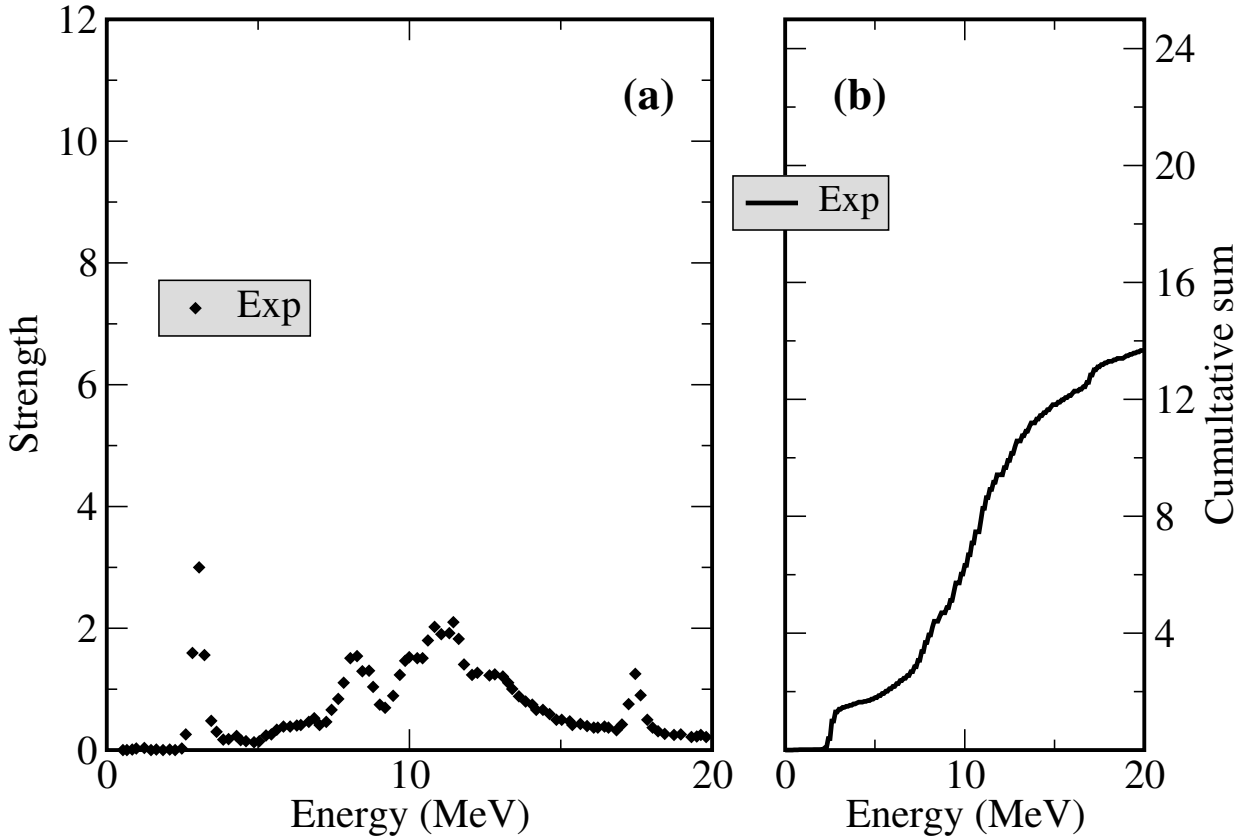

(a) GT^- strength in RPA and SSRPA compared with (GT^- plus IVSM) data.
(b) Cumulative strengths up to 20 MeV.
Data from: K. Yako *et al.*, Phys. Rev. Lett. 103, 012503 (2009)
From D.Gambacurta, M. Grasso, J. Engel, Phys. Rev. Lett. 125, 212501 (2020)

GT^- Strength Distribution ^{48}Ca, SGII interaction

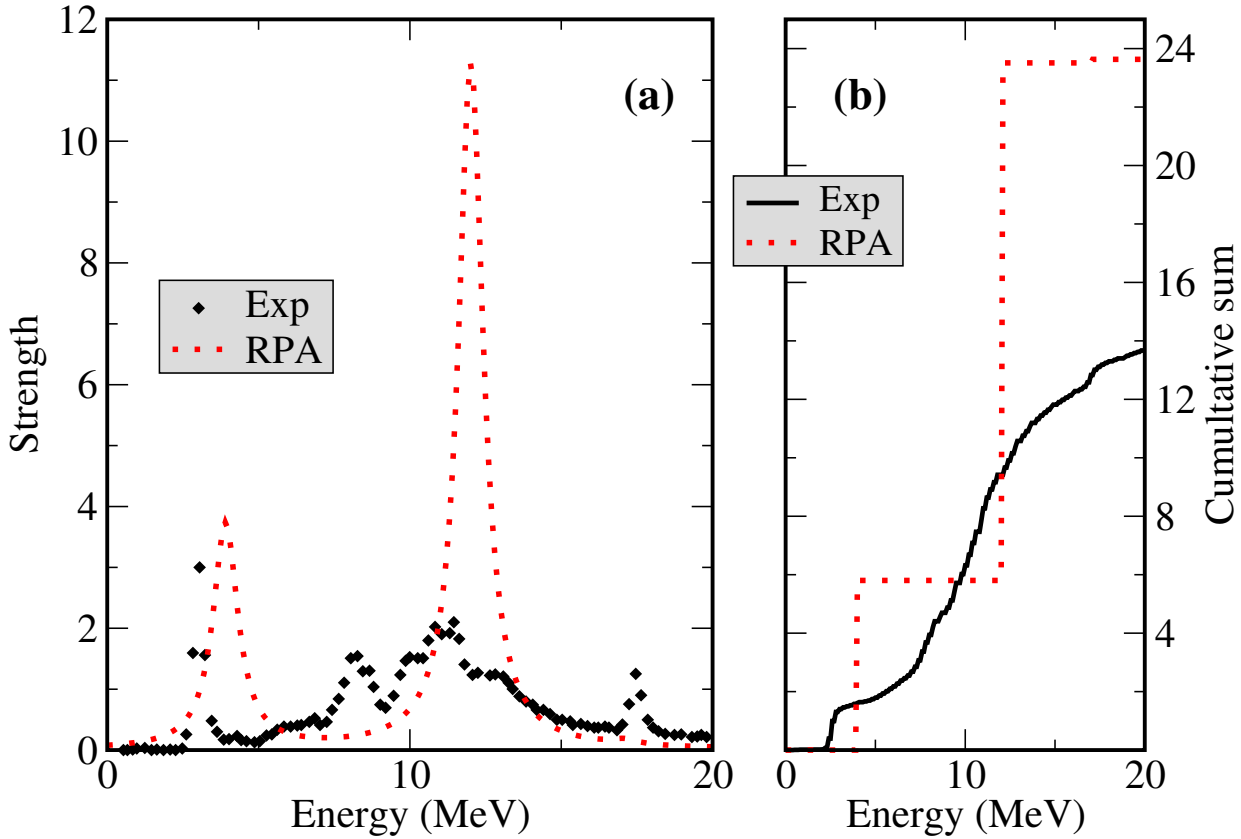

(a) GT^- strength in RPA and SSRPA compared with (GT^- plus IVSM) data.
(b) Cumulative strengths up to 20 MeV.
Data from: K. Yako *et al.*, Phys. Rev. Lett. 103, 012503 (2009)
From D.Gambacurta, M. Grasso, J. Engel, Phys. Rev. Lett. 125, 212501 (2020)

GT$^-$ Strength Distribution ^{48}Ca, SGII interaction

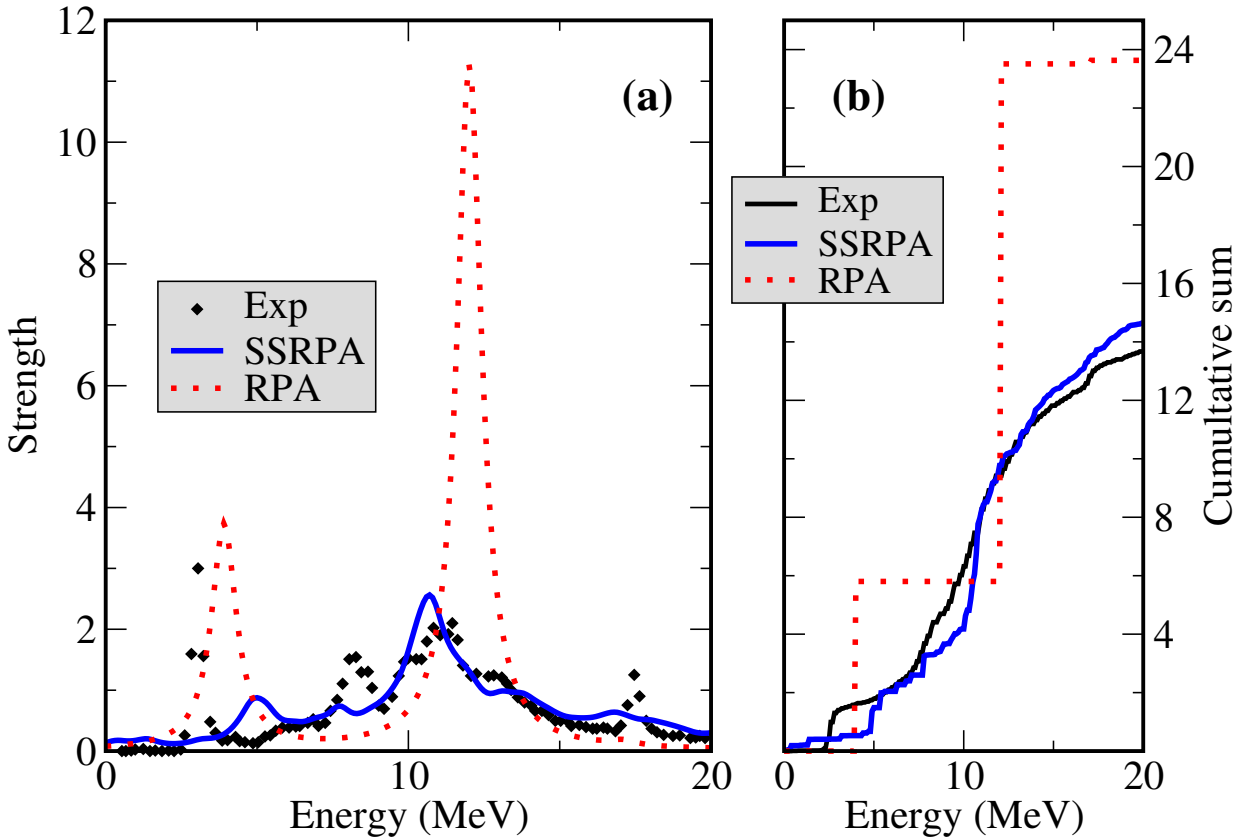

(a) GT$^-$ strength in RPA and SSRPA compared with (GT$^-$ plus IVSM) data.
(b) Cumulative strengths up to 20 MeV.
Data from: K. Yako *et al.*, Phys. Rev. Lett. 103, 012503 (2009)
From D.Gambacurta, M. Grasso, J. Engel, Phys. Rev. Lett. 125, 212501 (2020)

GT$^-$ Strength Distribution ^{48}Ca, sum rules in the two channels

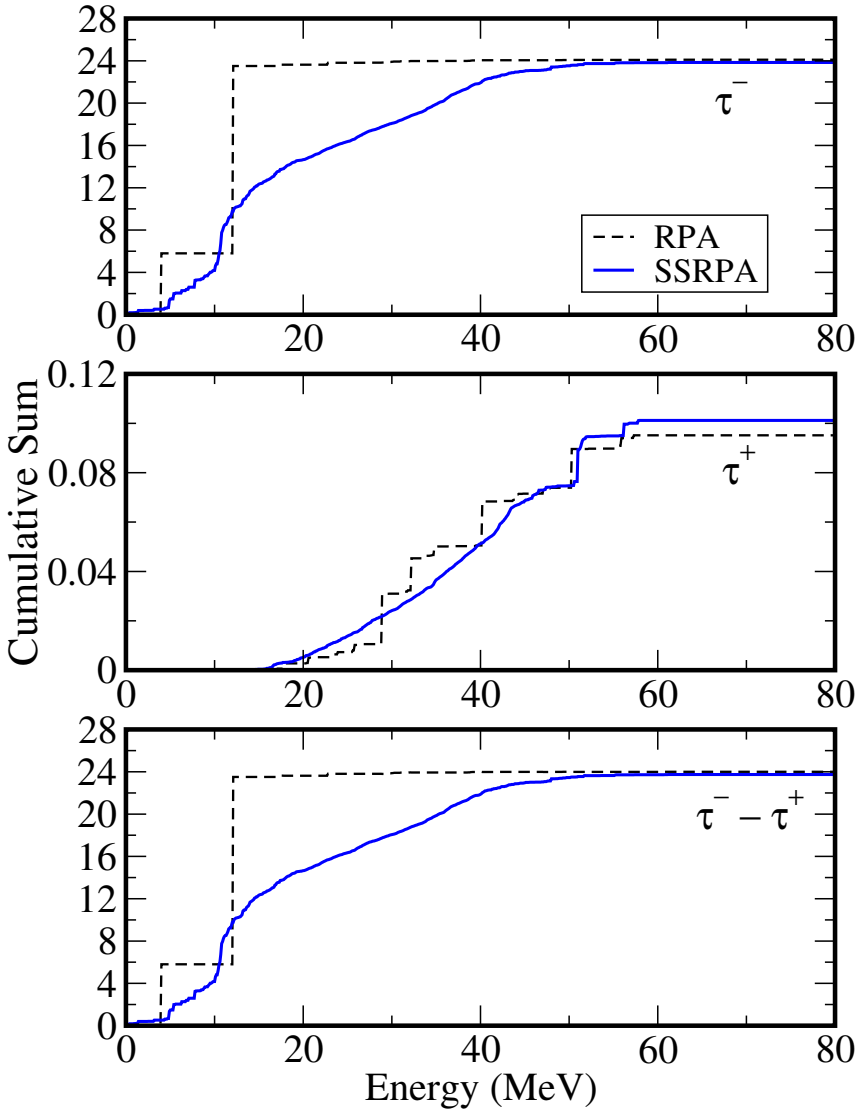

Calculations fo heavier systems

For heavier nuclei, the inversion of the A_{22} becomes prohibitive.
We checked that the diagonal approximation provides relieable results

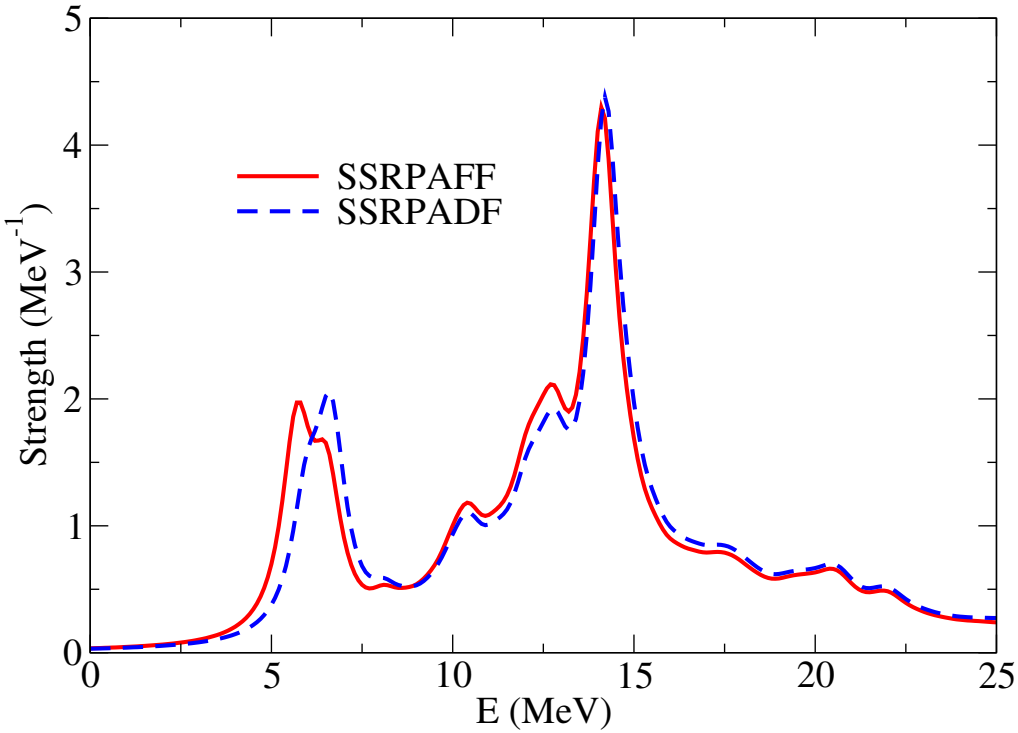

GT$^-$ strengths obtained for the nucleus ^{90}Zr in MeV^{-1}. SSRPAFF and SSRPADF spectra are shown.

From D.Gambacurta and M. Grasso, Phys. Rev. C 105, 014321, (2022)

GT^- Strength Distribution ^{90}Zr and ^{132}Sn

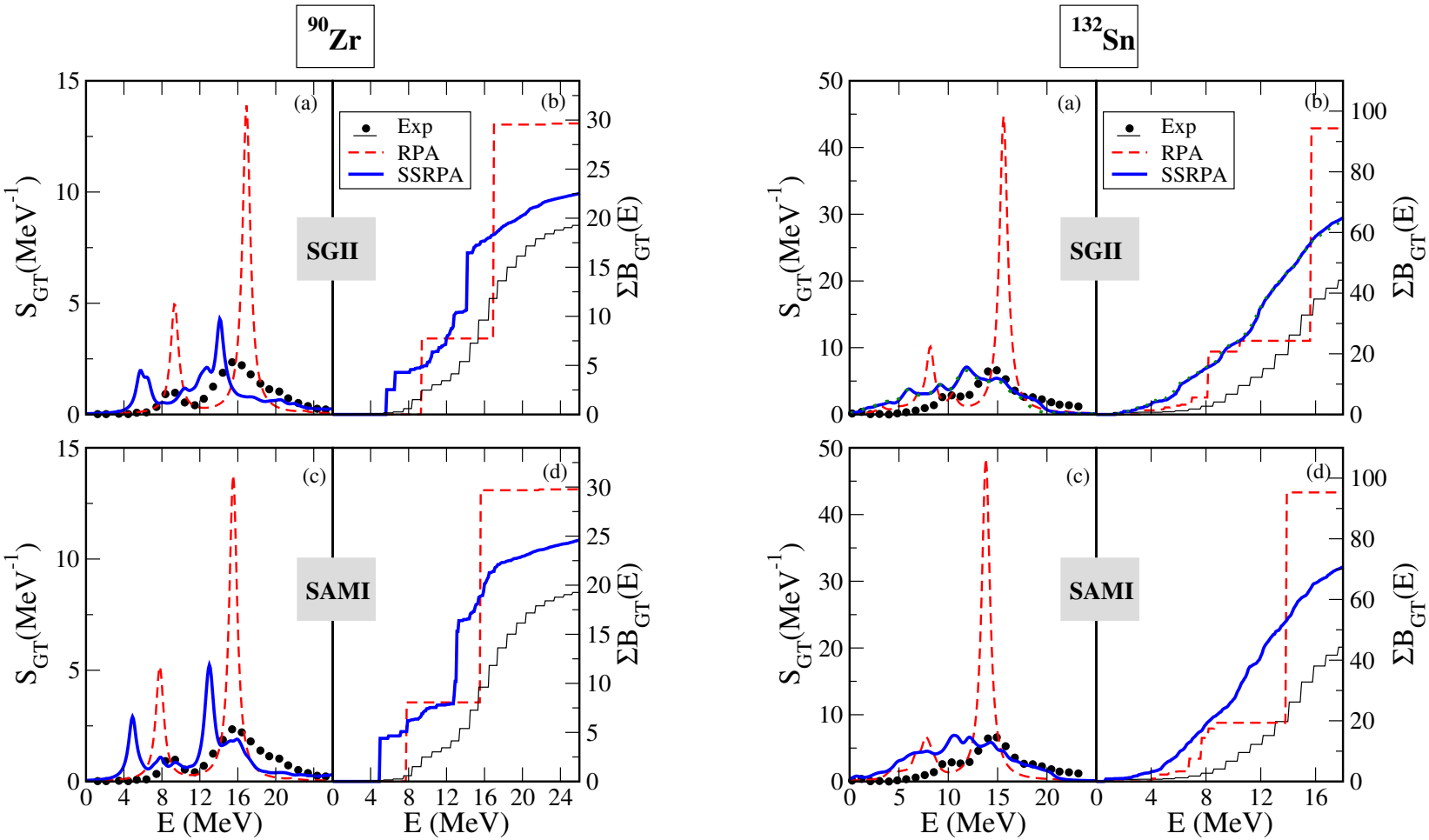

From: D. G. and M. Grasso, Phys. Rev. C 105, 014321, 2022

GT^- Strength Distribution ^{90}Zr and ^{132}Sn

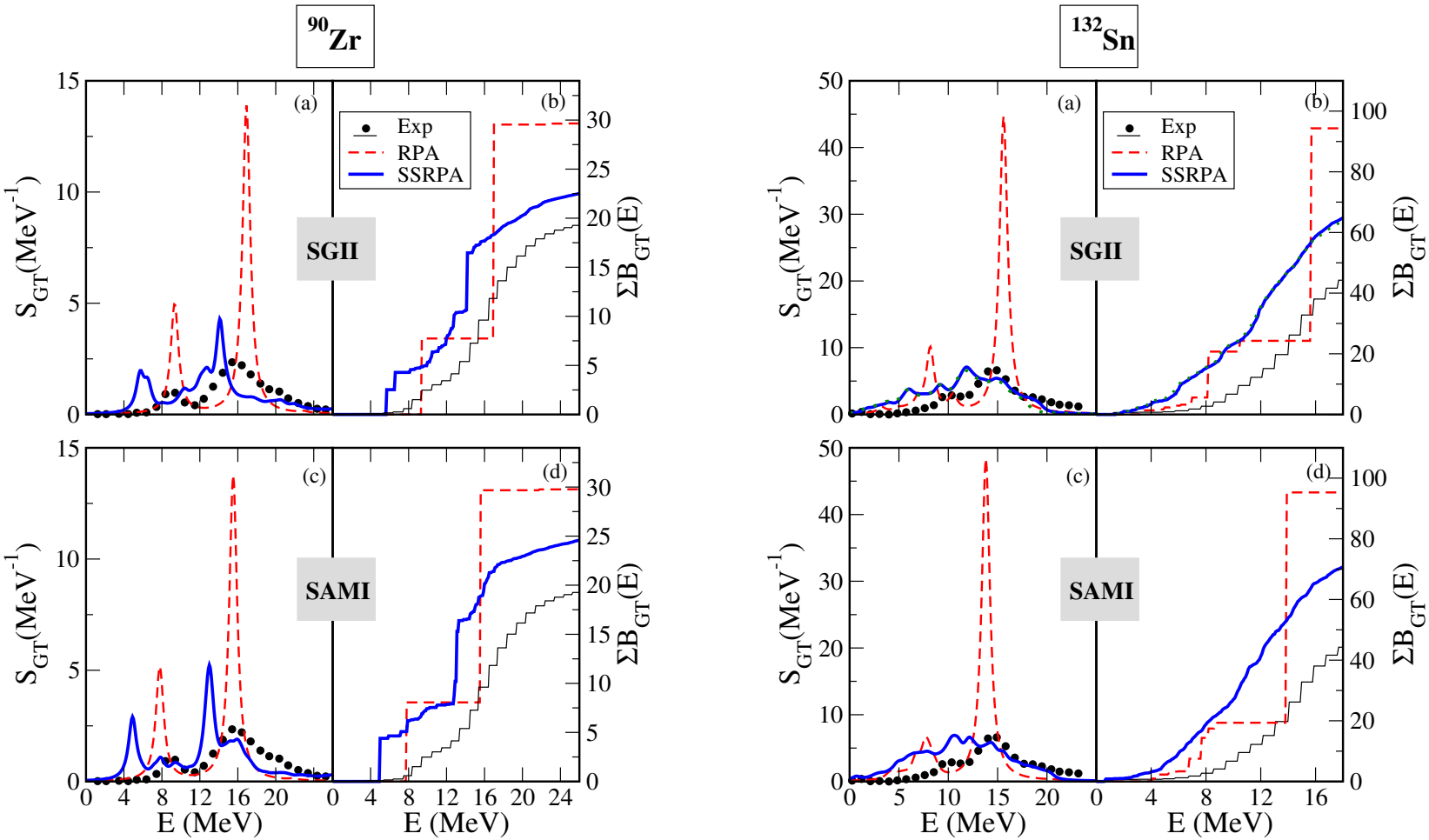

From: D. G. and M. Grasso, Phys. Rev. C 105, 014321, 2022
Other sources of queenching may be needed ...

GT^- Strength Distribution for the nuclei ^{22}O (blue) and ^{14}C (green): SSRPA versus *ab initio* Coupled Cluster including two-body currents [1].

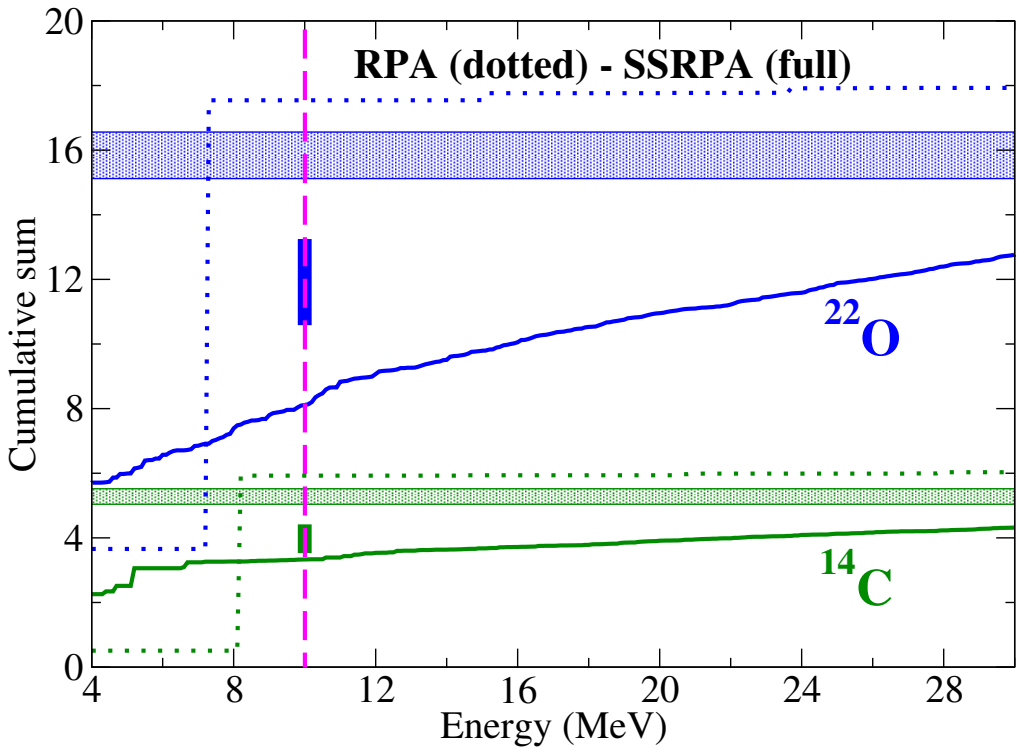

The blue and green horizontal areas represent the reduction of the total Ikeda sum rule $S_{GT-} - S_{GT+}$ from *ab initio* results [1].
The blue and green vertical intervals correspond to a reduction of (70-80 %) of the sum rule exhausted at 10 MeV.
[1] A. Ekstrom *et al.* Phys. Rev. Lett. 113, 262504 (2014)
See also Gysbers et al. Nature Phys. 15 428 (2019)

From D.Gambacurta and M. Grasso, Phys. Rev. C 105, 014321, (2022)

GT$^-$ Strength Distribution and β-decay half-life ^{78}Ni

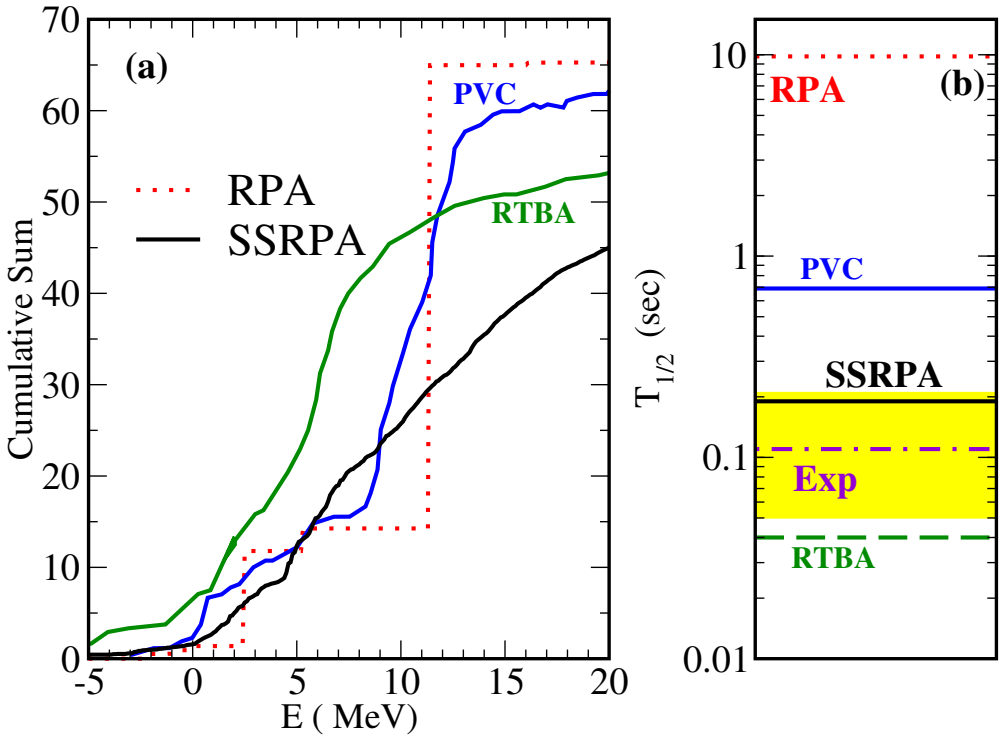

(a) Cumulative sum for the nucleus ^{78}Ni within the SSRPA, PVC and RTBA models;
(b) β-decay half-life for ^{78}Ni. **No quenching, bare** $g_a = 1.27$**;**
Data from: P. T. Hosmer *et al.* Phys. Rev. Lett. 94, 112501 (2005)
PVC: Y. F. Niu, G. Coló and E. Vigezzi, Phys. Rev. C 90, 054328 (2014)
RTBA:C. Robin and E. Litvinova, Phys. Rev. C 98, 051301(R), 2018

From D.Gambacurta, M. Grasso, J. Engel, Phys. Rev. Lett. 125, 212501 (2020)

β decay half-lives: PVC results

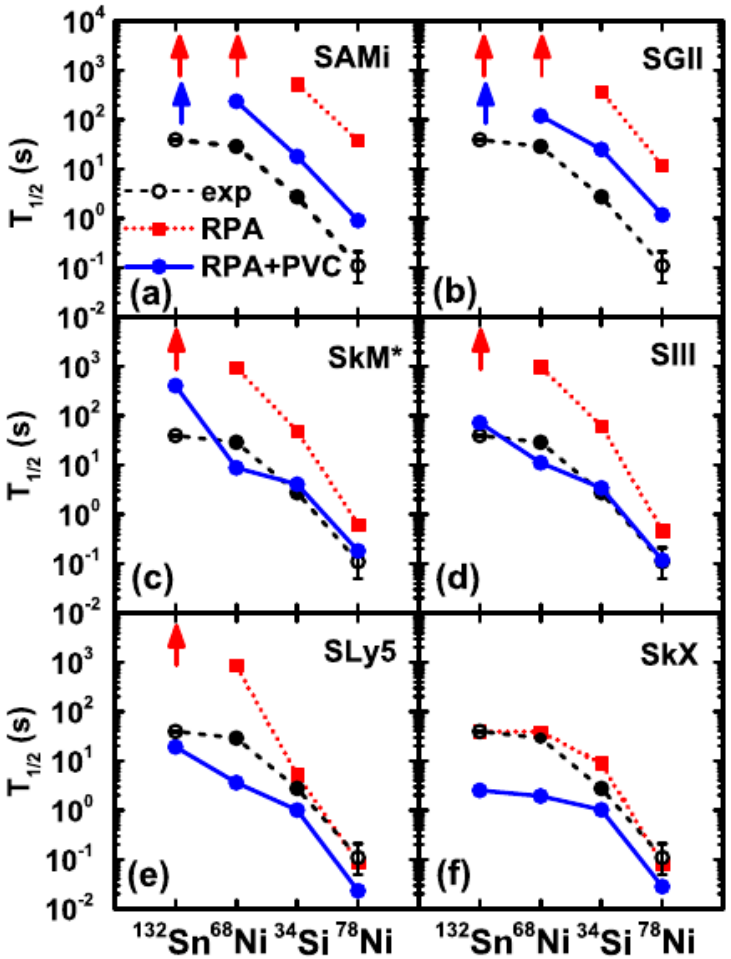

β decay half-lives: SSRPA results

PHYSICAL REVIEW C **107**, 014325 (2023)

Effects of two-particle–two-hole configurations and tensor force on β decay of magic nuclei

M. J. Yang,[1] H. Sagawa,[2,3] C. L. Bai,[1] and H. Q. Zhang[4]

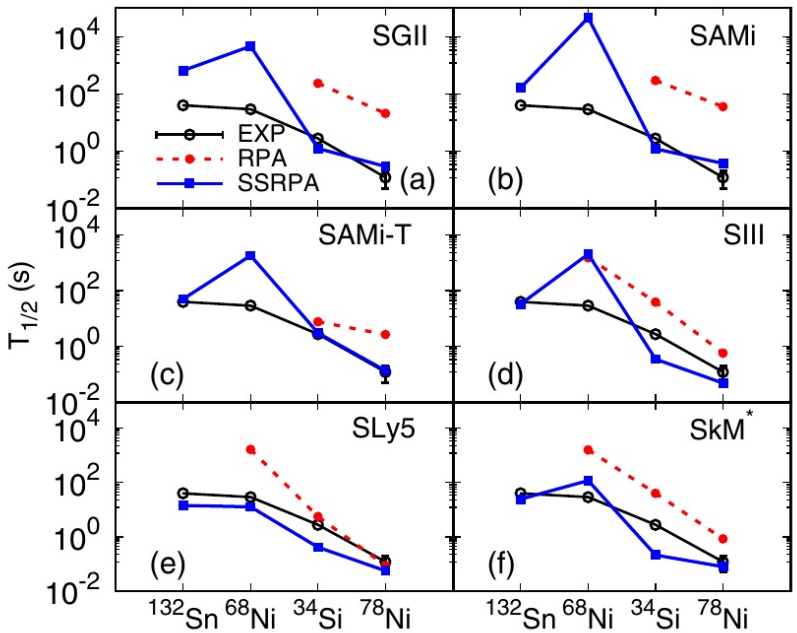

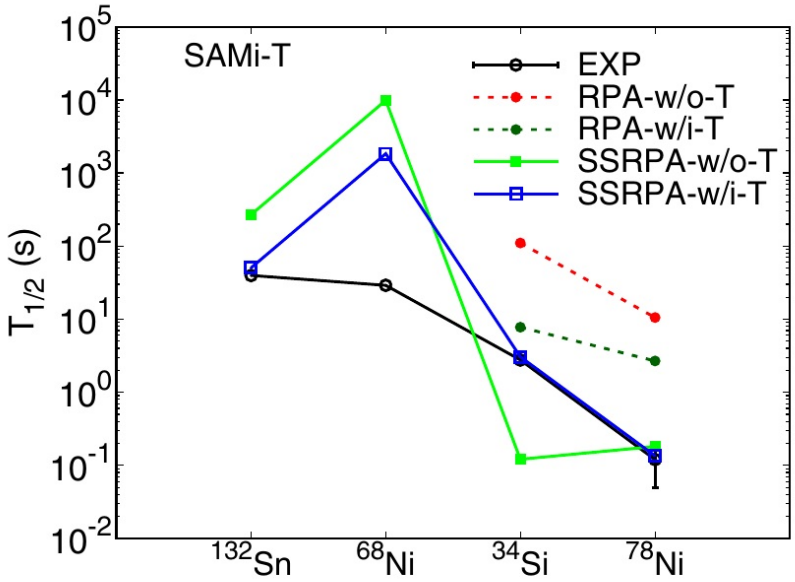

β decay half-lives: SSRPA preliminar results

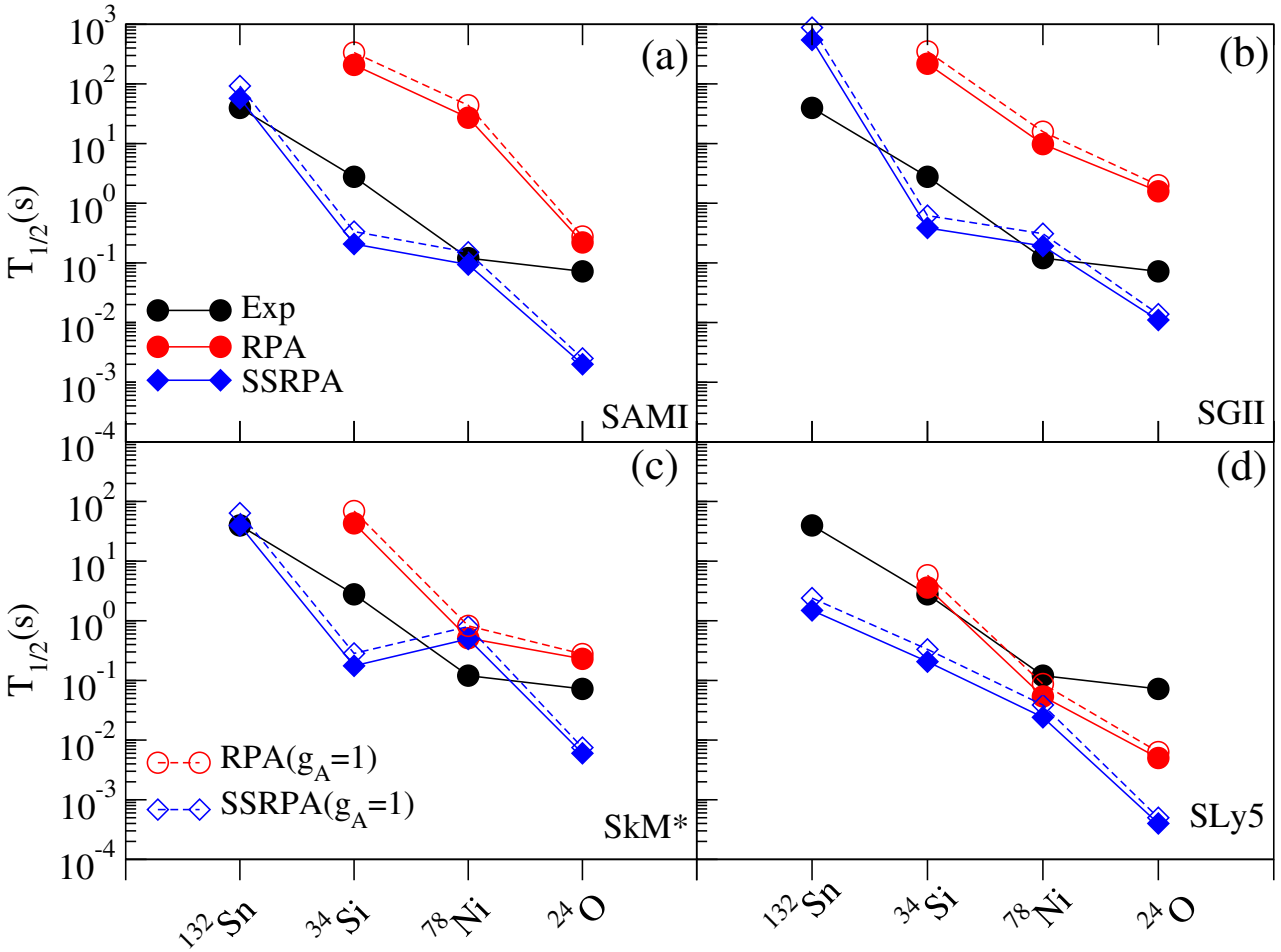

From D.Gambacurta and M. Grasso, *in preparation*

Conclusions and Outlook

SSRPA merits

- More general description than the RPA
- The EDF Subtracted SRPA is robust and reliable (double-counting free)
- Better description of Fragmentation, Spreading, Low-lying states

SSRPA limitations

- Numerically very demanding
- Transition Probabilities of 2ph states often underestimated
- Extension to deformed case not (at present) viable

SSRPA future work

- More systematic calculations
  (including also double-beta and -gamma decay and double-phonons?)
- Pairing, e.g. Second QRPA
- Comparison with PVC model (and possible merging)

Extra Slides

HPC implementation

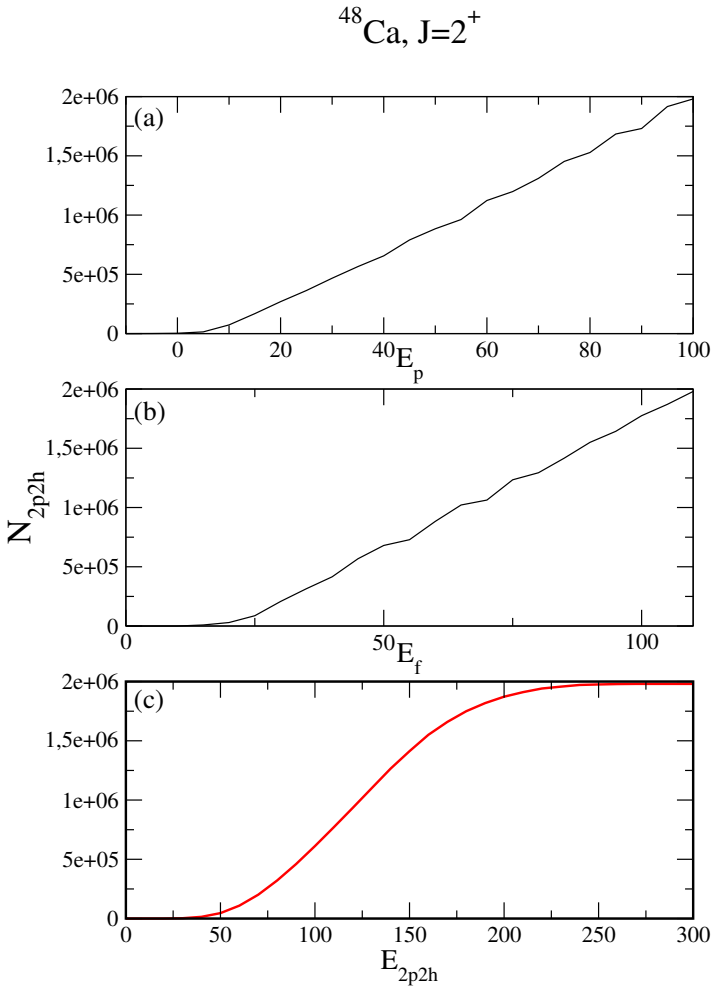

Numerical complexity

- The most demanding task is related to the treatment of the $A_{22'}$ matrix
- The number of 2p-2h configurations can be very large$\simeq 10^{6-8}$
- We need to calculate the "full" spectrum
- Most demanding tasks:
  a) subtraction procedure, $A_{22'}$ inversion
  b) diagonalization of the SSRPA eigenvalue problem

PETSc and SLEPc libraries

Portable, Extensible Toolkit for Scientific computation

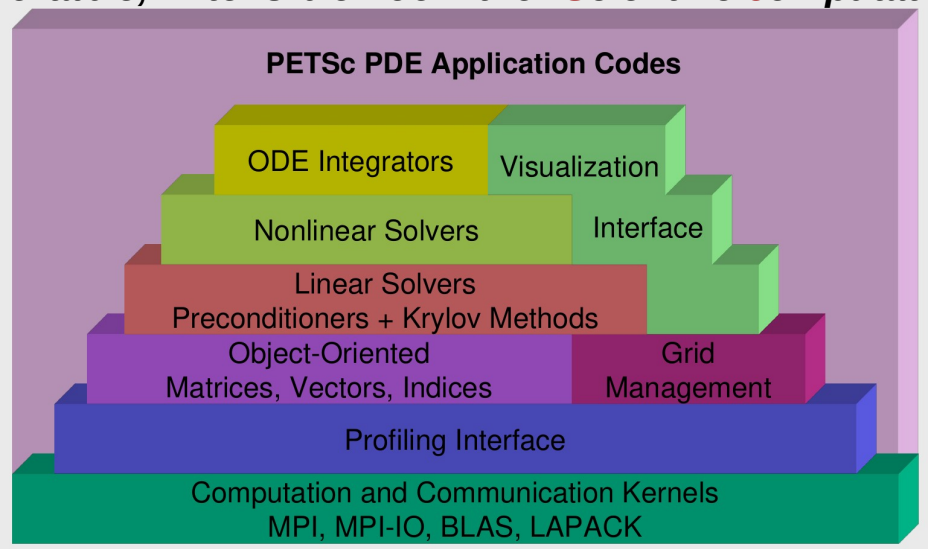

- Sequential and parallel data structures
- Sequential and parallel algebraic solvers
- Parallel computing, mostly transparent to the user

www.mcs.anl.gov/petsc

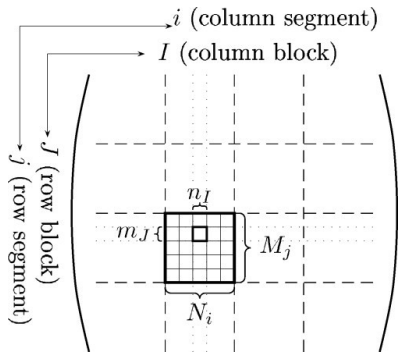

Scalable Library for Eigenvalue Problem computations https://slepc.upv.es/

SLEPc

SVD Solvers			
Cross Product	Cyclic Matrix	Lanczos	Thick Res. Lanczos

Eigensolvers			
Krylov-Schur	Arnoldi	Lanczos	Other

Spectral Transform			
Shift	Shift-and-invert	Cayley	Fold

Standard Eigenproblem $Ax = \lambda x$

Generalized Eigenproblem $Ax = \lambda Bx$

- Various problem characteristics
  - Real/complex, Hermitian/non-Hermitian
- Wanted solutions
  - Usually only a few eigenpairs, but may be many
  - Any part of the spectrum (exterior, interior), intervals

Spectral Transformation $Ax = \lambda x \Longrightarrow Tx = \theta x$

- State-of-the-art eigensolvers: Krylov-Schur | Arnoldi | Lanczos | Other

mpiexec -n 64 ./slepc -eps_nev 1000 -eps_target 12.5 -eps_type lanczos

Scalability test

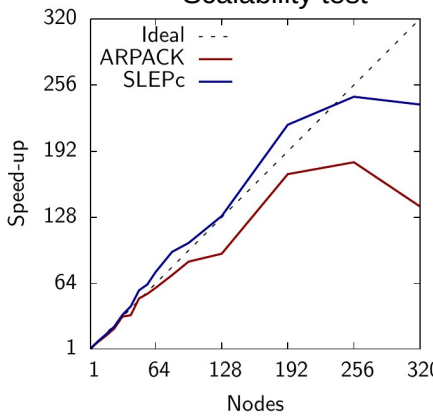

- Dimension 659,033
- 10 eigenvalues

First Applications

PHYSICAL REVIEW C **79**, 044305 (2009)

Global investigation of the fine structure of the isoscalar giant quadrupole resonance

A. Shevchenko,[1,*] O. Burda,[1] J. Carter,[2] G. R. J. Cooper,[3] R. W. Fearick,[4] S. V. Förtsch,[5] H. Fujita,[2,6] Y. Fujita,[6] Y. Kalmykov,[1,†] D. Lacroix,[7,8] J. J. Lawrie,[5] P. von Neumann-Cosel,[1,‡] R. Neveling,[5] V. Yu. Ponomarev,[1] A. Richter,[1] E. Sideras-Haddad,[2] F. D. Smit,[5] and J. Wambach[1]

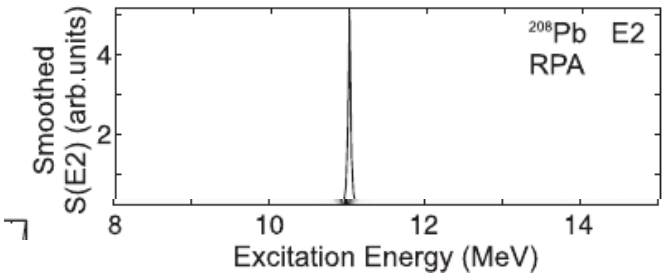

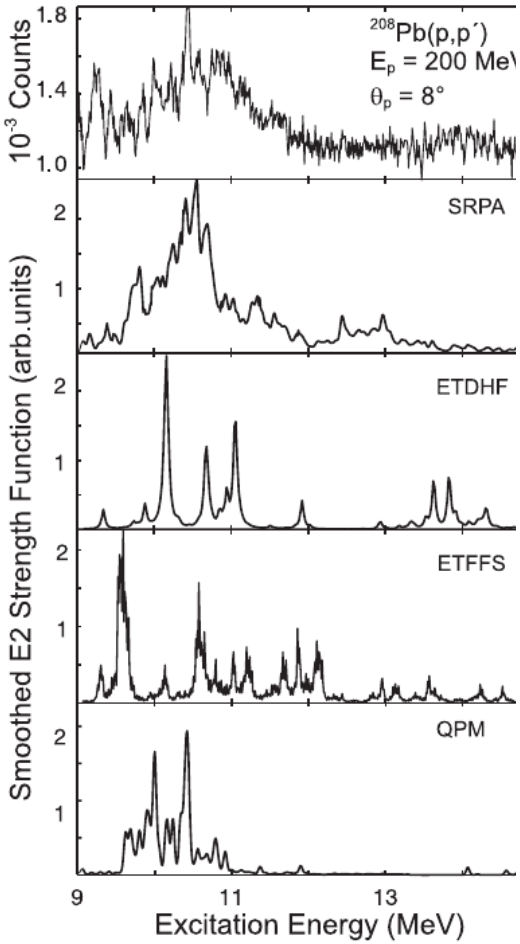

Nuclear Physics **A426** (1984) 253–275

FRAGMENTATION OF NUCLEAR STRENGTH DISTRIBUTIONS BY 2p2h EXCITATIONS†

B. SCHWESINGER*

J. WAMBACH

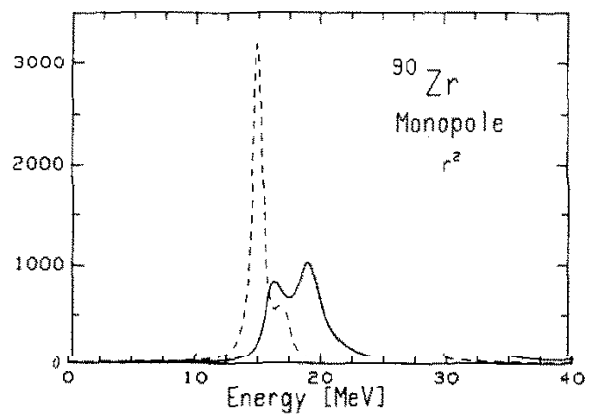

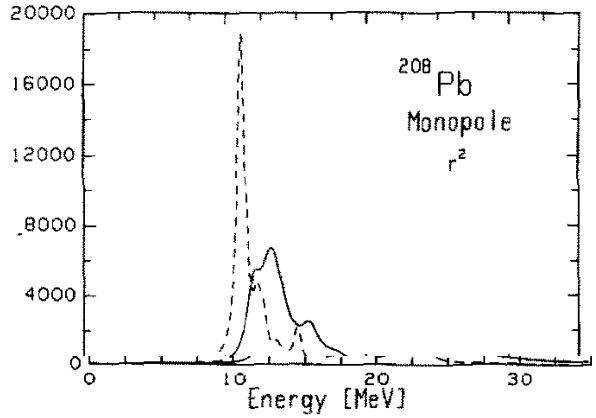

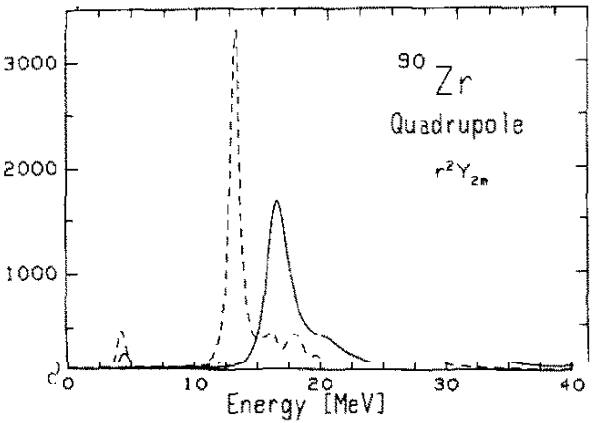

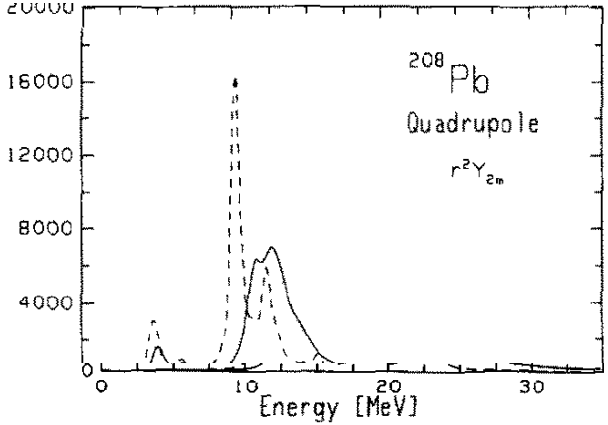

Physics Letters B 349 (1995) 7–10

Double-dipole excitations in ^{40}Ca

S. Nishizaki [1], J. Wambach [2]

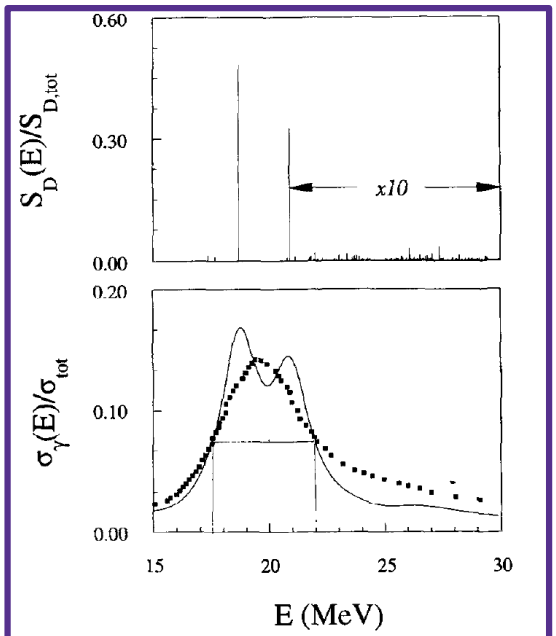

ig. 1. Upper part: the calculated dipole transition strength distri-ution in ^{40}Ca (Eq. (8)). The high-energy tail has been multi-ied by a factor of 10; lower part: the photoabsorption cross sec-on, normalized to the TRK sum rule. The data, indicated by the lled squares, are inferred from the Compton-scattering analysis f [11].

On the other hand, the single-dipole state

$$|D\rangle \equiv \sum_{i=1}^{Z} r_i \tau_i^z |0\rangle,$$

as well as the double-dipole state

$$|DD\rangle \equiv (\sum_{i=1}^{Z} r_i \tau_i^z)(\sum_{j=1}^{Z} r_j \tau_j^z)|0\rangle,$$

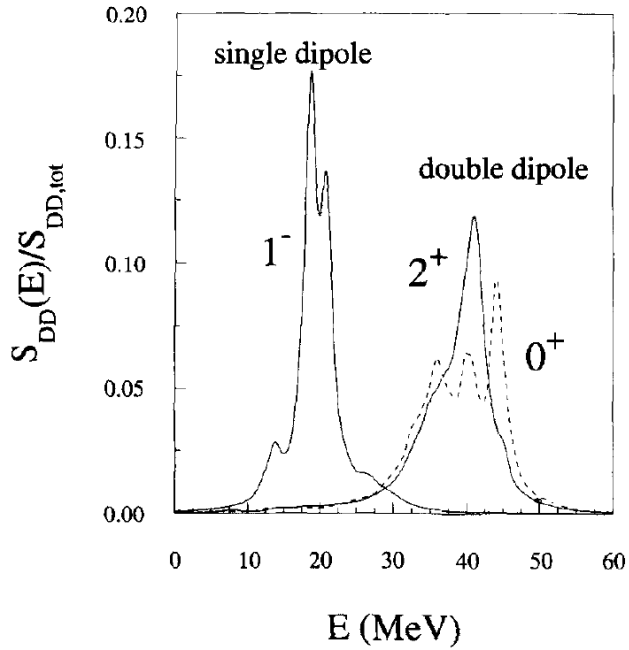

Fig. 2. The transition-strength distribution for the 0^+-component (dashed line) and 2^+-component (full line) the DGDR in ^{40}Ca. For comparison the single-dipole strength function is also given

Double Phonons: Data

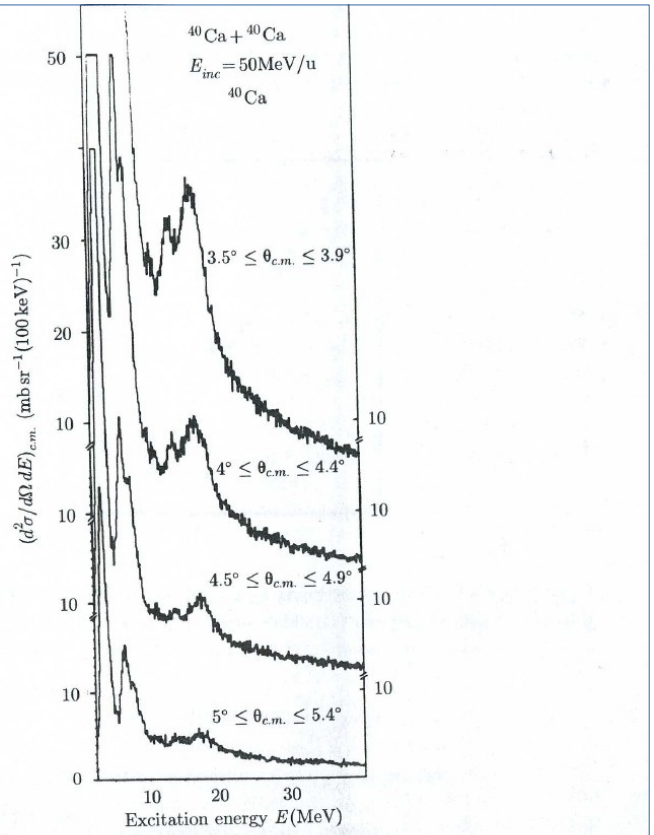

FIG. 9.12. The experimental inelastic-scattering spectrum of the $^{40}Ca + ^{40}Ca$ reaction at 50 MeV/u for different angles. From (CHO95a), by permission of Elsevier Science.

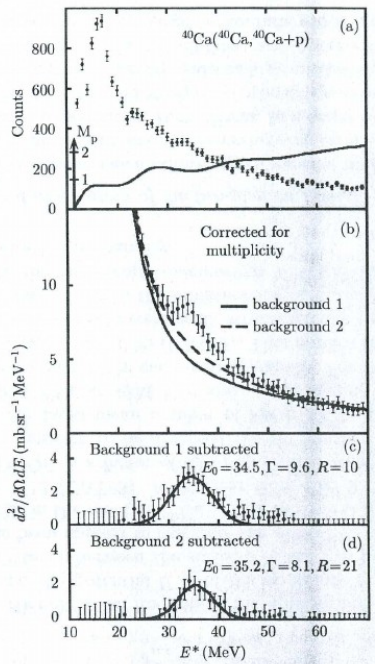

FIG. 9.14. ^{40}Ca ions resulting from $^{40}Ca + ^{40}Ca$ inelastic scattering at 50 MeV/u and at very forward scattering angles were detected in coincidence with protons emitted at backward angles. (a) The exclusive spectrum. The full line gives the calculated multiplicity of the protons assuming statistical decay. (b) Part of the inelastic exclusive spectrum corrected for the proton multiplicity. Two choices for the continuum underlying the observed bump are indicated. (c) and (d) The spectrum after subtraction of the background. The full lines indicate the fit to the resulting spectrum assuming a Gaussian shape with the parameters as indicated. R is the cross-section ratio between the ISGQR and the assumed DGQR. E_0 and Γ are in MeV. From (SCA97).

Double Phonons: UCOM-SRPA

PHYSICAL REVIEW C **81**, 024317 (2010)

Large-scale second random-phase approximation calculations with finite-range interactions

P. Papakonstantinou* and R. Roth

$$F_{\mathrm{DDR};J} = [F_{\mathrm{IVD}} \otimes F_{\mathrm{IVD}}]_{J^+}$$

$$\langle\lambda|F^{\dagger}_{\mathrm{DDR};J}|0\rangle = \sum_{\mathrm{ph}} \left[X^{\lambda}_{\mathrm{ph}}{}^{*} + (-1)^{J} Y^{\lambda}_{\mathrm{ph}}{}^{*}\right] f^{\mathrm{DDR};J}_{\mathrm{ph}} + \sum_{\mathrm{p_1p_2h_1h_2}} \left[X^{\lambda *}_{\mathrm{p_1p_2h_1h_2}} + Y^{\lambda *}_{\mathrm{p_1p_2h_1h_2}}\right] f^{\mathrm{DDR};J}_{\mathrm{p_1p_2h_1h_2}},$$

$$\begin{aligned} f^{\mathrm{DDR};J}_{\mathrm{ph}} &= (-1)^{j_{\mathrm{p}}+j_{\mathrm{h}}+J} \sum_{\mathrm{p}'} \begin{Bmatrix} 1 & 1 & J \\ j_{\mathrm{h}} & j_{\mathrm{p}} & j_{\mathrm{p}'} \end{Bmatrix} \\ &\times \langle \mathrm{p}||F_{\mathrm{IVD}}||\mathrm{p}'\rangle\langle \mathrm{p}'||F_{\mathrm{IVD}}||\mathrm{h}\rangle \\ &+ (-1)^{j_{\mathrm{p}}+j_{\mathrm{h}}+1} \sum_{\mathrm{h}'} \begin{Bmatrix} 1 & 1 & J \\ j_{\mathrm{p}} & j_{\mathrm{h}} & j_{\mathrm{h}'} \end{Bmatrix} \\ &\times \langle \mathrm{p}||F_{\mathrm{IVD}}||\mathrm{h}'\rangle\langle \mathrm{h}'||F_{\mathrm{IVD}}||\mathrm{h}\rangle, \end{aligned}$$

$$\begin{aligned} f^{\mathrm{DDR};J}_{\mathrm{p_1p_2h_1h_2}} &= 2\sqrt{\frac{(2J_{\mathrm{p}}+1)(2J_{\mathrm{h}}+1)}{(1+\delta_{\mathrm{p_1p_2}})(1+\delta_{\mathrm{h_1h_2}})}} \\ &\times \left[\langle \mathrm{p_1}||F_{\mathrm{IVD}}||\mathrm{h_1}\rangle\langle \mathrm{p_2}||F_{\mathrm{IVD}}||\mathrm{h_2}\rangle \begin{Bmatrix} j_{\mathrm{p_1}} & j_{\mathrm{h_1}} & 1 \\ j_{\mathrm{p_2}} & j_{\mathrm{h_2}} & 1 \\ J_{\mathrm{p}} & J_{\mathrm{h}} & J \end{Bmatrix} \right. \\ &- (-1)^{j_{\mathrm{h1}}+j_{\mathrm{h2}}-J_{\mathrm{h}}} \\ &\times \langle \mathrm{p_1}||F_{\mathrm{IVD}}||\mathrm{h_2}\rangle\langle \mathrm{p_2}||F_{\mathrm{IVD}}||\mathrm{h_1}\rangle \\ &\times \left. \begin{Bmatrix} j_{\mathrm{p_1}} & j_{\mathrm{h_2}} & 1 \\ j_{\mathrm{p_2}} & j_{\mathrm{h_1}} & 1 \\ J_{\mathrm{p}} & J_{\mathrm{h}} & J \end{Bmatrix} \right]. \end{aligned} \tag{A9}$$

PHYSICAL REVIEW C **81**, 024317 (2010)

Large-scale second random-phase approximation calculations with finite-range interactions

P. Papakonstantinou* and R. Roth

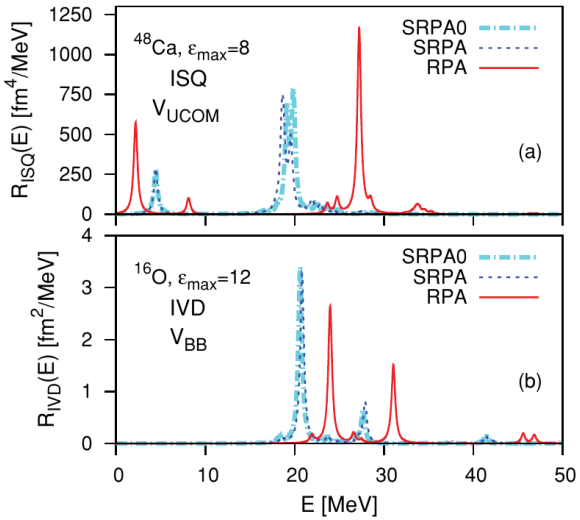

FIG. 2. (Color online) Quality of the diagonal approximation. (a) IS quadrupole response of ^{48}Ca in a single-particle basis with $\epsilon_{max} = 8$ and using V_{UCOM}. (b) IV dipole response of ^{16}O in a single-particle basis with $\epsilon_{max} = 12$ and $\ell_{max} = 8$ and using V_{BB}. Results are shown obtained with RPA, solving the full SRPA problem and using the diagonal approximation (SRPA0). (In all cases, $\Gamma = 0.5$ MeV.)

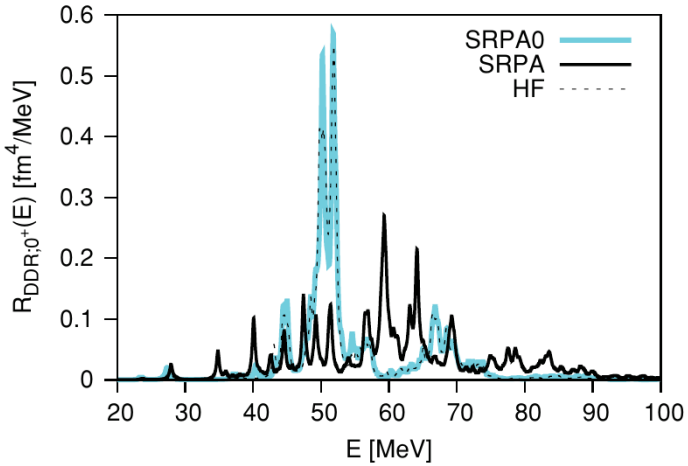

FIG. 3. (Color online) 0^+ component of the double dipole resonance of ^{16}O, calculated within a single-particle basis of seven oscillator shells. The strength function ($\Gamma = 0.5$ MeV) is calculated within SRPA and SRPA0 [diagonal approximation; Eq. (4)], as well as using the unperturbed (HF) ph and 2p2h states.

Transitions To Door-way States And Nuclear Responses Against 2-body External Fields

arXiv:2411.01709v1 [nucl-th] 3 Nov 2024

Futoshi Minato[1,2,3,*]

$$T_J \equiv [O_L P_L]^{(J)} \qquad |\langle \nu||T_J||0\rangle|^2 = \left| \sum_{mi} \left(X^{(\nu)}_{mi} + (-1)^J Y^{(\nu)}_{mi} \right) T^{(J)}_{mi} + \sum_{mnij} \sum_{J_p J_h} \left(\mathcal{X}^{(\nu)}_{mnij} + \mathcal{Y}^{(\nu)}_{mnij} \right) T^{(J_p J_h J)}_{mnij} \right|^2$$

$$T^{(J)}_{mi} = (-1)^{j_m+j_i+J} \sum_n \left\{ \begin{array}{ccc} j_i & j_m & J \\ L & L & j_n \end{array} \right\} \langle m||O_L||n\rangle\langle n||P_L||i\rangle + (-1)^{j_m+j_i+1} \sum_j \left\{ \begin{array}{ccc} j_i & j_m & J \\ L & L & j_j \end{array} \right\} \langle m||O_L||j\rangle\langle j||P_L||i\rangle,$$

$$T^{(J_p J_h J)}_{mnij} = 2 \frac{\hat{J}_p}{\sqrt{1+\delta_{mn}}} \frac{\hat{J}_h}{\sqrt{1+\delta_{ij}}} \left[\left(\begin{array}{ccc} j_m & j_n & J_p \\ j_i & j_j & J_h \\ L & L & J \end{array} \right) \times O^{(L)}_{mi} P^{(L)}_{nj} - (-1)^{j_i+j_j-J_h} \left(\begin{array}{ccc} j_m & j_n & J_p \\ j_j & j_i & J_h \\ L & L & J \end{array} \right) O^{(L)}_{mj} P^{(L)}_{ni} \right]$$

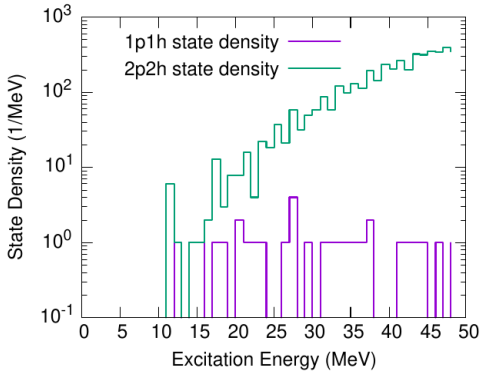

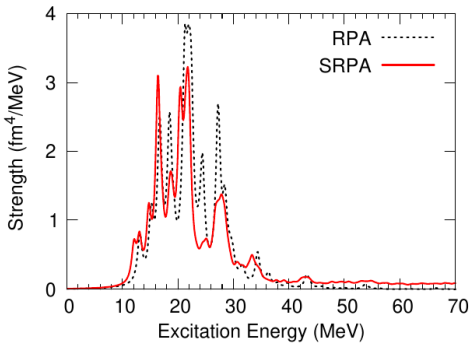

Figure 3. Strength distribution of isoscalar monopole excitations for ^{16}O. The dotted and solid lines are the results for RPA and SRPA, respectively. The lines are smoothed by a Lorentzian function with a width 1 MeV.

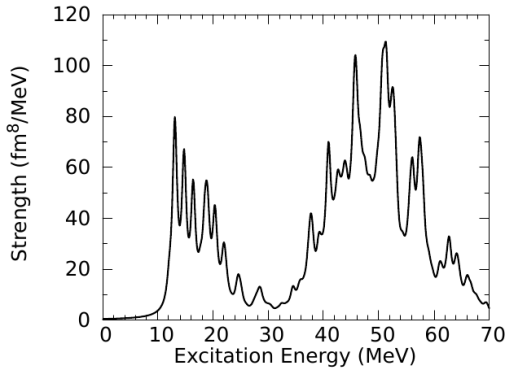

Figure 7. Calculated strength distribution of double isoscalar monopole operator for ^{16}O. The strength distribution is smoothed by a Lorentzian function with a width 1 MeV.

Backup Slides

RPA Matrices (1p-1h configurations)

$$A_{1,1'} = \langle HF \mid \left[a_h^\dagger a_p, [H, a_{p'}^\dagger a_{h'}]\right] \mid HF\rangle$$

$$B_{1,1'} = -\langle HF \mid \left[a_h^\dagger a_p, [H, a_{h'}^\dagger a_{p'}]\right] \mid HF\rangle.$$

SRPA Matrices (1p-1h and 2p-2h configurations)

$$A_{1,2} = A_{2,1}^* = \left\langle HF\middle|\left[a_h^\dagger a_p, [H, a_{p_1}^\dagger a_{p_2}^\dagger a_{h_1} a_{h_2}]\right]\middle|HF\right\rangle$$

$$A_{2',2} = \left\langle HF\middle|\left[a_{h_2'}^\dagger a_{h_1'}^\dagger a_{p_2'} a_{p_1'}, [H, a_{p_1}^\dagger a_{p_2}^\dagger a_{h_1} a_{h_2}]\right]\middle|HF\right\rangle$$

$$B_{1,2} = B_{2,1}^* = -\left\langle HF\middle|\left[a_p^\dagger a_h, [H, a_{p_2}^\dagger a_{p_2}^\dagger a_{h_1} a_{h_2}]\right]\middle|HF\right\rangle = 0$$

$$B_{2',2} = -\left\langle HF\middle|\left[a_{p_1'}^\dagger a_{p_2'}^\dagger a_{h_1'} a_{h_2'}, [H, a_{p_1}^\dagger a_{p_2}^\dagger a_{h_1} a_{h_2}]\right]\middle|HF\right\rangle = 0$$

RPA Matrices (1p-1h configurations)

$$A_{1,1'} \sim \epsilon_{1ph} + \langle ph|V|ph\rangle$$

$$B_{1,1'} \sim +\langle pp|V|hh\rangle$$

SRPA Matrices (1p-1h and 2p-2h configurations)

$$A_{1,2} \sim \langle ph|V|pp\rangle + \langle hh|V|hp\rangle$$

$$A_{2',2} \sim \epsilon_{2ph} + \langle ph|V|ph\rangle + \langle pp|V|pp\rangle + \langle hh|V|hh\rangle$$

SRPA diagrams

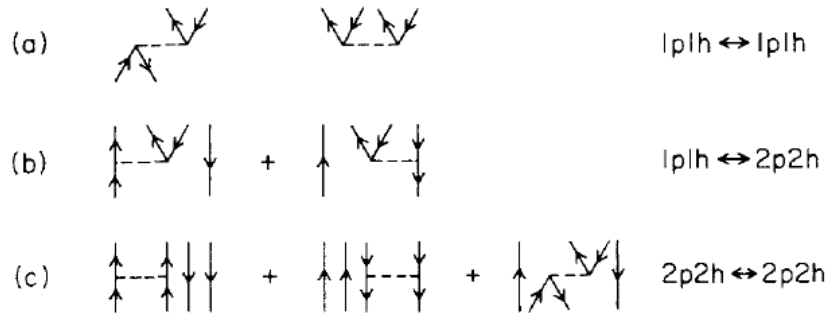

Fig. 2.1. Two-body interaction diagrams iterated by the SRPA equations. a. 1p1h RPA diagrams; b. coupling terms between 1p1h and 2p2h states; and c. mixing terms in the 2p2h subspace.

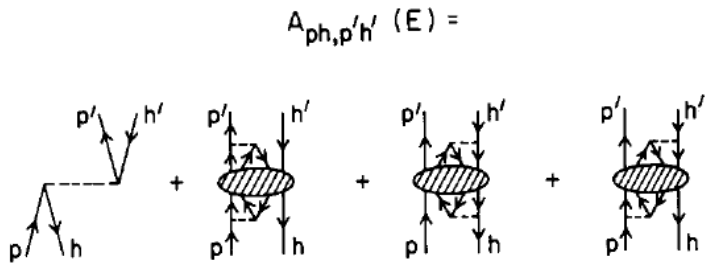

Fig. 2.2. Energy-dependent 1p1h interaction matrix elements after formal elimination of the 2p2h subspace.

Previous (1980s and 1990s) applications

Nuclear Physics A560 (1993) 765–796
North-Holland

NUCLEAR PHYSICS A

Second RPA calculations of the charge-exchange quadrupole response functions in closed-shell nuclei

S. Ait-Tahar [a,b] and D.M. Brink [a]

In the present calculations, we make a second approximation by not including the contributions from the real part of the self-energy term. The inclusion of this term is known to distort the spectrum and to shift the resonance energies so that the resonant peaks are no longer found at their RPA values [21,25]. The justification of this approximation rests upon the following arguments. The first problem, namely the resonance shift, can be avoided by simply omitting the on-shell part of the real part of $\Sigma(\omega)$ as described by, for example, Schwesinger and Wambach [26]. This can be justified on the grounds that we are using an effective interaction, namely the Skyrme interaction. The parameters of this interaction are adjusted phenomenologically to describe the bulk properties of nuclei and HF results with these parameters reproduce the gross properties of the experimental single-particle spectrum fairly well. The difficulty related to the effects of the real part inherent to the SRPA can be avoided if one works in the framework of the extended RPA theory [13,14,27] which unlike the SRPA incorporates correlations in the ground state. However, in such calculations, one should not use the effective interactions usual to ordinary HF–RPA calculations but, instead, adopt residual interactions derived from realistic potentials like the G-matrix interaction [28]. Such interactions are known to give unreasonable results for the HF calculations and thus, the single-particle energies need to be obtained from some model single-particle basis and not from realistic single-particle energies as these latter already incorporate all higher-order effects [14].

Beta-decay Half-life

$$T_{1/2} = \frac{D}{g_A^2 \int^{Q_\beta} S(E) f(Z,\omega) dE}.$$

$$f(Z,\omega) = \int_{m_e c^2}^{\omega} p_e E_e (\omega - E_e)^2 F_0(Z+1, E_e) dE_e,$$

Fermi function of the emitted electron

Gamow-Teller transition

ΔS=1 ΔL=0 ΔT=1

operator

$$\hat{O}_{\mathrm{GT}^-} = \sum_{i=1}^{A} \vec{\sigma}(i) \cdot \tau_-(i)$$

Transition probability

$$B(\mathrm{GT}^-) = \sum_{\nu} |\langle \nu | \hat{O} | 0 \rangle|^2$$

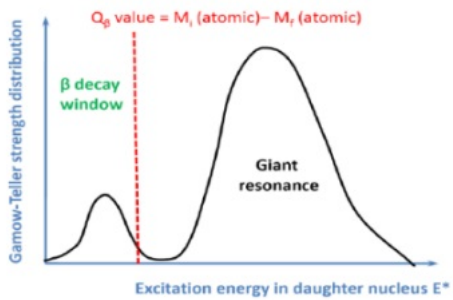

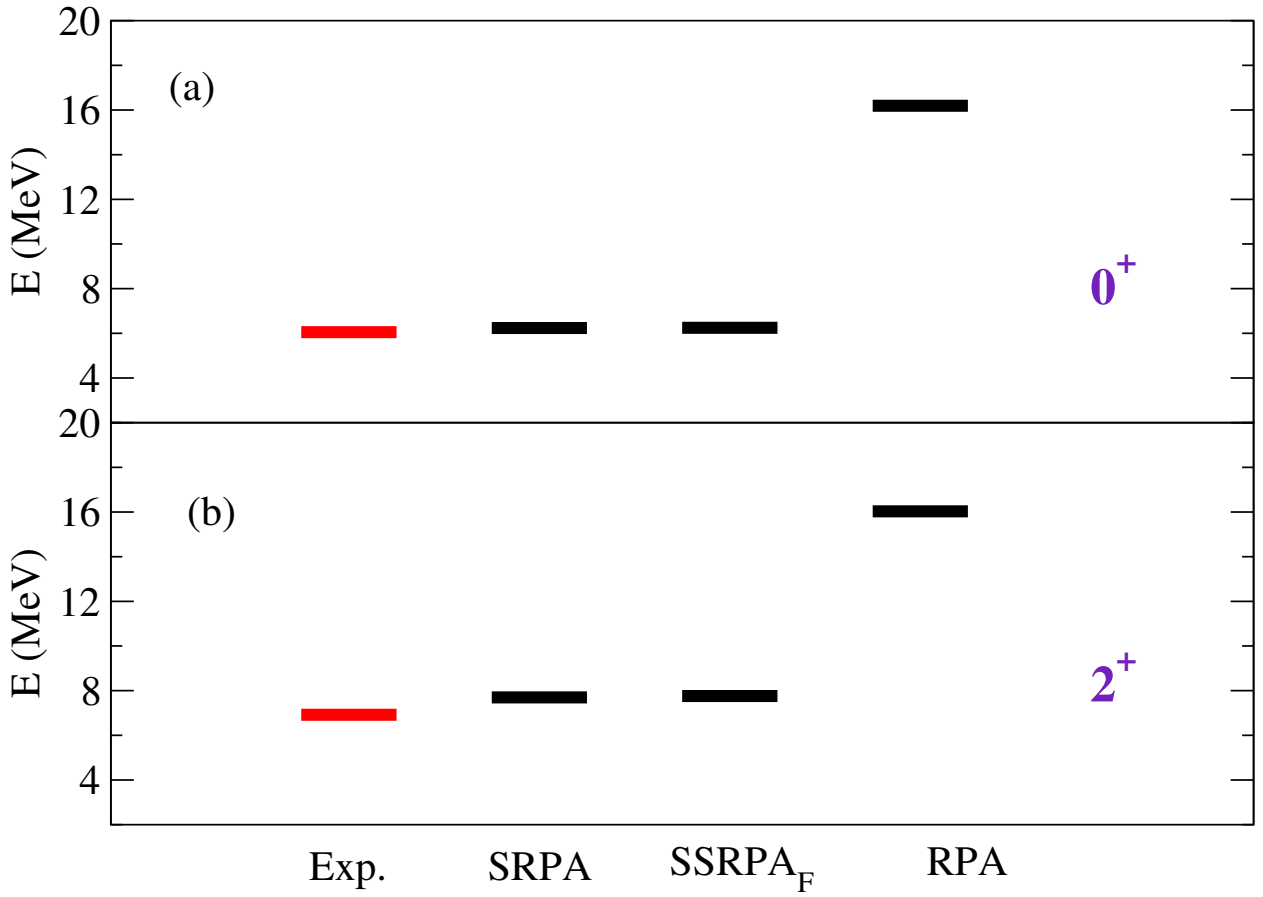

Comparison of values from the standard SRPA, the SSRPA$_F$, the RPA, and experiment for the energy of the first low–lying 0^+ (a) and 2^+ (b) states.

Transition densities

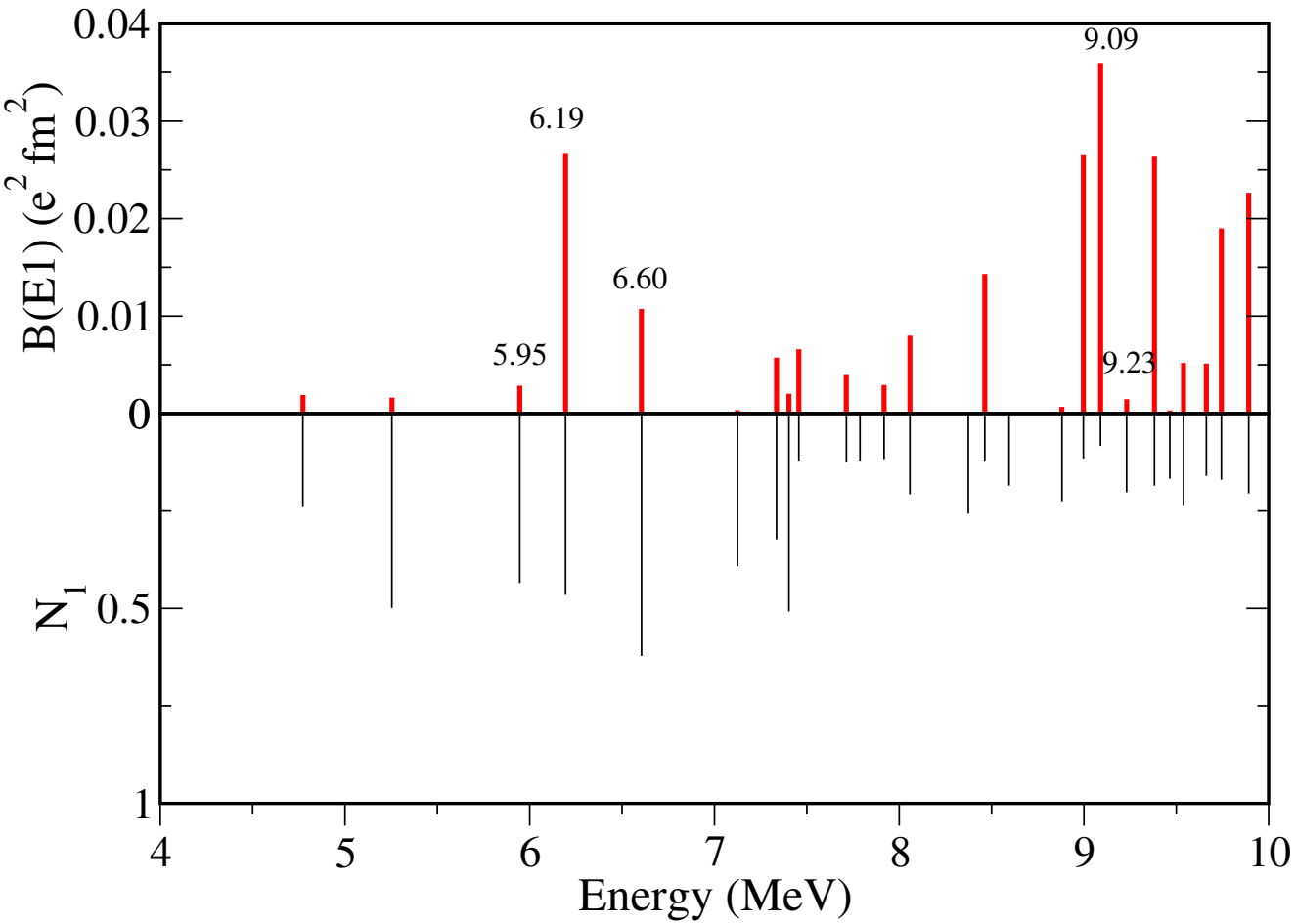

Transition densities

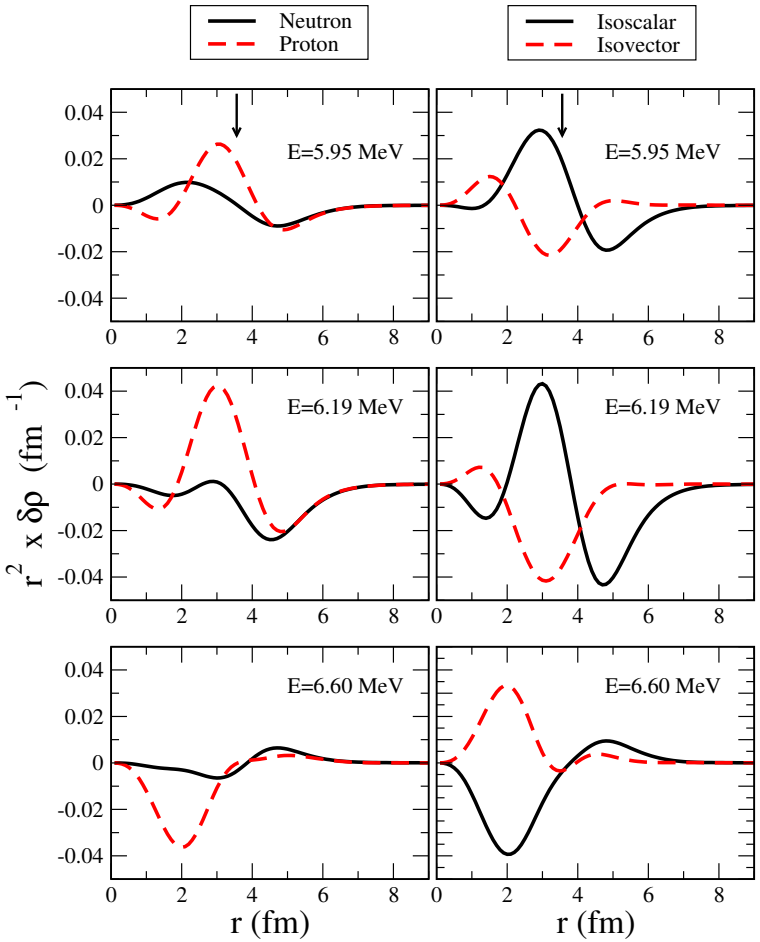

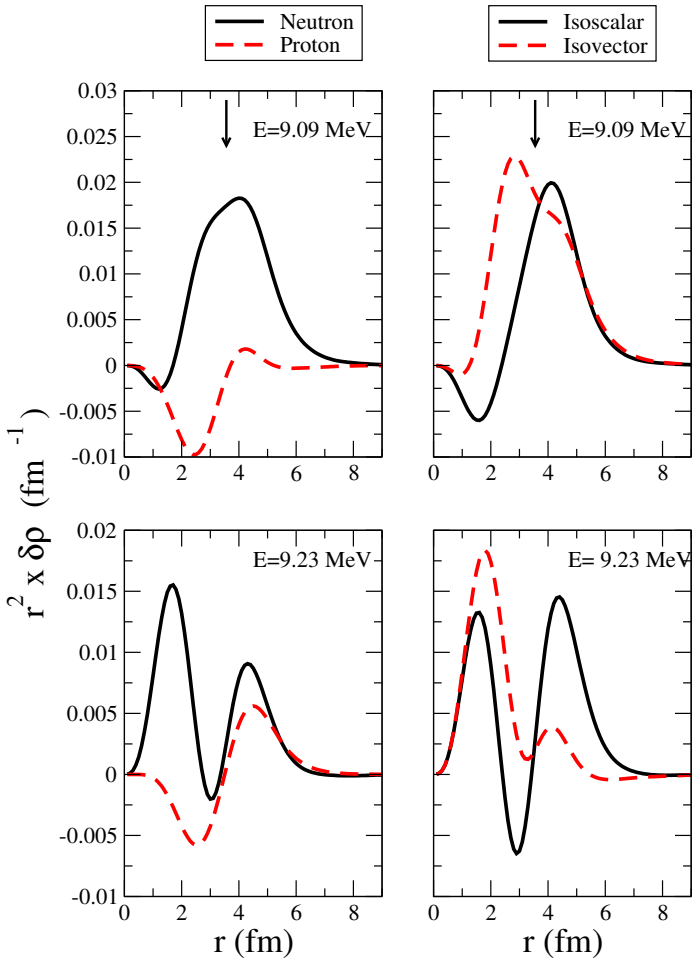

Low–energy states contribution to the EWSR.

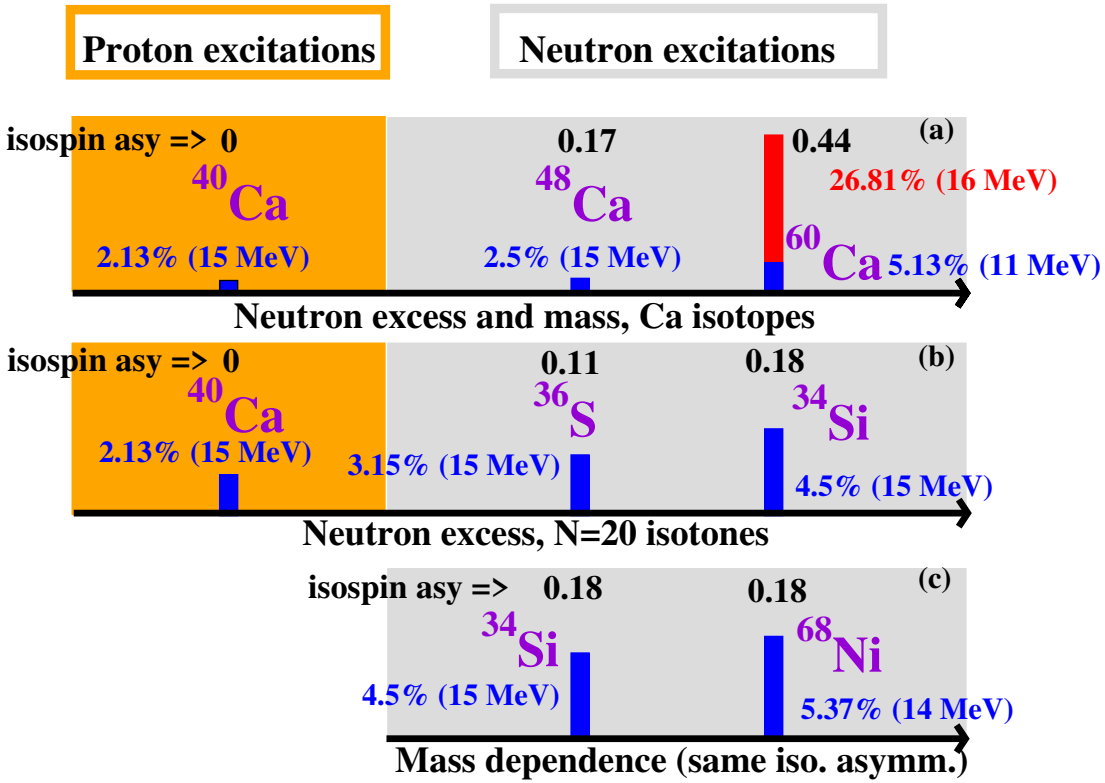

Percentages of the EWSR for several nuclei and corresponding isospin asymmetry $\delta = (N - Z)/A$.
(a) Ca isotopes: evolution as a function of the neutron excess and the mass;
(b) $N = 20$ isotones: evolution as a function of the neutron excess;
(c) Evolution as a function of the mass for two nuclei with the same isospin asymmetry, ^{34}Si and ^{68}Ni.

GT$^-$ Strength Distribution ^{48}Ca

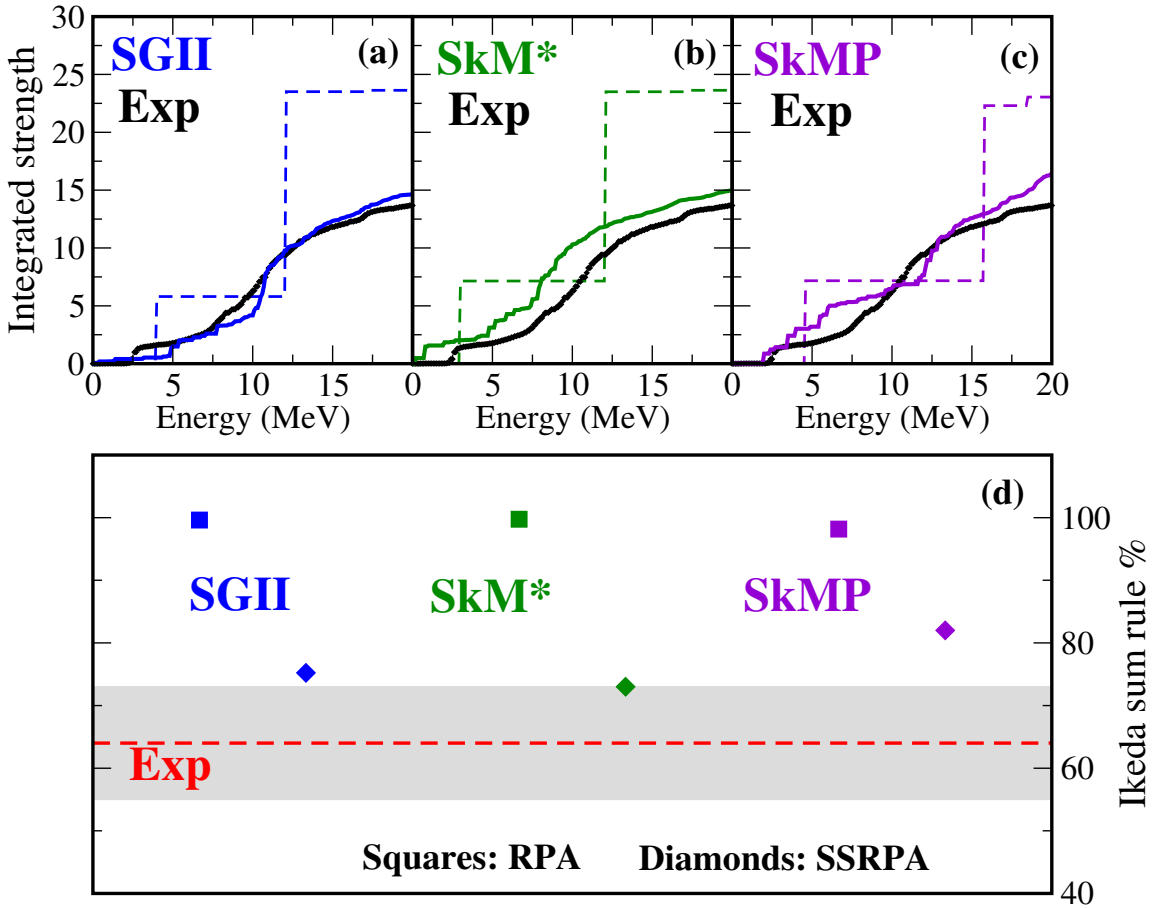

(a), (b), (c) Strengths integrated up to 20 MeV with different parameterizations.

(d) RPA and SSRPA percentages of the Ikeda sum rule below 30 MeV compared with the experimental one.

From D.Gambacurta, M. Grasso, J. Engel, Phys. Rev. Lett. 125, 212501 (2020)

GT$^-$ Strength Distribution ^{48}Ca, sum rules in the two channels

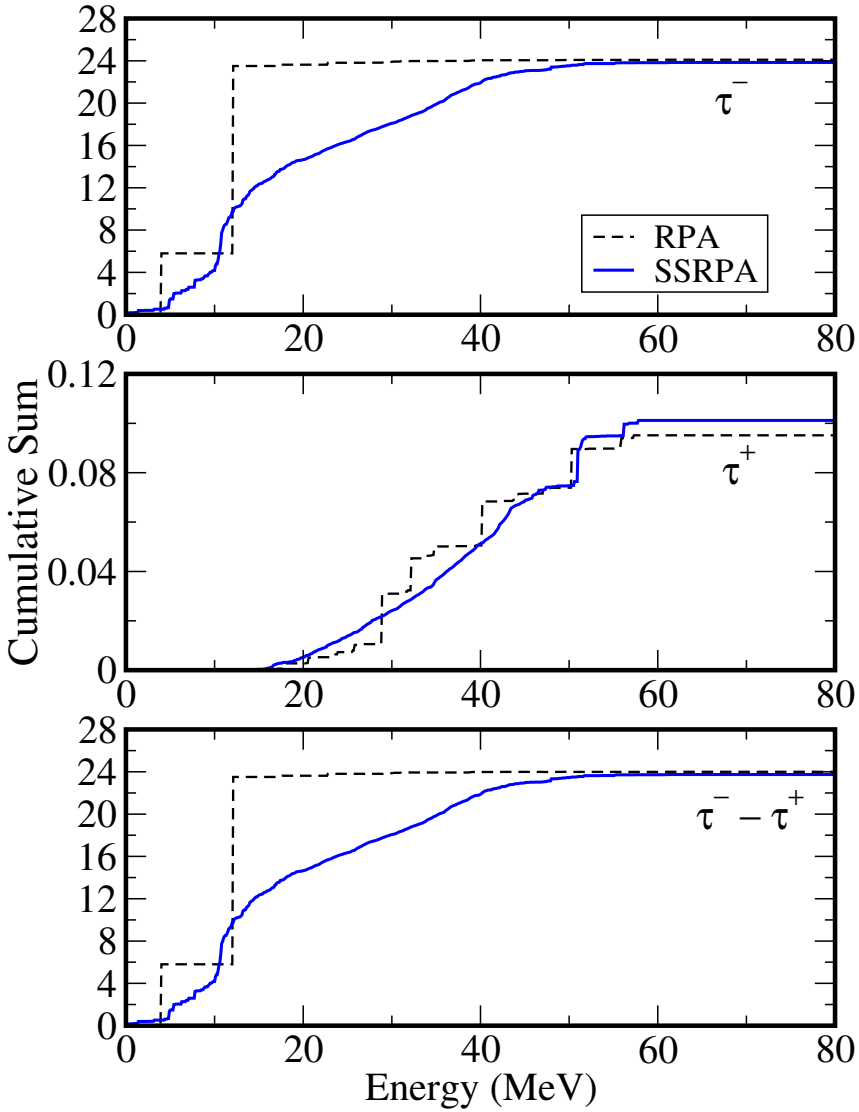

GT^- Strength Distribution for the nuclei ^{22}O (blue) and ^{14}C (green): SSRPA versus *ab initio* Coupled Cluster including two-body currents [1].

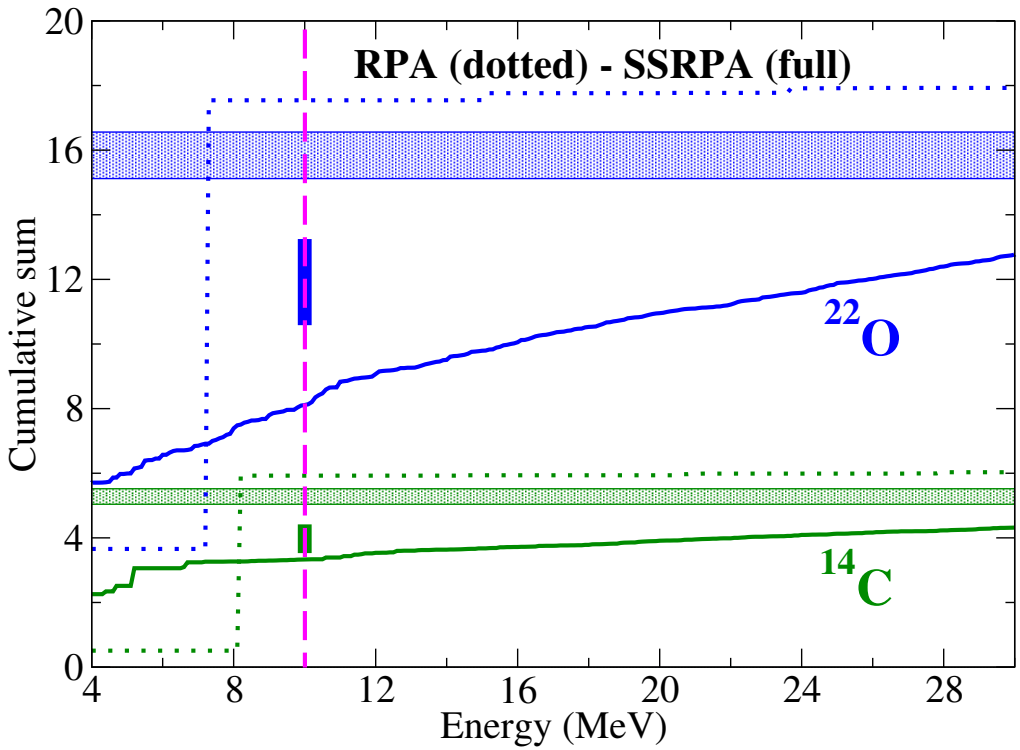

The blue and green horizontal areas represent the reduction of the total Ikeda sum rule $S_{GT-} - S_{GT+}$ from *ab initio* results [1].
The blue and green vertical intervals correspond to a reduction of (70-80 %) of the sum rule exhausted at 10 MeV.
[1] A. Ekstrom *et al.* Phys. Rev. Lett. 113, 262504 (2014)
See also Gysbers et al. Nature Phys. 15 428 (2019)

From D.Gambacurta and M. Grasso, Phys. Rev. C 105, 014321, (2022)

The Subtraction Method: Justification in EDF

- Residual interaction

$$V(\mathbf{r}_1,\mathbf{r}_2) = \left.\frac{\delta^2 E[\rho]}{\delta\rho(\mathbf{r}_1)\delta\rho(\mathbf{r}_2)}\right|_{\rho_0} \equiv V^{RPA}(\mathbf{r}_1,\mathbf{r}_2)$$

- In SRPA (due coupling with 2p2h) V becomes energy dependent:

$$V^{SRPA}(\mathbf{r}_1,\mathbf{r}_2) \longmapsto V^{SRPA}(\mathbf{r}_1,\mathbf{r}_2,\omega)$$

- We want to recover, in the static limit, the RPA response, therefore

$$V^{SRPA}(\mathbf{r}_1,\mathbf{r}_2) \longmapsto \tilde{V}^{SRPA}(\mathbf{r}_1,\mathbf{r}_2,\omega) =$$

$$V^{SRPA}(\mathbf{r}_1,\mathbf{r}_2,\omega) - V^{SRPA}(\mathbf{r}_1,\mathbf{r}_2,\omega=0) + V^{RPA}(\mathbf{r}_1,\mathbf{r}_2)$$

- assuring that

$$\tilde{V}^{SRPA}(\mathbf{r}_1,\mathbf{r}_2,\omega=0) = V^{RPA}(\mathbf{r}_1,\mathbf{r}_2)$$

Time-dependent version of the HK theorem (known as the Runge-Gross theorem [1]) RPA provides "exact" adiabating limit of the response

[1] E. Runge and E. K. U. Gross, Phys. Rev. Lett. 52, 997 (1984)

Why the Gogny interaction?

- SRPA: not only p-h matrix elements appear in the Eqs of Motion
- Gogny interaction adjusted both in the p-h and p-p channels
- Finite range interaction $\longmapsto$ more stability is expected
- However, density-dependent part is still zero range type
- D. Gambacurta, M. Grasso, V. De Donno, G. Co', and F. Catara, Phys. Rev. C 86, 021304 (2012)

Isoscalar Strength Distribution in ^{16}O, Gogny case (D1S)

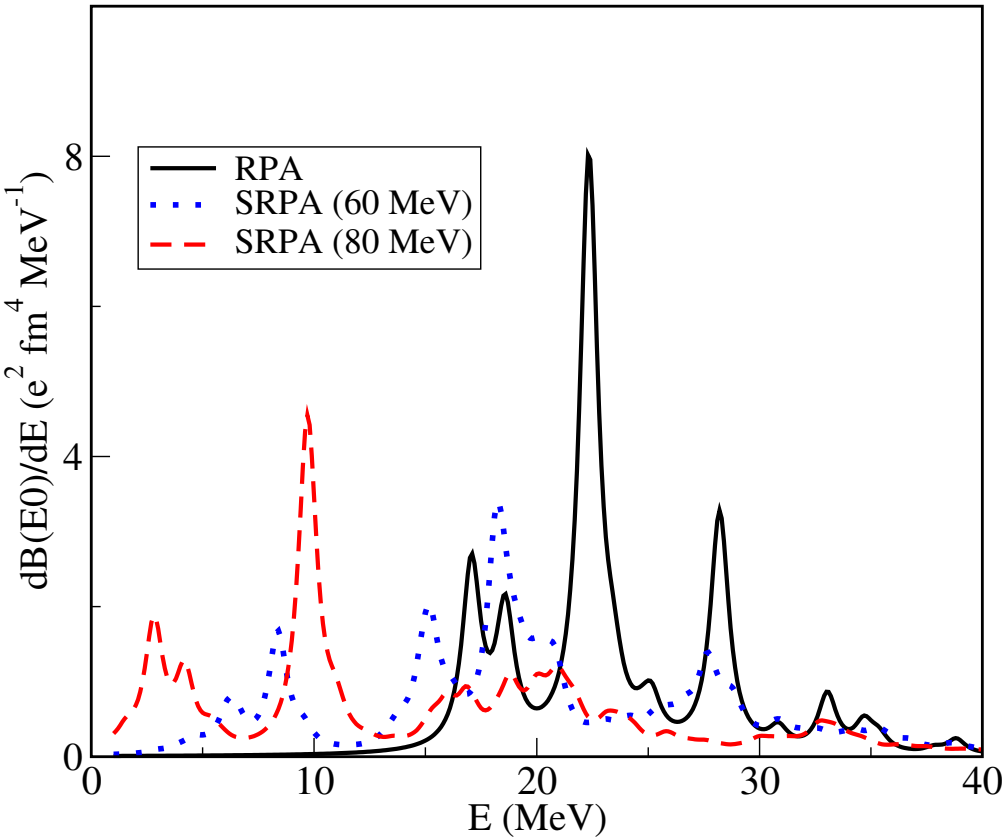

"Anomalous" $\nu - \pi$ matrix elements

- neutron-proton ($\nu\pi$) matrix elements in SRPA matrices, are very large (from 5 to 10 times larger)
- These matrix elements do not contribute to standard RPA calculations
- Their effects are especially strong in the matrix elements coupling 1ph and 2ph configurations.
- Similar behaviour found also in multiparticle-multihole calculations, N. Pillet *et al.*, Phys. Rev. C 85, 044315 (2012)

Two different kinds of calculations:

- (a) A full SRPA calculation where all the 2ph configurations are included
- (b) Only the 2ph configurations composed by pure neutron or proton excitations are included (SRPA*).

Isoscalar Strength Distribution in ^{16}O, Gogny case (D1S)

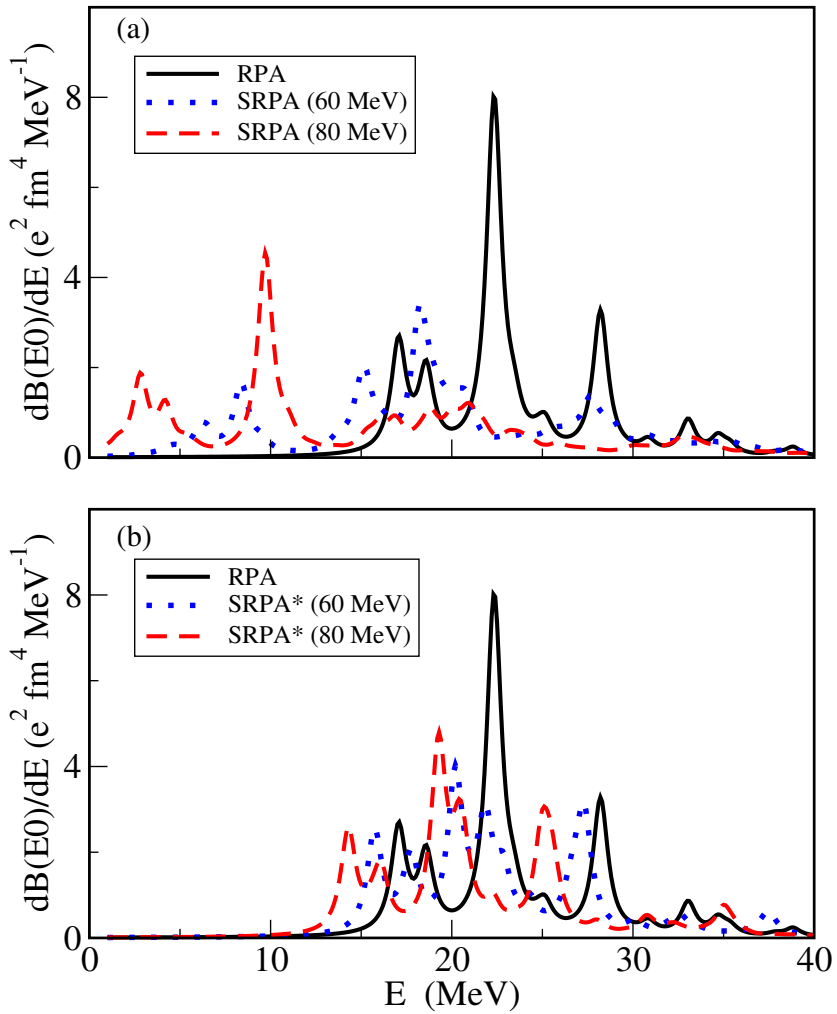

Monopole Strength Distribution in ^{16}O, Gogny case (D1S)

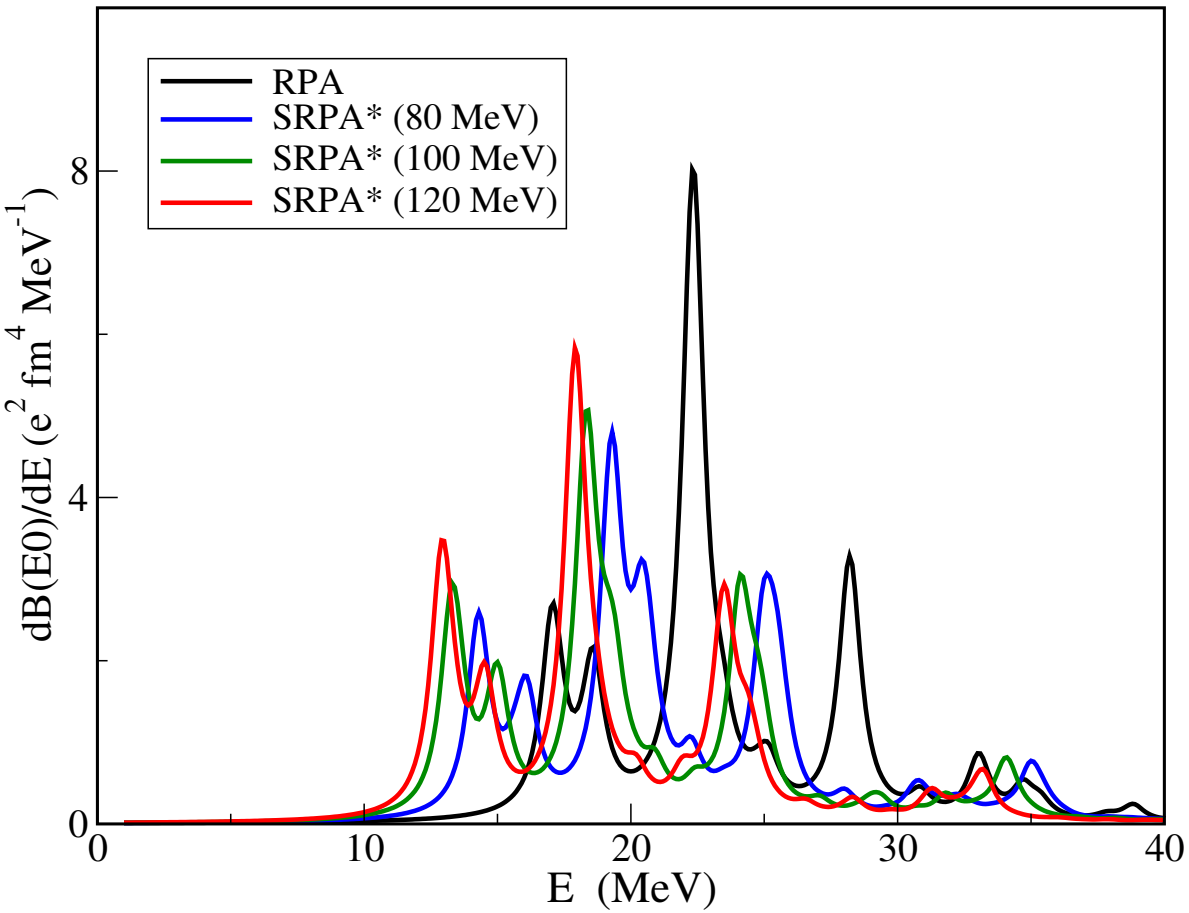

Monopole Strength Distribution: SRPA vs SSRPA:the Gogny (D1S) case

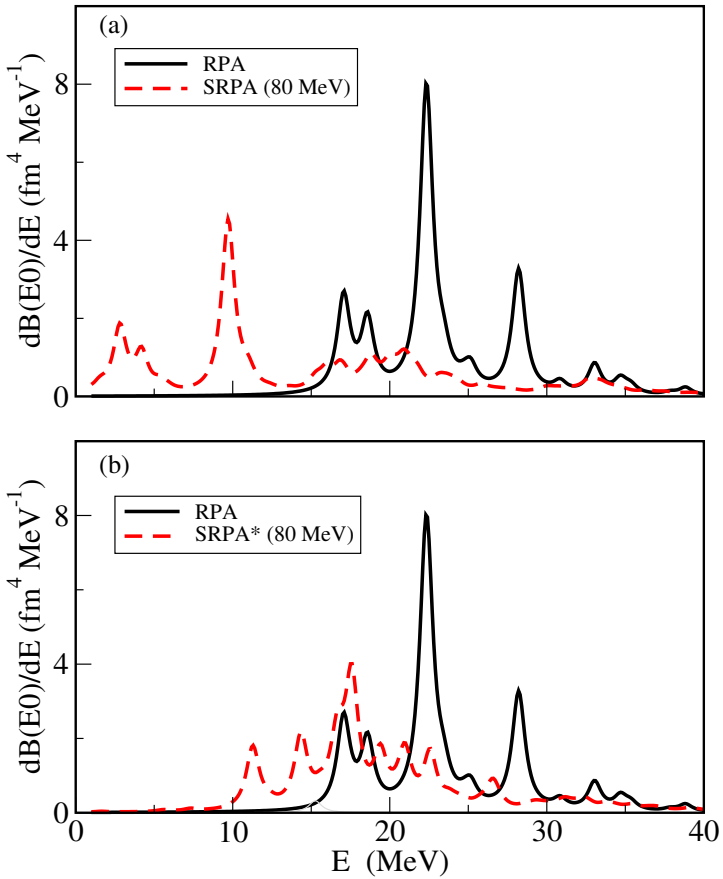

D. G. and M. Grasso, The European Physical Journal A, 52(7), 2016

Monopole Strength Distribution: SRPA vs SSRPA:the Gogny (D1S) case

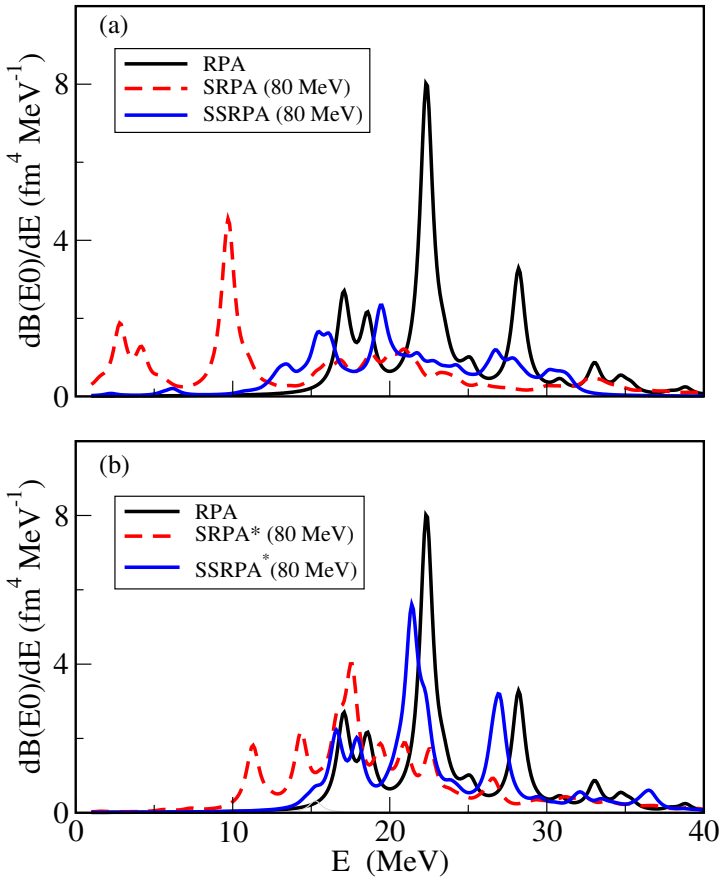

D. G. and M. Grasso, The European Physical Journal A, 52(7), 2016

Some applications of the SSRPA

- Dipole response in ^{48}Ca
- Low-lying monopole modes in neutron-rich nuclei
- Quadrupole response in closed-shell nuclei (ISGQR)
- Gamow-Teller excitation and Beta-decay

Dipole Polarizability

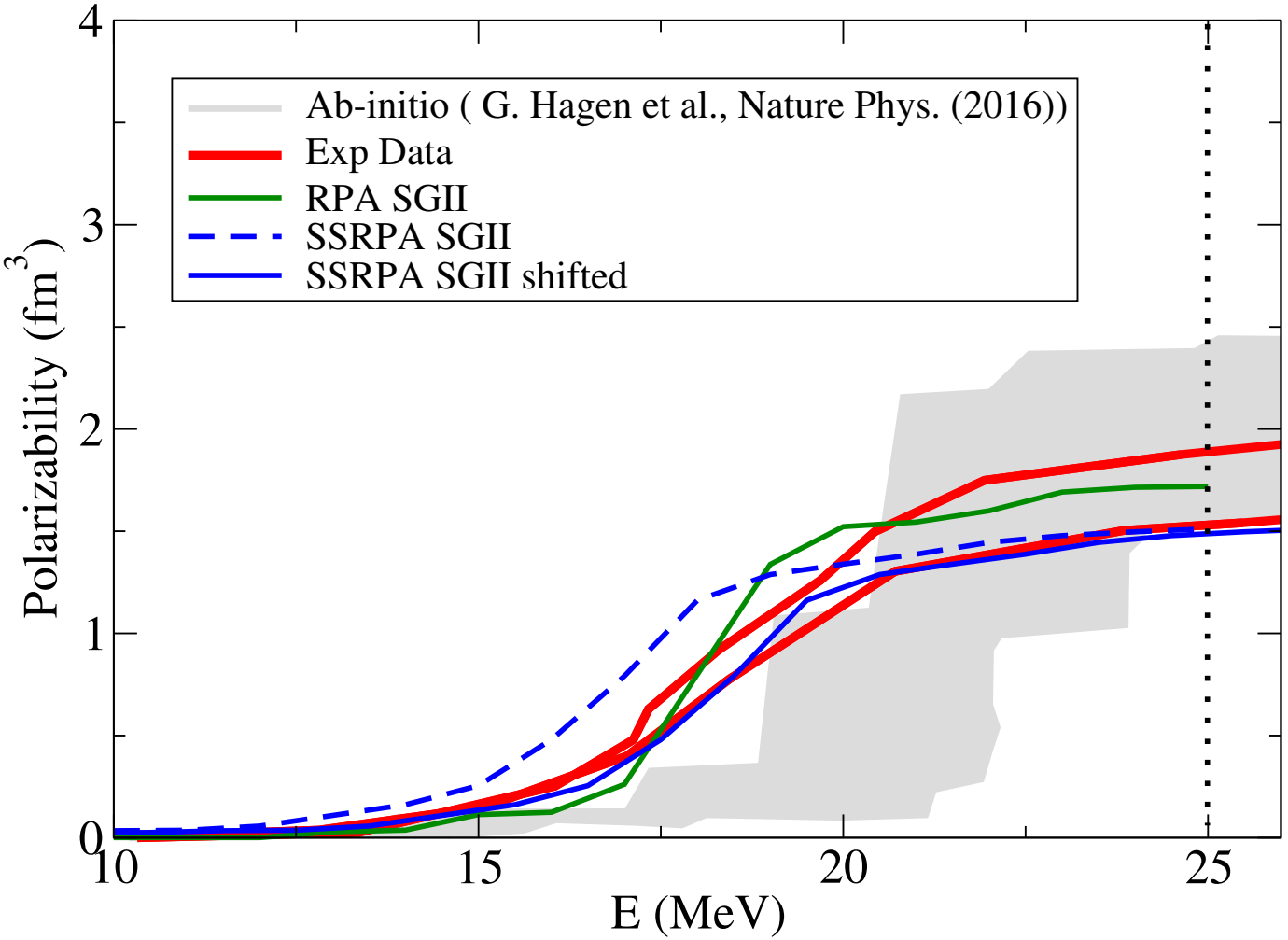

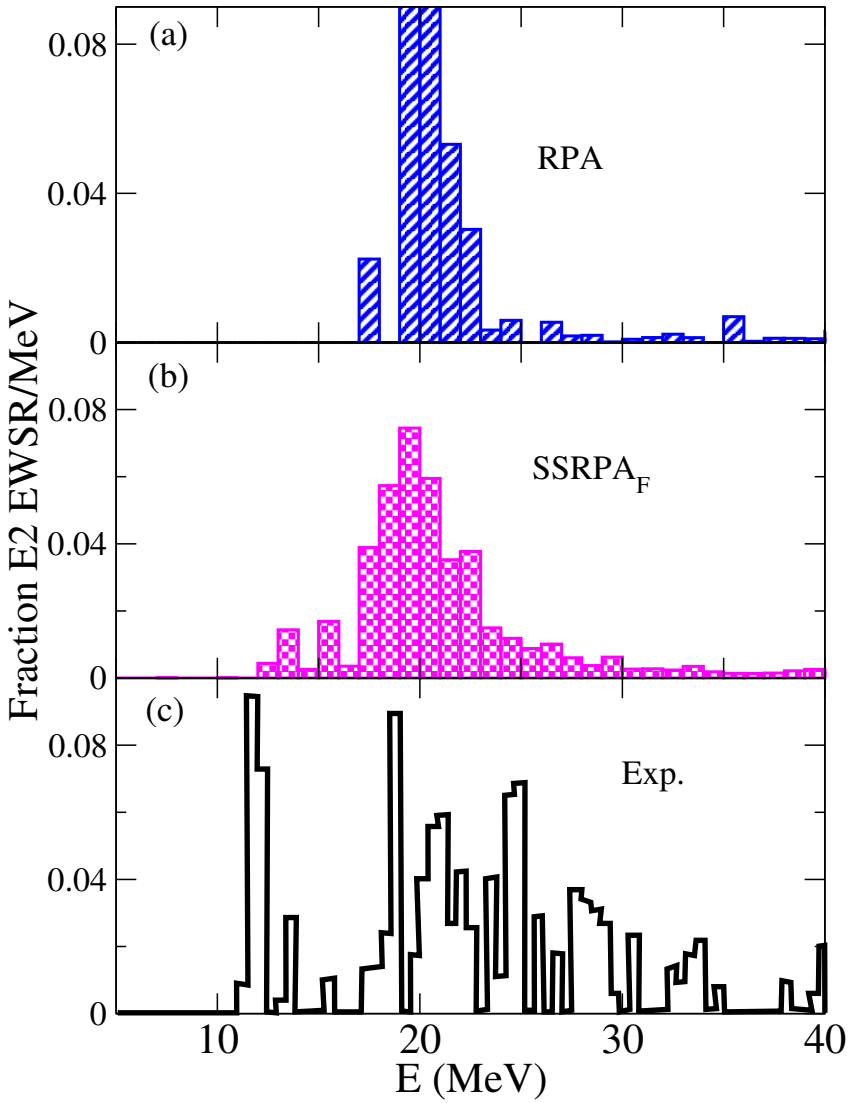

Same as in Fig. **??** but for the $E2$ EWSR.

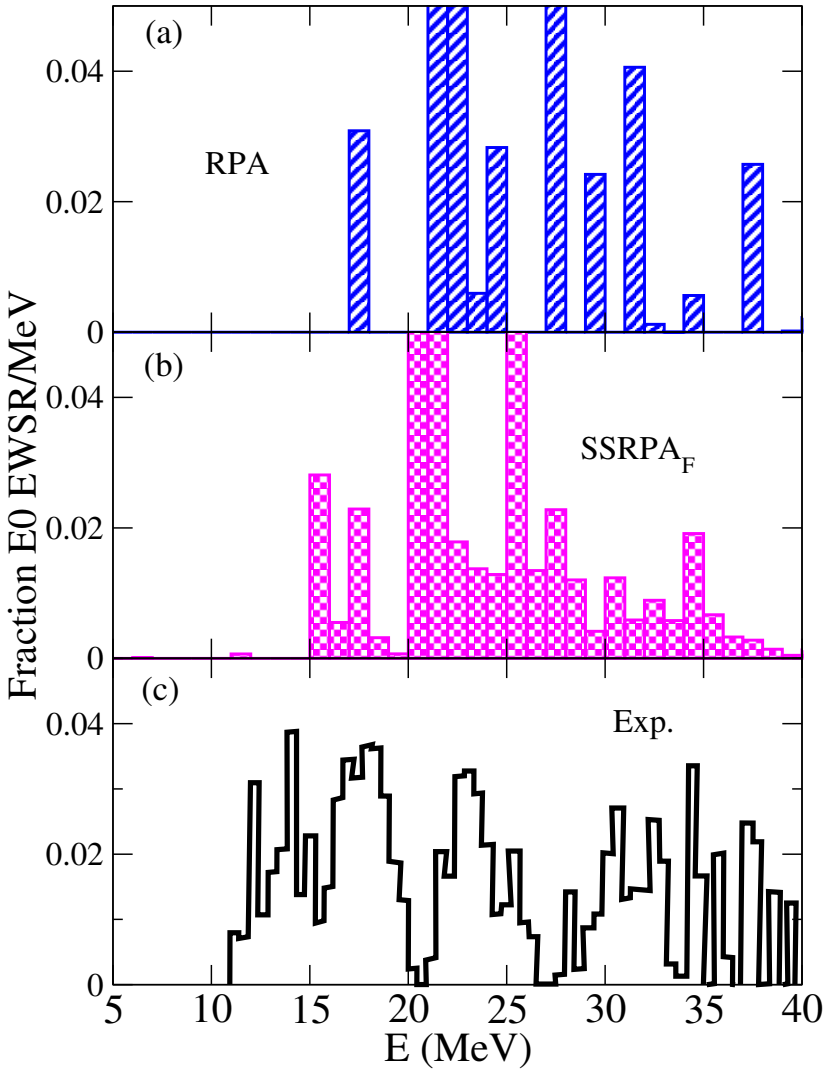

Fraction of the $E0$ EWSR in the RPA (a) and in the SSRPA$_F$ (b). The experimental fraction, from Y.-W. Lui, H.L. Clark, and D.H. Youngblood, Phys. Rev. C 64, 064308 (2001) is in panel (c).

Effect of J^2 terms

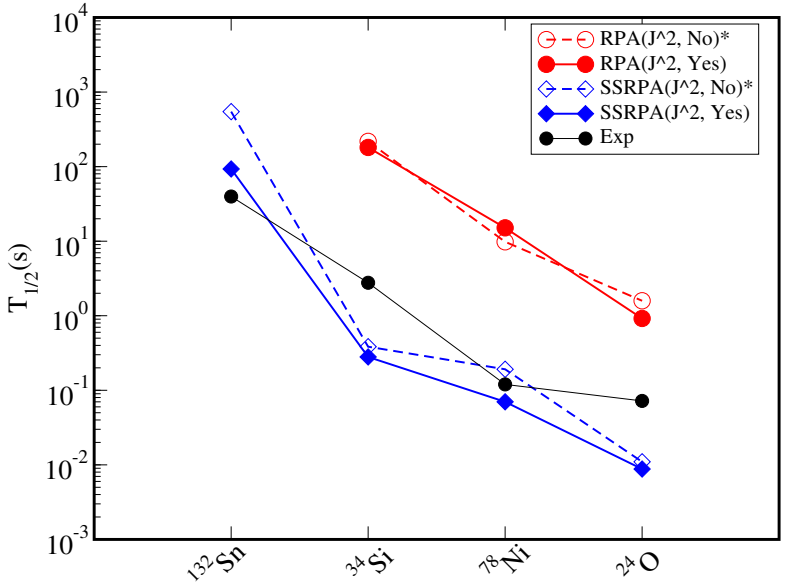

SGII interaction

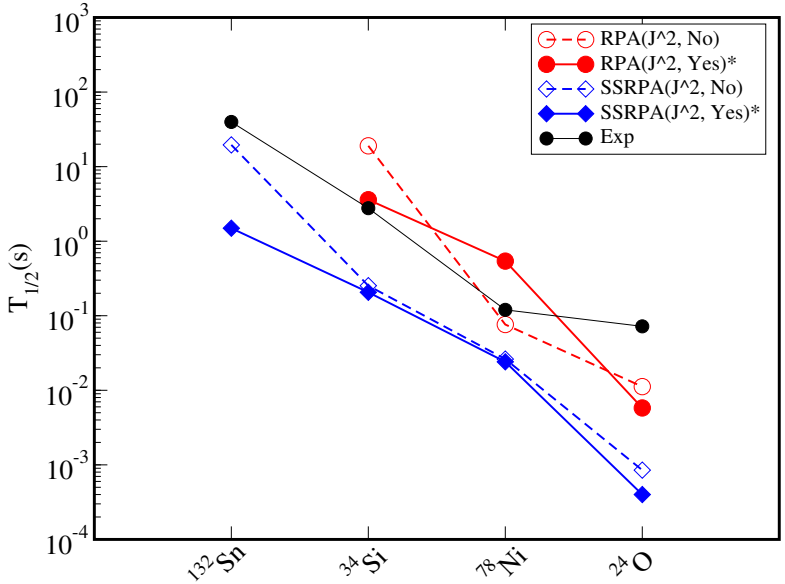

SLy5 interaction

Numerical complexity: different approximations schemes

Numerical complexity

- The most demanding task is related to the treatment of the $A_{22'}$ matrix
- The number of 2p-2h configurations can be very large$\simeq 10^7, 10^8$
- We need to calculate the "full" spectrum
- Most demanding tasks:
  a) subtraction procedure, $A_{22'}$ inversion
  b) diagonalization of the SSRPA eigenvalue problem
- Strong simplification if $A_{22'}$ is assumed to be diagonal

Different calculation scheme:

1. SSRPADD: $A_{22'}$ is Diagonal both in a) and b)
2. SSRPADF: $A_{22'}$ is Diagonal both in a) and Full in b)
3. SSRPAFF: $A_{22'}$ is Full both in a) and in b)

GT$^-$ Strength Distribution ^{48}Ca SSRPA results

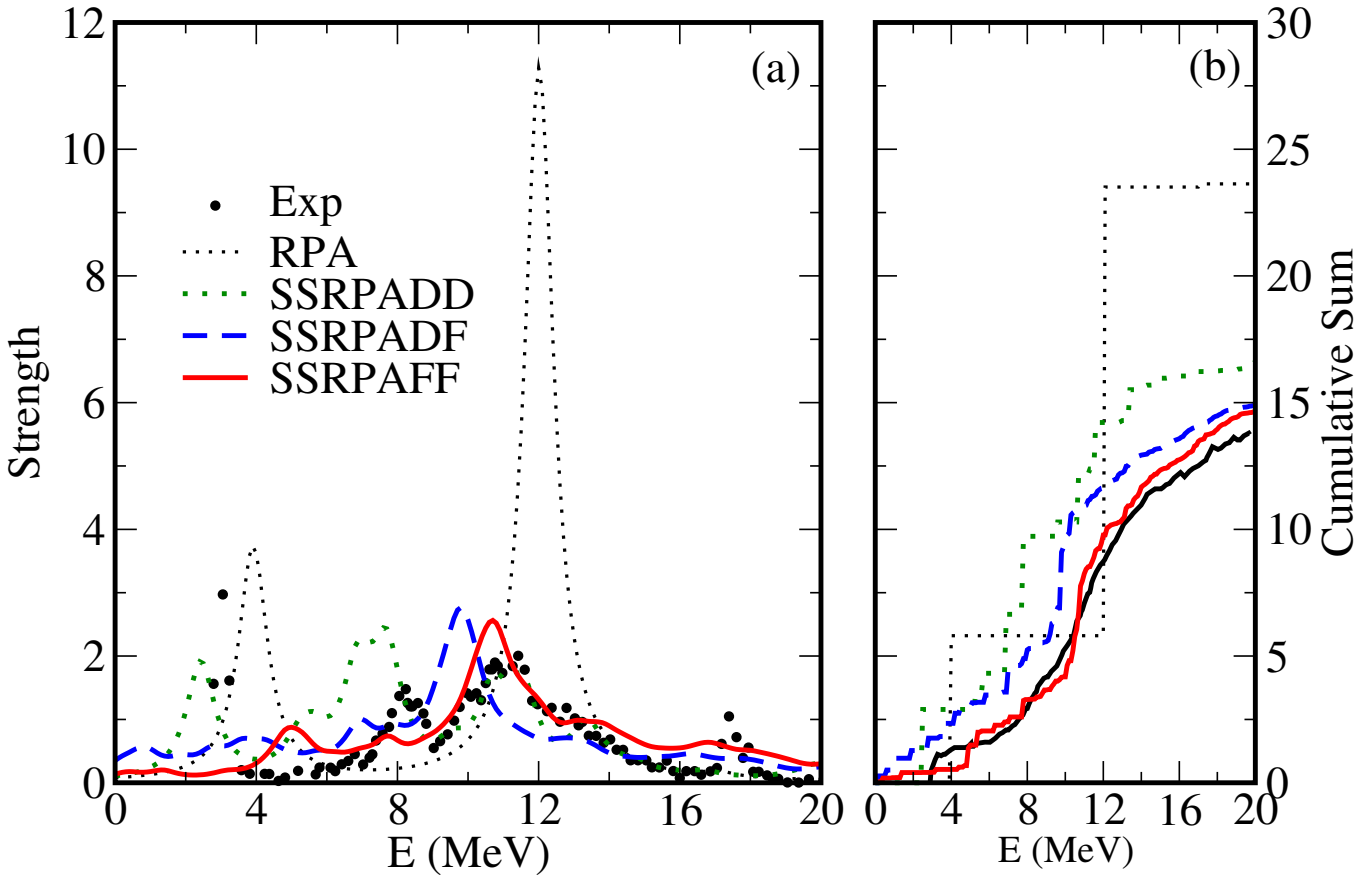

Comparison between SSRPADD, SSRPADF and SSRPAFF results .

From D.Gambacurta and M. Grasso, Phys. Rev. C 105, 014321, (2022)

GT$^-$ Strength Distribution ^{48}Ca, 2p2h cutoff EC (MeV) dependence

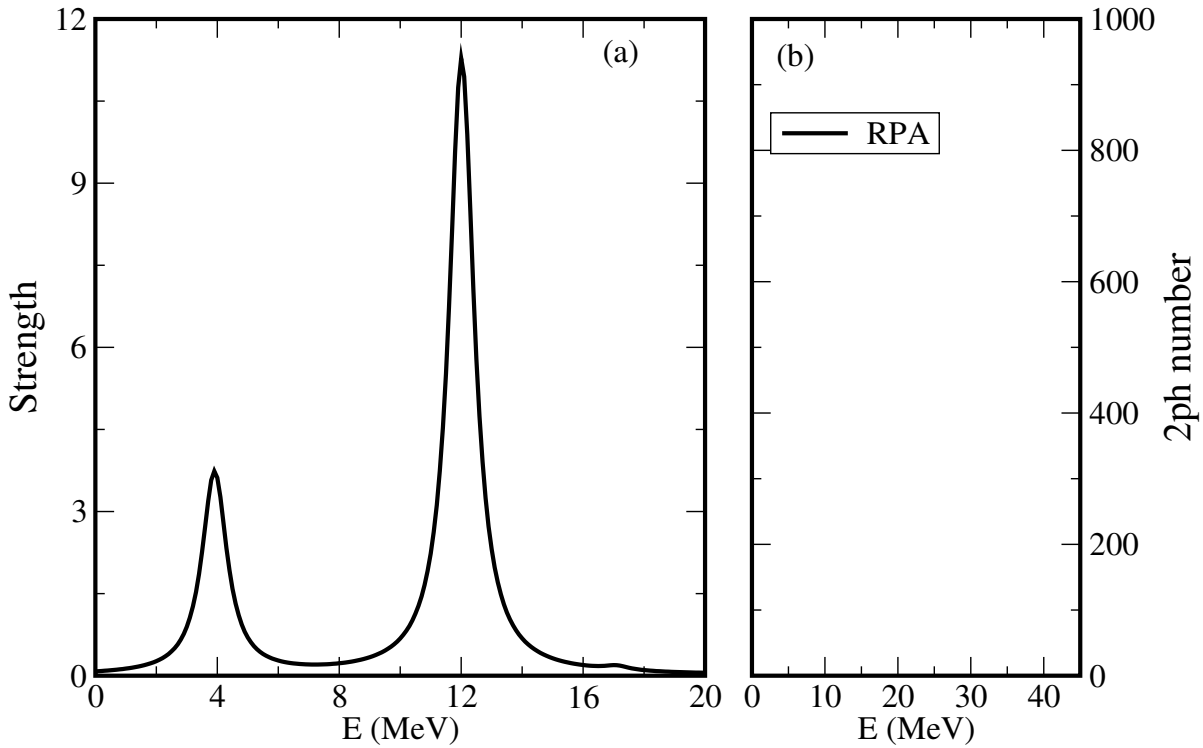

GT^- Strength Distribution ^{48}Ca, 2p2h cutoff EC (MeV) dependence

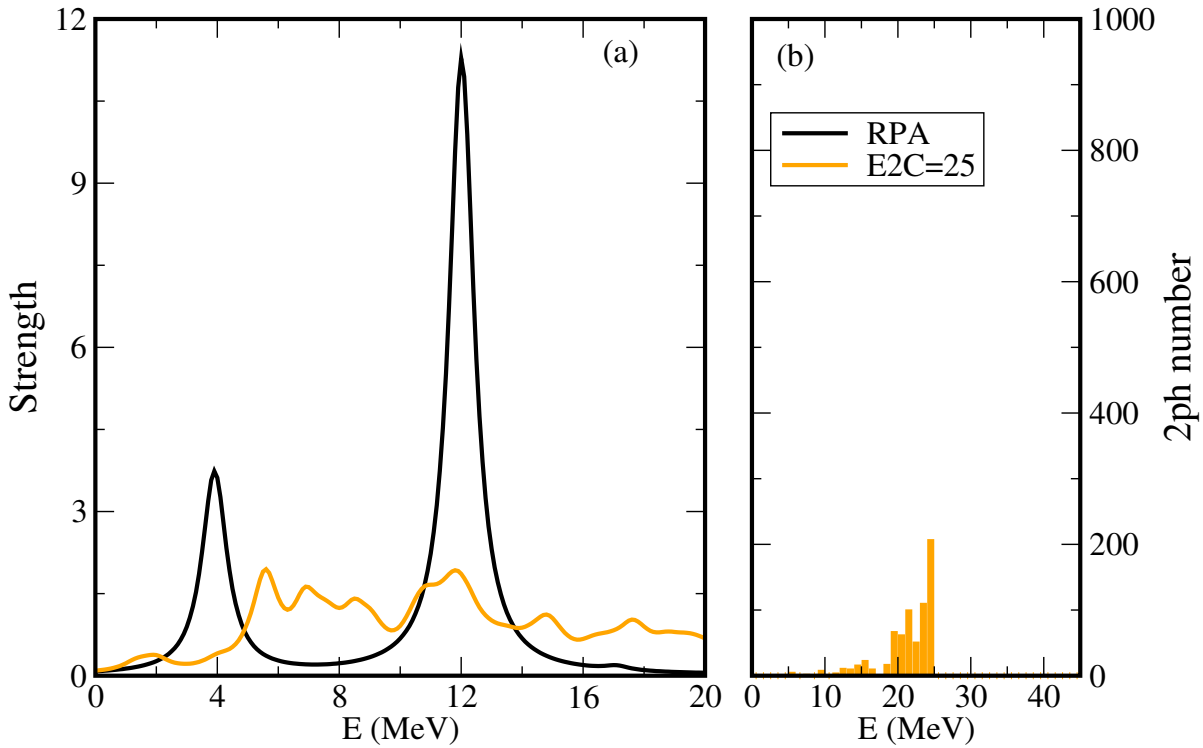

GT^- Strength Distribution ^{48}Ca, 2p2h cutoff EC (MeV) dependence

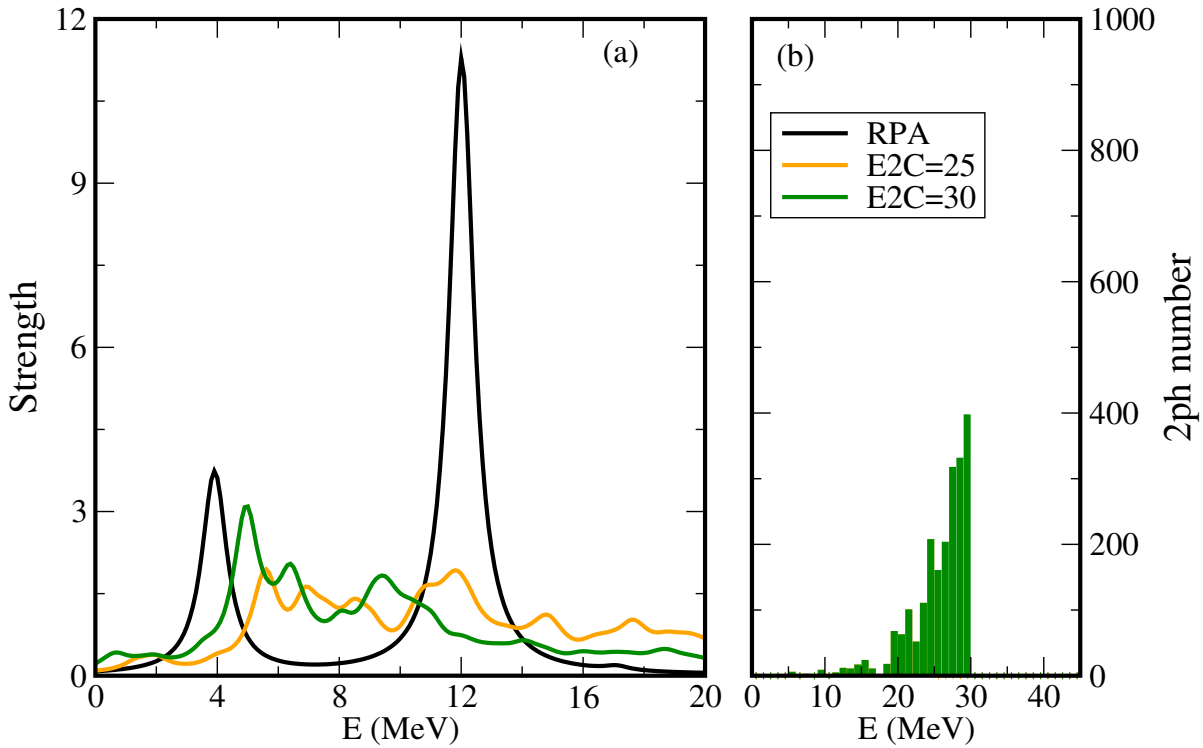

GT^- Strength Distribution ^{48}Ca, 2p2h cutoff EC (MeV) dependence

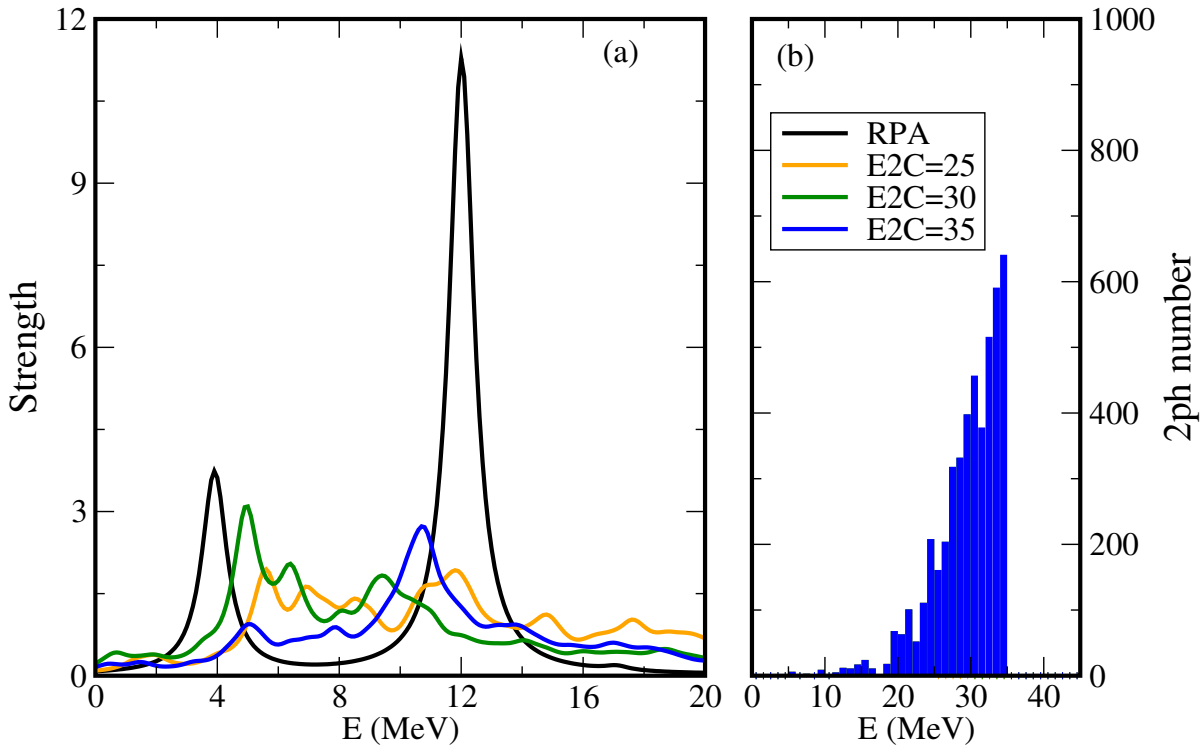

GT^- Strength Distribution ^{48}Ca, 2p2h cutoff EC (MeV) dependence

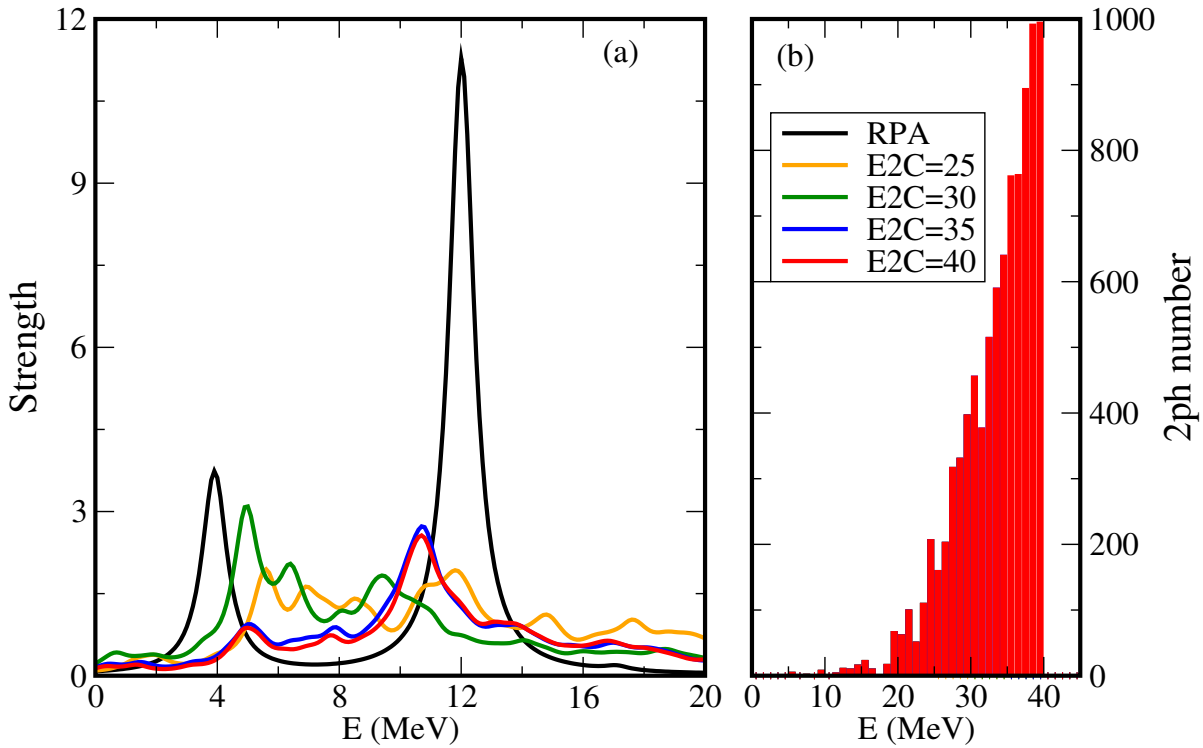

GT$^-$ Strength Distribution ^{48}Ca, 2p-2h cutoff dependence

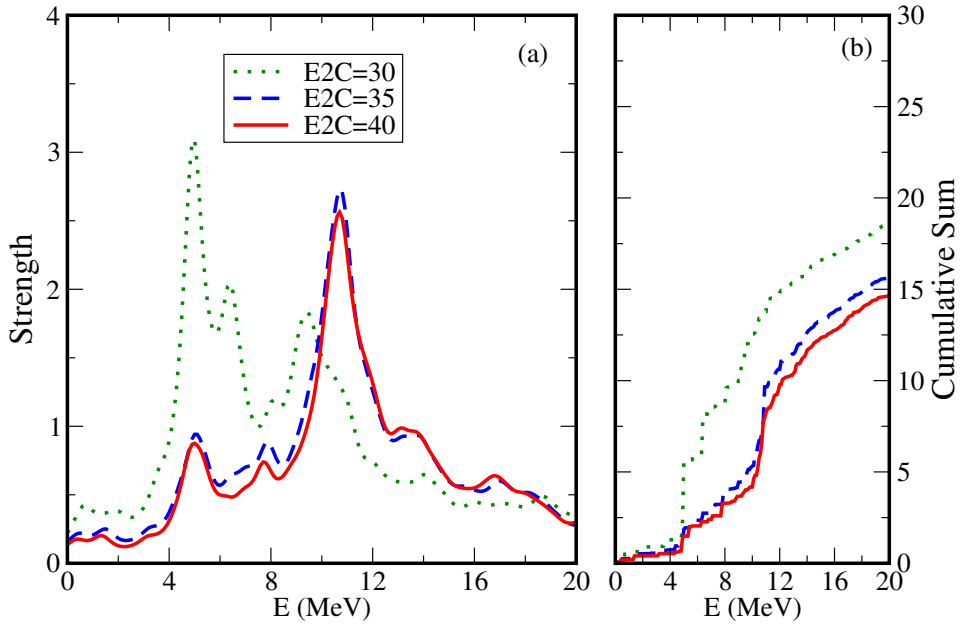

SSRPA results, 2p-2h cutoff E2C value in MeV units.